UNIVERSIDAD NACIONAL AUTÓNOMA DE MÉXICO
PROGRAMA DE MAESTRÍA Y DOCTORADO EN INGENIERÍA
INGENIERÍA ELÉCTRICA - CONTROL

CONTINUOUS HIGHER-ORDER SLIDING MODE CONTROL: IMPLEMENTATION ISSUES

TESIS
QUE PARA OPTAR POR EL GRADO DE:
DOCTOR EN INGENIERÍA

PRESENTA:
ALBERTO ISMAEL CASTILLO LÓPEZ

TUTOR(ES) PRINCIPAL(ES)
DR. LEONID FRIDMAN, FACULTAD DE INGENIERÍA
TUTOR
DR. JAIME A. MORENO, INSTITUTO DE INGENIERÍA
CO-TUTOR

MÉXICO, CD. MX., JULIO DE 2017

JURADO ASIGNADO:

Presidente:	Dr. Marco Antonio Arteaga Pérez
Secretario:	Dr. Jaime Alberto Moreno Pérez
Vocal:	Dr. Leonid Fridman
1er. Suplente:	Dr. Gerardo René Espinosa Pérez
2do. Suplente:	Dr. Luis A. Álvarez-Icaza Longoria

CIUDAD UNIVERSITARIA, CIUDAD DE MÉXICO, MÉXICO

TUTOR DE TESIS:

DR. LEONID FRIDMAN

- -

FIRMA

(Segunda hoja)

"... Consider again that pale blue dot we've been talking about. Imagine that you take a good long look at it. Imagine you're staring at the dot for any length of time, and then try to convince yourself that God created the whole Universe for one of the 10 million or so species of life that inhabit that speck of dust. Now take a step further: Imagine that everything was made just for a single shade of that species, or gender, or ethnic or religious subdivision. We can recognize here a shortcoming –in some circumstances serious– in our ability to understand the world. Characteristically, we seem compelled to project our own nature onto Nature.

Man in his arrogance thinks himself a great work, worthy of the interposition of a deity. Darwin wrote telegraphically in his notebook, "More humble and I think truer to consider him created from animals." We're Johnny-come-latelies. We live in the cosmic boondocks. We emerged from microbes and muck. Apes are our cousins. Our thoughts and feelings are not fully under our own control. And on top of all this, we're making a mess of our planet and becoming a danger to ourselves. The trapdoor beneath our feet swings open. We find ourselves in bottomless free fall. If it takes a little myth and ritual to get us through a night that seems endless, who among us cannot sympathize and understand?

We long to be here for a purpose, even though, despite much self-deception, none is evident. The significance of our lives and our fragile planet is then determined only by our own wisdom and courage. We are the custodians of life's meaning. We long for a Parent to care for us, to forgive us our errors, to save us from our childish mistakes. But knowledge is preferable to ignorance. Better by far to embrace the hard truth than a reassuring fable.

Modern science has been a voyage into the unknown, with a lesson in humility waiting at every stop. Our commonsense intuitions can be mistaken. Our preferences don't count. We do not live in a privileged reference frame. If we crave some cosmic purpose, then let us find ourselves a worthy goal. "

Carl Sagan

Acknowledgements

A mis padres y hermanos, por su apoyo, comprensión y consejo.

Al Dr. Leonid Fridman, por su guía, consejo y amistad.

Al Dr. Jaime Moreno cuya participación fue fundamental para el desarrollo de esta tesis.

A los miembros de mi comité tutoral y sinodales por sus valiosas observaciones y consejos.

A mis compañeros del grupo de Modos Deslizantes.

Al CONACyT y al Posgrado de Ingeniería Eléctrica de la UNAM.

Contents

List of Abbreviations

SMC	**S**liding **M**ode **C**ontrol
HOSM	**H**igher **O**rder **S**liding **M**odes
CHOSM	**C**ontinuous **H**igher **O**rder **S**liding **M**odes
STA	**S**uper **T**wisting **A**lgorithm
SSTA	**S**aturated **S**uper **T**wisting **A**lgorithm
GSTA	**G**eneralized **S**uper **T**wisting **A**lgorithm
SS	**S**liding **S**urface
RC	**R**elay **C**ontroller
OISM	**O**utput **I**ntegral **S**liding **M**ode **C**ontrol
MPC	**M**odel **P**redictive **C**ontrol

Chapter 1

Introduction: Continuous Sliding-Mode Control

1.1 Sliding Mode Control

The Sliding Mode Control (SMC) technique has been known as one of the most efficient tools for theoretically exact compensation of matched uncertainties and perturbations in control systems. The classical theory of First Order SMC (FOSMC) was stablish and reported by Prof. Utkin (see for example Utkin, 1992). The main advantage of Sliding Mode Control of theoretically exact compensate matched uncertainties (insensitivity) is achieved by a bounded (saturated) discontinuous of control law. Nevertheless, discontinuities in control law in presence of nonidealities (e.g. non-modeled dynamics, time delays, hysteresis, etc.) may produce high-frequency oscillations in the states and outputs which is the worst disadvantage of the SMC methodology, the called *chattering* effect (Utkin, 1992; Boiko and Fridman, 2005). The FOSMC allows the finite-time convergence of the trajectories of the system to the desired Sliding Surface (SS), but the state variables only converge asymptotically to the origin. This sliding surface design is restricted to have relative degree one with respect to the control input.

1.2 Continuous Higher-Order Sliding-Mode Features

During the last decades SMC theory has been developed in order to remove or attenuate the main disadvantages of the classical SMC. Chattering alleviation has lead to a new generations of Sliding Mode control algorithms that produce a continuous signal of control. For example, one of the most representative algorithms of Continuous Higher-Order Sliding Mode Control (CHOSMC) theory is the so-called Super-Twisting Algorithm (STA) (Levant, 1998). It was designed as an alternative to classical Sliding Mode controller reducing drastically the appearance of the chattering effect. STA introduces a *dynamic extension* to the system such that a discontinuous term is hidden behind an integrator, that is why it generates a continuous control signal ensuring theoretically exact compensation of *Lipschitz* perturbations as well as providing finite-time convergence of the output and its derivative (a second-order Sliding Mode). The properties of the STA are actively discussed (see for example Boiko and Fridman, 2005, Polyakov and Poznyak, 2009, Orlov, Aoustin, and Chevallereau, 2011, Utkin, 2013, Bernuau et al., 2013, Utkin, 2016), as well as the possibilities of its adaptation (see for example Shtessel, Taleb, and Plestan, 2012, Utkin and Poznyak, 2013).

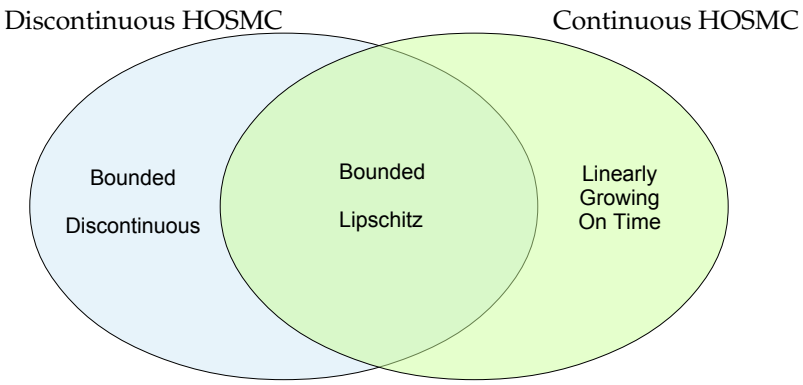

FIGURE 1.1: Class of perturbations of Discontinuous and Continuous controllers.

1.2.1 Class of perturbation/uncertainties compensation

Nature of control signal generated by the STA controller is closely related with the class of perturbations that can be exactly compensated: Discontinuous controllers generate a bounded control signal that is able to compensate bounded matched disturbances that can even be discontinuous as dry friction or backlash effect. On the other hand, Continuous controllers can only compensate Lipschitz continuous disturbances, but they can be growing linearly on time without bounds. Figure 1.1 shows the class of perturbations for the two families of HOSMC.

1.2.2 Chattering Reduction

During the last decades *chattering* effect was associated to the nature of the control signal, i.e. *chattering* was though as a consequence for applying discontinuous control signal into the system making higher-order non-modeled dynamics to excite. Then, the application of continuous signal of control would reduce drastically the appearance of *chattering*.

Recent studies (Pérez-Ventura and Fridman, 2016; Utkin, 2016) have shown that the amplitude and frequency of output oscillations in the *chattering* effect also depend in the parameters of the parasitic non-modeled dynamics affecting the relative degree of the output with respect to the control input, and in the gain selection of the HOSM algorithm. Nevertheless, the present work focuses its efforts on the study of STA as the solution, in most practical of cases, to the alleviation of *chattering* effect.

1.2.3 Accuracy

Almost all known HOSM controllers possess specific homogeneity properties (Levant 2005). This properties, apart from providing standard methods for stability proofs, provide the highest possible asymptotic accuracy in the presence of measurement noises, delays and discrete measurements Levant, 1993.

It is also shown in Levant, 2010 that in the presence of an actuator of the form $\tau\dot{z} = a(z,u)$, $v = v(z)$, $z \in \mathbb{R}^m$, $v \in \mathbb{R}$ with u the input of the actuator, v its output and μ the time constant, this accuracy properties also hold under reasonable assumptions.

1.3 STA Implementation Issues

Continuous HOSM have become one of the most important achievements in SMC Theory. The integral discontinuous term in control law allows to ensure the SMC properties with a continuous signal of control. Nevertheless, when substituting discontinuous controllers by continuous ones, several drawbacks arise on experimental setups that must be addressed.

As STA is the most representative Continuous HOSMC in SMC theory, the present work focuses in the further development of STA properties in the following fields. The achievements in this aspects will be the base for further development in general (r-th order) HOSMC.

Super-Twisting Algorithm (STA) (Levant, 1993), as mentioned before, has been one of the most well-known Continuous HOSM algorithms in the last decades. It was designed as a possibility to substitute the discontinuous FOSMC by a continuous one. STA as any Continuous HOSMC allows the exact rejection of Lipschitz perturbations. It ensures a quadratic precision of the output with respect to the sampling time due to its homogeneity properties and a second order Sliding Mode achieved in finite-time, i.e. output and its derivative are robustly driven to zero in finite-time. It is also one of the most cited nonlinear algorithms as author's original work. See https://scholar.google.com/citations?user=_A_QeKgAAAAJ.

Classic form of STA (Levant, 1998) is defined by

$$\begin{aligned} u = & \quad -k_1 \lceil x_1 \rfloor^{\frac{1}{2}} + z; \\ \dot{z} = & \quad -k_2 \text{sign}\,(x_1)\,, \end{aligned} \tag{1.1}$$

where the notation $\lceil a \rfloor^b = |a|^b \text{sign}\,(a)$ is used during the rest of the work. The first term is a function proportional to the square root of the state while the second one is an integral of a discontinuous function. STA works as a nonlinear Proportional-Integral (PI) controller, making it a unbounded controller, i.e. proportional term can be very big depending on the initial condition of the system, and the integral term can grow linearly with respect to time.

The class of systems to which STA can be applied consists in first order (relative degree 1) systems represented by

$$\dot{x} = \gamma(x,t)u + \phi(x,t). \tag{1.2}$$

where $x \in \mathbb{R}$ is the state, $u \in \mathbb{R}$ the control input, and $\gamma(x,t)$ and $\phi(x,t)$ uncertain functions of the state and time.

1.3.1 State dependent perturbations and uncertain control coefficient

CHOSMC are insensible with respect to Lipschitz continuous matched perturbations. Even though, when considering a plant's mathematical model with parametric uncertainty, perturbations become state dependent, that in general are just locally Lipschitz. This means that in implementation setups STA cannot maintain its properties globally:

In Levant, 1993, the STA proof of convergence was made by means of geometrical arguments for the case when uncertainty in the control coefficient and perturbations only dependent on time.

Different Lyapunov functions (see for example Moreno and Osorio, 2008, Moreno, 2011, Polyakov and Poznyak, 2009, Orlov, Aoustin, and Chevallereau, 2011, Utkin,

2013) were recently designed in order to get convergence conditions and estimations of the reaching time.

Nevertheless, this Lyapunov proofs are made under conservative assumptions:

1. the perturbations are dependent only on time (Levant, 1993,Moreno, 2011).
2. the control coefficient is known (Levant, 1993, Moreno, 2011,Gonzalez, A., and Fridman, 2012,Picó et al., 2013,Guzmán and Moreno, 2015).
3. perturbations are dependent on state and time, but it is supposed that their total time derivative, i.e. control signal is *a priori* bounded by some constant (Shtessel, Taleb, and Plestan, 2012,Gonzalez, A., and Fridman, 2012).

In reality, for example, any uncertainty in the inertia moment of a mechanical system can cause time and state dependent uncertainties/perturbations and also time and state dependent uncertain control coefficient.

In this work the possibility of implementation of Generalized STA (GSTA) (Moreno, 2009) under this scenario is considered: the case when *both, the perturbation and control coefficient are state and time dependent and, moreover, the control coefficient is* ***uncertain.***

Chapter 2 and 3 will present further robustness properties of GSTA with respect to state and time dependent perturbations, and an uncertain coefficient of control, respectively.

1.3.2 Saturation

STA, as mentioned before, achieve their continuous control signal by means of a discontinuous function *hidden* through an integrator. Then, any version of STA is a control law with integral action and as any integral control law is in general unbounded. Control signal can grow without bounds depending on the perturbations (who also can be linearly growing in time), and bounds of overshoots during the transient process cannot be *a priori* determined.

The original version of STA, as it was introduced in Levant, 1993, Theorem 5, p.1257, is a saturated control law, i.e. the control signal is bounded. To ensure the saturation, the author proposed a switching logic saturating both, the term of STA proportional to the square root of the state and the integral term separately. However, this switching logic can generate undesired oscillations on the border of the integrator saturation (see Fig. 4.5).

In practical implementations control effort is always limited and it is well known (Hippe, 2006) that the application of controllers with integral action in feedback loops with bounded control signal may lead to the so-called *integral windup* effect. This refers to the situation where a significant change in the set-point causes actuator saturation and as a result accumulating significant error in the integral term during the rise. This produces undesired overshooting or even destabilizing the origin of the system. Some classic anti-windup techniques consist in:

- Disabling the integral function until the variable to control has entered a controllable region,
- Reseting the integral controller to a desired value.

Chapter 4 proposes two different structures of SSTA, using classical anti-windup techniques, in order to make the STA's control signal not to exceed predefined bounds. The main idea is to design a controller using a Relay Controller (RC) with a given

level of saturation outside some neighborhood of the origin where the integral function will be disabled. The size of this vicinity is calculated ensuring that, crossing the border of this vicinity, the controller will switch to STA and will ensure finite-time convergence to the origin without saturation.

Chapter 5 is focused on experimental setups to test the performance of the proposed scheme of saturation. Three different experiments are performed. The first one is the velocity tracking of a mechanical system where the relative degree of the output is 1 and therefore SSTA is directly applicable.

The second one is the application of the classical Sliding Variable (SV) design on a Reaction Wheel Pendulum and the SSTA as the controller to enforce the system trajectories to the SS.

The third one is an application of continuous Output Integral Sliding Modes (OISM) to a Model Predictive nominal controller (MPC). The design of MPC allows to include restrictions on the states and in the control signal in the controller design. Continuous OISM will protect the nominal MPC granting insensitivity to the closed-loops system with respect to Lipschitz matched perturbations.

Finally, Chapter 6 summarizes the theoretical and experimental results of the present work.

Chapter 2

State Dependent Perturbations

2.1 Introduction

In this section Generalized Super-Twisting Algorithm is applied to a class of systems whose perturbations are time and state dependent. A non-smooth strict Lyapunov function is used to obtain the conditions for the global finite-time stability and to estimate the time of convergence.

2.1.1 Motivation example:

Consider the problem of velocity tracking in mechanical system

$$(1+\cos^2(q))\ddot{q} + g\sin(q) + b(\dot{q} + \arctan\dot{q}) = u,$$

where $q \in \mathbb{R}$ and $\dot{q} \in \mathbb{R}$ are the state variables and $u \in \mathbb{R}$ the torque control input. The terms of the differential equation represent a varying inertia moment, gravitational term and viscous and dry friction, respectively. It is desired to realize exact velocity tracking to a desired trajectory $\dot{q}_d$. In this statement, the dependence of the functions on the variable q can be considered as exogenous functions of time. By defining the error variable $e_1 = \dot{q} - \dot{q}_d$, the velocity error dynamics are

$$\dot{e}_1 = \gamma(q)u - \gamma(q)g\sin(q) - \gamma(q)b\left(e_1 + \dot{q}_d + \arctan\left(e_1 + \dot{q}_d\right)\right) - \ddot{q}_d, \tag{2.1}$$

where $\gamma(q) = 1/(1+\cos^2(q))$. Here, the time-varying function $\gamma(q(t))$ is an uncertain time-varying control coefficient. Let us remark that $\gamma(q(t))$ is bounded by $0 < 0.5 \leq \gamma(q(t)) \leq 1$, with a bounded time derivative.

If the standard STA $u_{st} = -k_1\lceil e_1\rfloor^{1/2} + z$, $\dot{z} = -k_2\lceil e_1\rfloor^0$, is applied to the plant, the closed-loop can be written as

$$\dot{e}_1 = -k_1\gamma(q)\lceil e_1\rfloor^{1/2} + \gamma(q)\underbrace{\left[z - g\sin(q) + b\left(e_1 + \dot{q}_d + \arctan\left(e_1 + \dot{q}_d\right)\right) - \frac{\ddot{q}_d}{\gamma(q)}\right]}_{e_2}. \tag{2.2}$$

Note that the function $-k_1\lceil e_1\rfloor^{1/2}$ is not able to compensate any of the non vanishing perturbation terms, so they need to be compensated through the integral action. One of the specific features of the STA lies in the equation of the dynamic extension

$$\dot{e}_2 = -k_2\lceil e_1\rfloor^0 + \underbrace{g\cos(q) - \left[\frac{\dddot{q}_d}{\gamma(q)} - \frac{\ddot{q}_d}{\gamma^2(q)}\dot{\gamma}(q)\right] + bc\ddot{q}_d}_{\dot{\varphi}} + bc\dot{e}_1, \tag{2.3}$$

$c = \left(\frac{(e_1+\dot{q}_d)^2+2}{(e_1+\dot{q}_d)^2+1}\right)$, where the discontinuous function $-k_2\lceil e_1 \rfloor^0$ has to overcome the derivative of the perturbations. Replacing in (2.3) the value of the last term we get

$$\begin{aligned} \dot{e}_2 = \quad & -\boldsymbol{k_2}\lceil e_1 \rfloor^0 + \dot{\varphi} \underbrace{-bc\gamma \boldsymbol{k_1} \lceil e_1 \rfloor^{1/2} - bc\gamma \boldsymbol{k_2} \int_0^t \lceil e_1(\tau) \rfloor^0 d\tau}_{u(t)} \\ & + bc\gamma \int_0^t \left[\dot{\varphi}(\tau) - b\left(k_1 \lceil e_1(\tau) \rfloor^{1/2} - e_2(\tau)\right)\right] d\tau \end{aligned} \tag{2.4}$$

Here, an **algebraic loop** occurs in the gains design since the gains themselves become part of the perturbation to overcome, as shown in equation (2.4). In Shtessel, Taleb, and Plestan, 2012 and Gonzalez, A., and Fridman, 2012, the control signal $u(t)$ is assumed to be bounded *a priori*, and the algebraic loop never occurs.

Moreover, a necessary condition of stability of the STA is that $k_2 > |\dot{\varphi} + bc\dot{e}_1|$. Is easy to see that the terms in $\dot{\varphi}$ can be bounded by a constant, nevertheless, non-bounded terms related with the dynamics of the controller itself appear in equation (2.4). These cannot be globally dominated by the sign function $-k_2\lceil e_1 \rfloor^0$. This behavior can be interpreted as perturbations that can grow exponentially in time.

Several problems arise when trying to find STA gains k_1 and k_2 that ensure the stability of the closed-loop and dominate the derivative of such perturbation:

1. STA gain k_2 needs to be designed based on functions depending on STA gains k_1 and k_2! This is an algebraic loop that has not been addressed in any previous work.

2. Although the perturbations $\dot{\varphi}$ can be bounded by a constant, the terms $-bc\gamma \boldsymbol{k_1} \lceil e_1 \rfloor^{1/2} - bc\gamma \boldsymbol{k_2} \int_0^t \lceil e_1(\tau) \rfloor^0 d\tau$ can be very big depending on the initial conditions $e_1(0)$ and perturbations.

3. The time variation in the control coefficient $\gamma(q(t))$ introduces the term $\frac{\ddot{q}_d}{\gamma^2(q(t))}\dot{\gamma}(q(t))$ to the total time derivative, and the bounds of $\gamma(q(t))$ and its derivative $\dot{\gamma}(q(t))$ should be also taken into account in the controller gains design.

4. State dependent perturbations implies state dependent derivatives which makes the perturbation to grow exponentially in time.

It is worth noting that the standard STA cannot be designed for the situations (1) and (2). Moreover, it is not clear if the stability of the system is preserved in spite of the unknown variations of the coefficients in equation (2.2) due to the uncertain control coefficient $\gamma(q)$.

The standard gain design for STA Levant, 1998 is not applicable here. Even more, the non-linear terms of the Standard STA are not enough to maintain the global stability of the system in presence of uncertain control coefficient and state dependent perturbation. Then, an improved STA will be used to solve this problem.

Generalized Super-Twisting Algorithm (GSTA)

Moreno, 2011, Moreno, 2009 is defined by

$$\begin{aligned} u &= -k_1\phi_1(x) + z, \quad \dot{z} = -k_2\phi_2(x), \\ \phi_1(x) &= \lceil x \rfloor^{\frac{1}{2}} + \beta x, \quad \phi_2(x) = \tfrac{1}{2}\lceil x \rfloor^0 + \tfrac{3}{2}\beta\lceil x \rfloor^{\frac{1}{2}} + \beta^2 x. \end{aligned} \tag{2.5}$$

Note that the Generalized STA (GSTA) has an extra linear term βx in function $\phi_1(x)$ and growing terms $\frac{3}{2}\beta\lceil x\rfloor^{\frac{1}{2}}$ and $\beta^2 x$ in function $\phi_2(x)$.

Note that function ϕ_2 is defined such that

$$\phi_2(x) = \phi_1'(x)\phi_1(x) \quad \text{with} \quad \phi_1'(x) = \left(\frac{1}{2|x_1|^{\frac{1}{2}}} + \beta\right). \tag{2.6}$$

With the extra linear term, three degrees of freedom in the GSTA gains design are obtained: k_1, k_2 and β. The growing terms help to counteract the effects of state dependent perturbations which can grow exponentially in time.

Contribution

This chapter proposes a global finite-time stability analysis for the GSTA based on a strict non-smooth Lyapunov function when there is a known control coefficient with state and time dependent perturbations.

The more general situation, where the control coefficient is also an uncertainty dependent on state and time will be addressed in the next chapter.

2.2 Chapter Problem Statement and Main Result

The main goal of this chapter is to find the conditions for GSTA gains $\{k_1, k_2, \beta\}$ design taking into account the known bounds of perturbations as well as its partial derivatives with respect to the time and state, such that the trajectories of the system globally converge to zero in finite-time.

2.2.1 State Dependent Perturbations and Known Coefficient of Control

2.2.2 Separation of Perturbations

Consider the first order system

$$\dot{x} = u + \varphi(x, t), \tag{2.7}$$

where $x \in \mathbb{R}$ is the state, $u \in \mathbb{R}$ is the control input, and φ a Lipschitz continuous function with respect to t and $\varphi \in \mathscr{C}^1$ with respect to x.

The term $\varphi(x, t)$ in an uncertain function dependent on the state and time. The control coefficient function is assumed to be known and without loss of generality, equals to 1. Terms of perturbation can be split in two terms as in Gonzalez, A., and Fridman, 2012:

$$\varphi(x, t) = \varphi_1(x, t) + \varphi_2(x, t) \tag{2.8}$$

such that the first term is vanishing at the origin, i.e. $\varphi_1(0, t) = 0, \quad \forall t \geq 0$ and bounded by

$$|\varphi_1(x, t)| \leq \alpha|\phi_1(x)|, \quad \phi_1(0) = 0, \tag{2.9}$$

and the second term is meant to be compensated through the integral action.

System (2.7) in closed-loop with (2.5) takes the form

$$\dot{x} = -k_1\phi_1(x) + z + \varphi_1(x, t) + \varphi_2(x, t). \tag{2.10}$$

Defining $x_1 = x$ and $x_2 = z + \varphi_2(x_1, t)$, we have

$$\dot{x}_1 = -k_1\phi_1(x_1) + x_2 + \varphi_1(x_1, t), \tag{2.11a}$$

$$\dot{x}_2 = -k_2\phi_2(x_1) + \frac{d}{dt}\left(\varphi_2(x_1, t)\right). \tag{2.11b}$$

The first equation can be rewritten as

$$\dot{x}_1 = \left(-\tilde{k}_1\phi_1(x_1) + x_2\right)$$

where

$$\tilde{k}_1 = k_1 - \frac{\varphi_1(x_1, t)}{\phi_1(x_1)}. \tag{2.12}$$

Note that from (2.9),

$$\left|\frac{\varphi_1(x, t)}{\phi_1(x_1)}\right| \leq \alpha\frac{|\phi_1(x_1)|}{|\phi_1(x_1)|} \leq \alpha,$$

then, $\tilde{k}_1$ is considered as a positive varying bounded gain.

The time derivative of the second term of perturbation (2.8) is given by

$$\begin{aligned}\frac{d}{dt}\left(\varphi_2(x_1, t)\right) &= \underbrace{\frac{\partial\varphi_2}{\partial t}}_{\delta_1(x_1,t)} + \underbrace{\left(\frac{\partial\varphi_2}{\partial x_1}\right)}_{\delta_2(x_1,t)}\dot{x}_1 \\ &= \delta_1(x_1, t) + \delta_2(x_1, t)\dot{x}_1.\end{aligned} \tag{2.13}$$

Moreover, the partial derivatives of the perturbation

$$\delta_1(x, t) = \frac{\partial\varphi_2(x, t)}{\partial t}, \quad \delta_2(x, t) = \frac{\partial\varphi_2(x, t)}{\partial x} \tag{2.14}$$

are assumed to be bounded by positive constants

$$|\delta_1(x_1, t)| \leq \quad \bar{\delta}_1, \quad |\delta_2(x_1, t)| \leq \quad \bar{\delta}_2. \tag{2.15}$$

From (2.2.2), we rewrite the second equation as

$$\begin{aligned}\dot{x}_2 &= -k_2\phi_2(x_1) + \delta_1(x_1, t) + \delta_2(x_1, t)\dot{x}_1 \\ &= -k_2\phi_2(x_1) + \delta_1(x_1, t) + \delta_2(x_1, t)\left(-\tilde{k}_1\phi_1(x_1) + x_2\right) \\ &= -k_2\phi_2(x_1) + \delta_1(x_1, t) - \delta_2(x_1, t)\tilde{k}_1\phi_1(x_1) + \delta_2(x_1, t)x_2.\end{aligned}$$

Due to the fact that $\phi_2(x_1) = \phi_1(x_1)\phi_1'(x_1)$ (see equations (2.5) and (2.6)), here it is possible to see that the unbounded third term of $-\delta_2(x_1, t)\tilde{k}_1\phi_1(x_1)$ can be compensated by the function $-k_2\phi_2(x_1)$. We group this terms in the following expression

$$\begin{aligned}\dot{x}_2 &= \phi_1'(x_1)\left[-k_2\phi_1(x_1) + \frac{\delta_1(x_1, t)}{\phi_1'(x_1)} - \frac{\delta_2(x_1, t)\tilde{k}_1}{\phi_1'(x_1)}\phi_1 + \frac{\delta_2(x_1, t)}{\phi_1'(x_1)}x_2\right] \\ &= \phi_1'(x_1)\left[-\left(k_2 + \frac{\delta_2(x_1, t)}{\phi_1'(x_1)}\tilde{k}_1\right)\phi_1(x_1) + \frac{\delta_1(x_1, t)}{\phi_1'(x_1)} + \frac{\delta_2(x_1, t)}{\phi_1'(x_1)}x_2\right].\end{aligned}$$

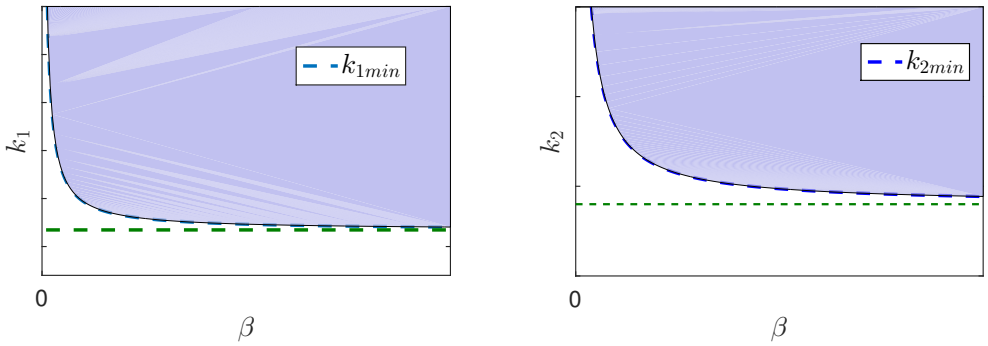

(A) asd (B) asd

FIGURE 2.1: Decrease of k_{1min} and k_{2min} vs β.

Note that the multiplicative inverse of function $\phi_1'(x_1)$ is bounded

$$\left|\frac{1}{\phi_1'(x_1)}\right| = \left|\frac{2|x_1|^{\frac{1}{2}}}{1+2\beta|x_1|^{\frac{1}{2}}}\right| \leq \frac{1}{\beta},$$

therefore any singularity occurs.

Global finite-time stability analysis of the closed-loop system (2.11) is based on a strict non-smooth Lyapunov function in Moreno, 2009, and it is given in the Appendix. Results of the analysis are stated in the following theorem.

Theorem 1. *Suppose that $\varphi(x,t)$ of the system (2.7) satisfy (2.8) and (2.15). Then, the states x_1 and x_2 converge to zero and z converges to $-\varphi(x,t)$, globally and in finite-time, if GSTA gains k_1, k_2 and $\beta > 0$ are designed as follows: for any $\epsilon > 0$:*

$$k_1 > \frac{2(1+\epsilon)\bar{\delta}_2}{\beta} + \alpha, \tag{2.16a}$$

$$k_2 > \frac{1}{4\underline{h}\epsilon}\left(\frac{(1+\epsilon)}{(k_1-\alpha)}\left(\frac{\bar{\delta}_2\alpha}{\beta}+2\bar{\delta}_1\right)+\frac{\bar{\delta}_2\epsilon}{\beta}+\alpha\right)^2+2\bar{\delta}_1. \tag{2.16b}$$

$$\underline{h} = 1-\frac{\bar{\delta}_2}{\beta}\frac{1+\epsilon}{(k_1-\alpha)} > 0,$$

△

Remark 1. *When the perturbation in the system is state dependent, the function $\delta_2(x_1,t)$ appears in the total time derivative, and it is worth noting that the extra terms in functions $\phi_1(x_1)$ and $\phi_2(x_1)$ related with the gain β, are necessary to guarantee the global stability of the equilibrium point. This behavior can be observed in (2.16a) and (2.16b), where the gain β appears in the ratio $\frac{\bar{\delta}_2}{\beta}$. This allows to arbitrarily decrease the effects of the perturbation $\bar{\delta}_2$ by increasing the gain β.* △

GSTA gain β does not only allow to guarantee the global stability of the system. It can be used to reduce the *chattering* effect by reducing the minimum values of gains k_1 and k_2 (see Figs. 2.1a and 2.1b). Once the gain β is fixed, the possible set of gains k_1 and k_2 are depicted in Fig. 2.2a.

The parameter $\epsilon > 0$, also allows to adjust the minimum values k_{1min} and k_{2min}. Fig. (2.2a) shows how the parameter ϵ can be selected such that k_{1min} and k_{2min} are in their lowest values.

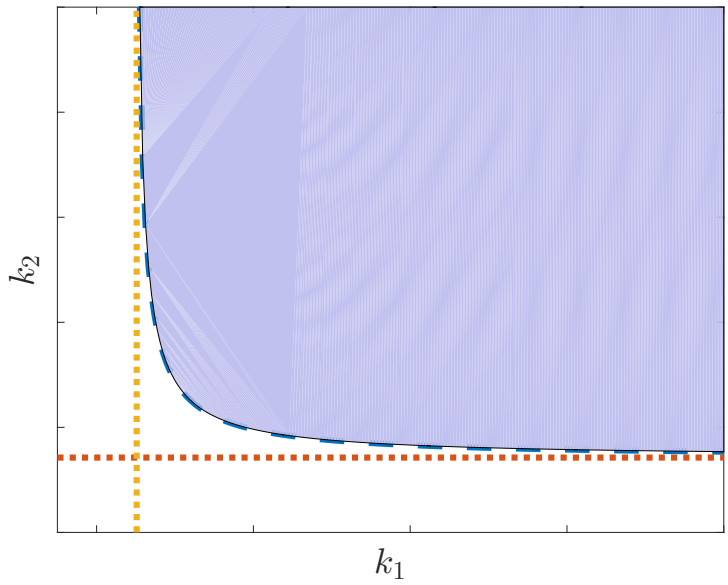

(A) Set of GSTA gains $\{k_1, k_2\}$, when β and parameter ϵ are fixed.

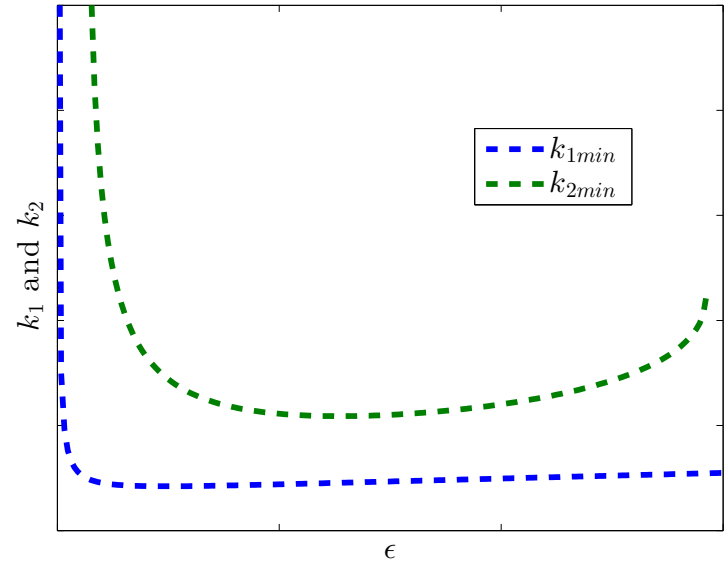

(B) Minimum values of k_1 and k_2 vs ϵ.

FIGURE 2.2: Theorem 1. Set of possible selection of gains $\{k_1, k_2, \beta\}$.

Chapter 3

Uncertain Coefficient of Control

3.1 Introduction

In this chapter, the Generalized Super-Twisting Algorithm is applied to a class of systems whose control coefficient is uncertain. Two cases are analyzed: i) perturbations and uncertain coefficient of control are dependent on time and the general case when ii) perturbation and uncertain control coefficient are time and state dependent. A non-smooth strict Lyapunov function is used to obtain the conditions for the global finite-time stability and to estimate the time of convergence.

3.2 General case

Consider the scalar dynamic system represented by the differential equation

$$\dot{x} = \gamma(x,t)u + \varphi(x,t), \tag{3.1}$$

where $x \in \mathbb{R}$ is the state and $u \in \mathbb{R}$ is the control input. The functions $\varphi(x,t)$ and $\gamma(x,t)$ are uncertain functions dependent on the state and time. The uncertain control coefficient function is also assumed to be bounded by positive constants

$$0 < k_m \leq \gamma(x,t) \leq k_M. \tag{3.2}$$

In order to guarantee a continuous control signal, the uncertain control coefficient $\gamma(x,t)$ and perturbation $\varphi(x,t)$ should be also continuous, since $x \equiv 0 \rightarrow \dot{x} \equiv 0$, and therefore

$$0 = \gamma(x,t)u + \varphi(x,t) \rightarrow u_{eq}(x,t) = -\frac{\varphi(x,t)}{\gamma(x,t)}.$$

Hence, φ and γ are assumed to be Lipschitz continuous functions with respect to t and $\varphi, \gamma \in \mathscr{C}^1$ with respect to x.

Following Gonzalez, A., and Fridman, 2012, we split the perturbations into two parts

$$\varphi(x,t) = \varphi_1(x,t) + \varphi_2(x,t), \tag{3.3}$$

such that the first term is vanishing at the origin, i.e. $\varphi_1(0,t) = 0$ for all $t \geq 0$, and bounded by

$$|\varphi_1(x,t)| \leq \alpha|\phi_1(x)|, \quad \phi_1(0) = 0. \tag{3.4}$$

The total time derivative of the second term (divided by the control coefficient $\gamma(x,t)$) can be represented as

$$\frac{d}{dt}\left(\frac{\varphi_2(x,t)}{\gamma(x,t)}\right) = \underbrace{\frac{1}{\gamma}\frac{\partial\varphi_2}{\partial t} - \frac{\varphi_2}{\gamma^2}\frac{\partial\gamma}{\partial t}}_{\delta_1(x,t)} + \underbrace{\left(\frac{1}{\gamma}\frac{\partial\varphi_2}{\partial x} - \frac{\varphi_2}{\gamma^2}\frac{\partial\gamma}{\partial x}\right)}_{\delta_2(x,t)}\dot{x} \tag{3.5a}$$

$$= \delta_1(x,t) + \delta_2(x,t)\dot{x}. \tag{3.5b}$$

System (3.1) in closed-loop with GSTA (2.5) has the form

$$\dot{x} = -k_1\gamma(x,t)\phi_1(x) + \varphi_1(x,t) + \gamma(x,t)\left[z + \frac{\varphi_2(x,t)}{\gamma(x,t)}\right],$$

and defining $x_1 = x$ and $x_2 = z + \dfrac{\varphi_2(x_1,t)}{\gamma(x_1,t)}$, we obtain

$$\dot{x}_1 = \gamma(x_1,t)\left[-k_1\phi_1(x_1) + \frac{\varphi_1(x_1,t)}{\gamma(x_1,t)} + x_2\right], \tag{3.6a}$$

$$\dot{x}_2 = -k_2\phi_2(x_1) + \frac{d}{dt}\left(\frac{\varphi_2(x_1,t)}{\gamma(x_1,t)}\right). \tag{3.6b}$$

Moreover, according to the previous discussion we assume that the perturbation terms are such that the functions

$$\begin{aligned}\delta_1(x_1,t) &= \frac{1}{\gamma(x_1,t)}\frac{\partial\varphi_2(x_1,t)}{\partial t} - \frac{\varphi_2(x_1,t)}{\gamma^2(x_1,t)}\frac{\partial\gamma(x_1,t)}{\partial t},\\ \delta_2(x_1,t) &= \frac{1}{\gamma(x_1,t)}\frac{\partial\varphi_2(x_1,t)}{\partial x_1} - \frac{\varphi_2(x_1,t)}{\gamma^2(x_1,t)}\frac{\partial\gamma(x_1,t)}{\partial x_1}\end{aligned} \tag{3.7}$$

are bounded by positive constants

$$|\delta_1(x_1,t)| \leq \bar{\delta}_1, \quad |\delta_2(x_1,t)| \leq \bar{\delta}_2. \tag{3.8}$$

Theorem 2. *Suppose that $\gamma(x,t)$ and $\varphi(x,t)$ of system (3.1) satisfy (3.2) and (3.8). Then, the states x_1 and x_2 converge to zero and z converges to $-\varphi(x,t)$, globally and in finite-time, if GSTA gains k_1, k_2 and $\beta > 0$ are designed as follows: for any $\epsilon > 0$:*

$$k_1 > \frac{(1+\epsilon)}{4\epsilon k_m}\left(\frac{\alpha}{k_m}(k_M - k_m) + \frac{\bar{\delta}_2\epsilon}{\beta}(k_M + k_m + 2)\right) + \frac{(1+\epsilon)}{4\epsilon k_m}\sqrt{\Lambda_{k_1}} + \frac{\alpha}{k_m}, \tag{3.9a}$$

$$\Lambda_{k_1} = \left(\frac{\alpha}{k_m}(k_M - k_m) + \frac{\bar{\delta}_2\epsilon}{\beta}(k_M + k_m + 2)\right)^2 + 8\epsilon(k_M - k_m)\left(\frac{\bar{\delta}_2\alpha}{\beta} + 2\bar{\delta}_1\right).$$

$$k_2 \in \left[k_M\left(2\sqrt{\underline{h}\epsilon}\bar{c} - \frac{\bar{c}}{2}\sqrt{\Delta_{k_2}}\right)^2 + 2\bar{\delta}_1, k_M\left(2\sqrt{\underline{h}\epsilon}\bar{c} + \frac{\bar{c}}{2}\sqrt{\Delta_{k_2}}\right)^2 + 2\bar{\delta}_1\right], \tag{3.9b}$$

$$\Delta_{k_2} = 16\underline{h}\epsilon - 8\left(\frac{(1+\epsilon)(k_M - k_m)}{\underline{k}_1 k_m}\right)\left(\frac{(1+\epsilon)}{\underline{k}_1 k_m}\left[\frac{\bar{\delta}_2\alpha}{\beta} + 2\bar{\delta}_1\right] + \frac{\bar{\delta}_2\epsilon}{\beta} + \frac{\alpha}{k_m}\right).$$

$$\underline{h} = 1 - \frac{\bar{\delta}_2}{\beta}\frac{k_m + \epsilon}{(k_1 k_m - \alpha)}, \quad \bar{c} = \frac{\underline{k}_1 k_m}{(1+\epsilon)(k_M - k_m)}, \quad \underline{k}_1 = k_1 - \frac{\alpha}{km}.$$

Moreover, a system trajectory starting at $x(0) = (x_1(0), x_2(0))$ *reaches the origin in a time smaller than*

$$T(x(0)) = \frac{2}{\mu_2} \ln \left(\frac{\mu_2}{\mu_1} V^{\frac{1}{2}}(x_1(0), x_2(0)) + 1 \right). \tag{3.9c}$$

where

$$V = \xi^T P \xi, \quad P = \begin{bmatrix} p_1 & -1 \\ -1 & p_2 \end{bmatrix} > 0, \quad \xi^T = [\phi_1(x_1) \;\; x_2]. \tag{3.9d}$$

△

Selection of matrix P and the proof of the Theorem is given in the Appendix A.

Remark 2. *When the control coefficient is known or it is unknown but constant, the partial derivatives of* $\gamma(\cdot)$ *with respect to the state and time are zero* $\left(\frac{\partial \gamma(\cdot)}{\partial t} = \frac{\partial \gamma(\cdot)}{\partial x} = 0 \right)$*, GSTA is able to ensure the global finite-time stability even in the case of unbounded perturbations* $\varphi(\cdot)$*.* △

3.3 Time dependent uncertain control coefficient and perturbation

The last case of analysis is taking into account an uncertain control coefficient and a perturbation, both Lipschitz continuous functions of time,

$$\dot{x} = \gamma(t)u + \varphi(t), \tag{3.10}$$

where $x \in \mathbb{R}$ is the state and $u \in \mathbb{R}$ is the control input. The uncertain control coefficient is assumed to be bounded by positive constants

$$0 < k_m \leq \gamma(t) \leq k_M. \tag{3.11}$$

The total derivative of the second term in the perturbation (3.3) has the form

$$\delta_1(t) := \frac{d}{dt} \left(\frac{\varphi_2(t)}{\gamma(t)} \right) = \frac{1}{\gamma} \frac{d\varphi_2}{dt} - \frac{\varphi_2}{\gamma^2} \frac{d\gamma}{dt}. \tag{3.12}$$

System (3.10) in closed-loop with GSTA has the form

$$\dot{x} \;\; = -k_1 \gamma(t) \phi_1(x) + \varphi_1(t) + \gamma(t) \left[z + \tfrac{\varphi_2(t)}{\gamma(t)} \right],$$

and defining $x_1 = x$ and $x_2 = z + \frac{\varphi_2(t)}{\gamma(t)}$,

$$\begin{aligned} \dot{x}_1 &= \gamma(t) \left[-k_1 \phi_1(x_1) + \frac{\varphi_1(t)}{\gamma(t)} + x_2 \right], \\ \dot{x}_2 &= -k_2 \phi_2(x_1) + \frac{d}{dt} \left(\frac{\varphi_2(t)}{\gamma(t)} \right). \end{aligned}$$

The total time derivative of the perturbation is assumed to be bounded by a positive constant

$$|\delta_1(t)| \leq \bar{\delta}_1. \tag{3.13}$$

Corollary 1. *Suppose that $\gamma(t)$ and $\varphi(t)$ of system (3.10) satisfy (3.11) and (3.13). Then, the states x_1 and x_2 converge to zero and z converges to $-\frac{\varphi(t)}{\gamma(t)}$, globally and in finite-time, if GSTA gains k_1, k_2 and $\beta \geq 0$ are designed as follows: for any $\epsilon > 0$:*

$$k_1 > \frac{(1+\epsilon)}{4\epsilon k_m}\left(\frac{\alpha}{k_m}(k_M - k_m)\right) + \frac{(1+\epsilon)}{4\epsilon k_m}\sqrt{\Lambda_{k_1}} + \frac{\alpha}{k_m}. \tag{3.14a}$$

$$\Lambda_{k_1} = \left(\frac{\alpha}{k_m}(k_M - k_m)\right)^2 + 16\epsilon(k_M - k_m)\bar{\delta}_1.$$

$$k_2 \in \left[k_M\left(2\sqrt{\epsilon}\bar{c} - \frac{\bar{c}}{2}\sqrt{\Delta_{k_2}}\right)^2 + 2\bar{\delta}_1, k_M\left(2\sqrt{\epsilon}\bar{c} + \frac{\bar{c}}{2}\sqrt{\Delta_{k_2}}\right)^2 + 2\bar{\delta}_1\right], \tag{3.14b}$$

$$\Delta_{k_2} = 16\epsilon - 8\left(\frac{(1+\epsilon)(k_M - k_m)}{\underline{k}_1 k_m}\right)\left(\frac{(1+\epsilon)}{\underline{k}_1 k_m}2\bar{\delta}_1 + \frac{\alpha}{k_m}\right).$$

$$\bar{c} = \frac{\underline{k}_1 k_m}{(1+\epsilon)(k_M - k_m)}, \quad \underline{k}_1 = k_1 - \frac{\alpha}{k_m}.$$

△

Proof is given in the Appendix A.

Example 1: Let be $\varphi(t) = t$ and $\gamma(t) = \frac{1}{t+1} + 1$. The time derivatives are $\dot{\varphi}(t) = 1$ and $\dot{\gamma}(t) = \frac{-1}{(t+1)^2}$ which are bounded by 1, and $k_m = 1$, $k_M = 2$. Using (3.12) and (3.13),

$$\left|\dot{\varphi}(t) + \frac{\varphi(t)}{k_m}\dot{\gamma}(t)\right| \leq 1.3.$$

Following (3.14), we design the GSTA gains $\epsilon = 1$, $k_1 = 3$, $k_2 = 5$ and $\beta = 0$. Fig. 3.1a shows the functions $\varphi(t)$ and $\gamma(t)$. Fig. 3.1b shows the behavior of $\frac{d}{dt}\left(\frac{\varphi(t)}{\gamma(t)}\right)$, and the value of the bound $\bar{\delta}_1$. It can be seen how the perturbation term never exceeds the calculated bound. The Sliding Mode is achieved almost at the beginning of the simulation and remains there for all future time (Fig. 3.1c). Note that the perturbation grows without limit, and the GSTA is able to compensate it globally and for all time.

GSTA compensates uncertainties coming from both, uncertain control coefficient and perturbation, as the ratio $-\frac{\varphi(\cdot)}{\gamma(\cdot)}$. Note that boundedness in (3.8) and (3.13) implies that the product $\frac{d\gamma(\cdot)}{dt}\varphi(\cdot)$ should be bounded. This is an example where the term $\varphi(\cdot)$ can be growing in time while the derivative $\frac{d\gamma(\cdot)}{dt}$ decreases such that bounds (3.13) and (3.8) exist. △

Example 2: $\varphi(t) = \sin(t) + 1 \leq 2$ and $\gamma(t) = 1 + 0.5\cos(t)$. The time derivatives are $\dot{\phi}(t) = \cos(t) \leq 1$, $\dot{\gamma}(t) = -0.5\sin(t) \leq 0.5$, $k_m = 0.5$, $k_M = 1.5$. Using (3.12) and (3.13)

$$\delta_1(t) = \frac{\cos(t)}{1 + 0.5\cos(t)} + \frac{0.5\sin(t)(\sin(t) - 1)}{(1 + 0.5\cos(t))^2}, \quad |\delta_1(t)| \leq 6.$$

In Figure 3.2, it is possible to observe the set of possible selection of gains following (3.14), for example $k_1 = 12$, $k_2 = 23$ and $\beta = 0$. Also the set of possible gains following Levant, 1993 is depicted. It is possible to see that the obtained gain conditions for GSTA in presence of time dependent uncertain control coefficient and perturbations is much less restrictive. △

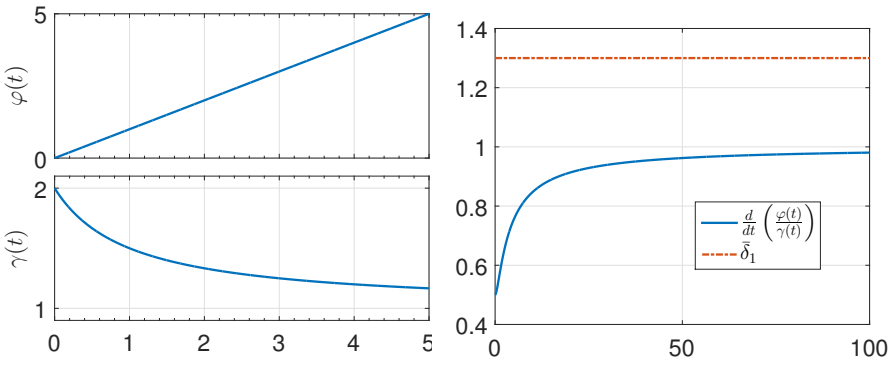

(A) Perturbation and uncertain control coefficient.

(B) $\frac{d}{dt}\left(\frac{\varphi(t)}{\gamma(t)}\right)$ vs $\bar{\delta}_1$.

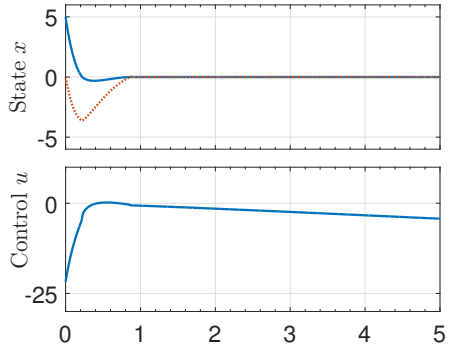

(C) Finite-time convergence to Sliding Mode and control signal.

FIGURE 3.1: Example 1.

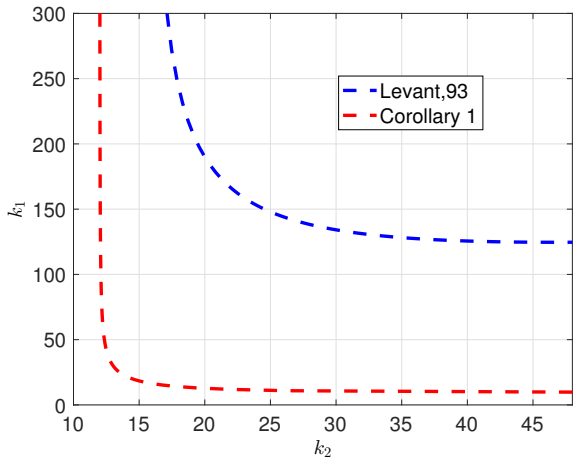

FIGURE 3.2: Example 2: Set of possible gain selection according to Corollary 1 and according to Levant, 1993.

Remark 3. *It is worth noting that system perturbations in Example 1 cannot be covered by conditions found in Levant, 1993. Moreover, in Example 2, the STA gain conditions (3.14) is much less restricctive than those found in Levant, 1993.*

△

3.4 Motivation Example of Chapter 2 (revisited)

Consider again the system (2.1) and the desired speed as $\dot{q}_d = a\sin(\omega t)$. System parameters are $b = 1$, $g = 10$, $a = 2$, $\omega = 2$, $k_m = 0.5$, $k_M = 1$. The closed-loop with the GSTA, and perturbations split in two parts

$$\dot{e}_1 = -k_1\gamma(q)\phi_1(e_1)\underbrace{-\gamma(q)be_1}_{\varphi_1(e_1,t)} + \gamma(q)[\underbrace{z - g\sin(q) - b\left(\dot{q}_d + \arctan\left(e_1 + \dot{q}_d\right)\right) - \frac{\ddot{q}_d}{\gamma(q)}}_{\frac{\varphi_2(e_1,t)}{\gamma(q)}}]. \tag{3.15}$$

Then, the system with dynamic extension $e_2 = z + \frac{\varphi_2(e_1,t)}{\gamma(q)}$, can be rewritten in the form

$$\dot{e}_1 = -\gamma(q)k_1\phi_1(e_1) + \gamma(q)e_2 + \varphi_1(e_1,t) \tag{3.16a}$$

$$\dot{e}_2 = -k_2\phi_2(e_1) + \frac{d}{dt}\left(\frac{\varphi_2(e_1,t)}{\gamma(q)}\right), \tag{3.16b}$$

$$\frac{\varphi(e_1,t)}{\gamma(t)} = -g\sin(q) - b\left(\dot{q}_d + \arctan\left(e_1 + \dot{q}_d\right)\right) - \frac{\ddot{q}_d}{\gamma(q)}. \tag{3.16c}$$

The partial derivatives are

$$\begin{aligned}
\frac{\partial\gamma(q)}{\partial t} &= \frac{2\cos(q)\sin(q)}{(1+\cos^2(q))^2},\\
\frac{\partial\gamma(q)}{\partial e_1} &= 0,\\
\frac{\partial\varphi(e_1,t)}{\partial t} &= -\dot{\gamma}(q)\left(g\sin(q) + b\dot{q}_d + b\arctan(e_1+\dot{q}_d)\right)\\
&\quad -\gamma(q)\left(g\cos(q) + b\ddot{q}_d\left(1 + \frac{1}{(e_1+\dot{q}_d)^2+1}\right)\right) - \dddot{q}_d,\\
\frac{\partial\varphi(e_1,t)}{\partial e_1} &= \frac{-b\gamma(q)}{(e_1+\dot{q}_d)^2+1}.
\end{aligned}$$

Following the proposed analysis, from (2.9), we get that

$$|-b\gamma(q)e_1| < \alpha\beta|e_1| \quad \Rightarrow \beta = 6 > bk_M \text{ and } \alpha = 0.2,$$

and the bounds (3.8) are

$$\begin{aligned}
|\delta_1(x_1,t)| &\leq 2a\omega(1+b+\omega) + g = 42\\
|\delta_2(x_1,t)| &\leq bk_M = 1.
\end{aligned}$$

Then, using (2.16a) and (3.9b) we can select $\epsilon = 1$ and $k_1 = 24 > k_{1min} = 19.18$, and $k_2 = 172 > k_{2min} = 170.59$.

Fig. (3.3a) shows the speed variable converging to the desired reference in finite-time and the continuous control signal. Fig. (3.3b) shows the state dependent perturbation and the uncertain control coefficient.

With the proposed design the problem of the algebraic loop, uncertain control coefficient and state dependent perturbations can be solved.

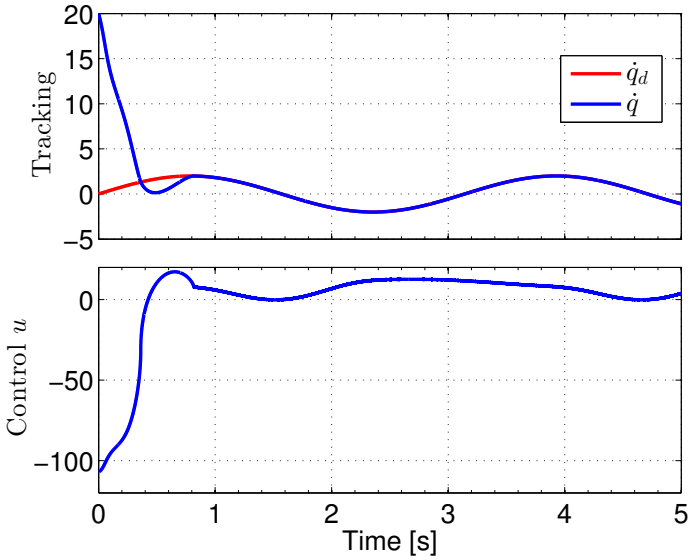

(A) Finite-time convergence of the states [rad/s] and control signal [Nm].

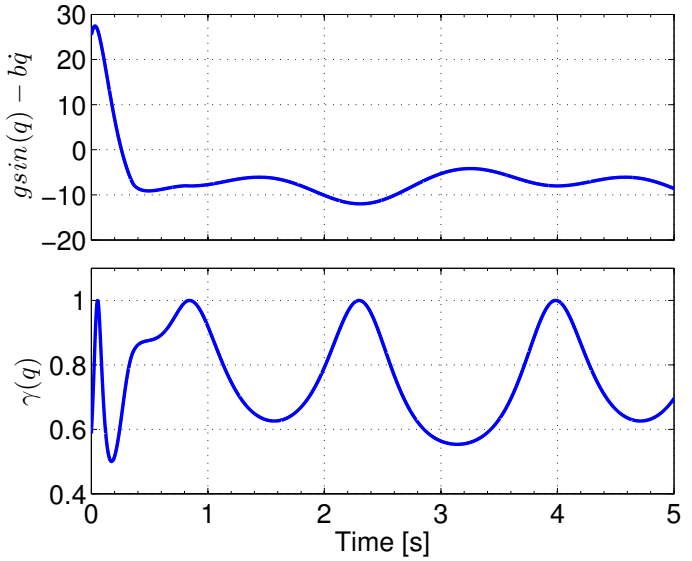

(B) State dependent perturbation and the uncertain control coefficient.

FIGURE 3.3: System trajectories with initial condition $q(0) = 10$, $\dot{q}(0) = 20$. GSTA gains are designed with the proposed method. The state and control converge to zero in finite-time.

Chapter 4

Saturation of STA

4.1 Introduction

Two different structures of Saturated Super-Twisting Algorithm (SSTA) combining Relay Controller (RC) and standard STA are presented. Both structures switch RC and STA through a dynamic switching law based on Lyapunov level curves. The RC enforce the system trajectories to a neighborhood of the origin such that crossing the border of this vicinity, the STA dynamics will ensure finite-time convergence to the origin without saturation.

In order to increment the maximum bound of the supported perturbations, the second algorithm also includes a perturbation estimator setting STA's integrator to the theoretically exact perturbation estimation.

Contribution

Two different versions of Saturated Super-Twisting Algorithms (SSTA) are presented. The first algorithm (Castillo et al., 2016b), the switching condition is designed based on a Positively Invariant Set (PINS) formed by the level curve of the Lyapunov function from Moreno and Osorio, 2008 lying between the saturation curves. The RC will enforce the trajectory of the system to reach this PINS in finite-time where the switching to the STA will take place. STA controller will produce continuous control signal and will be able to drive system trajectory to zero in finite-time fulfilling the saturation condition. Finally this controller will produce just one switch. The main disadvantage of this first scheme is that the maximum supported perturbation bound is less then the half of the saturation level.

In the second algorithm (Castillo et al., 2016a), the performance of the closed loop system is improved with the addition of a perturbation estimator which takes advantage of the intervals of time where the RC controller is active, and resetting the STA's integrator term to the theoretically exact value of the perturbation when it becomes active. This change improves the maximum perturbation bound supported by the SSTA.

Prescribed finite-time convergence gains of the estimator are obtained with the Lyapunov function from Polyakov and Poznyak, 2009 in order to improve the behavior of the transient process. Experimental validations on a mechanical systems are included in Chapter 5 to illustrate the performance of the of the proposed scheme.

Section 4.2 presents the problem statement and the proposed algorithm. In Section 4.3, the algorithm and gain designs are presented with simple examples and section 4.4 the second algorithm with perturbation estimator.

4.2 Problem Statement

For the sake of simplicity, we consider the simplest case of first order perturbed system of the first chapters. Later on, we will show that the following results can be extended for the case of state dependent perturbations and GSTA,

$$\dot{x} = u + \varphi(t), \quad x_0 = x(0), \tag{4.1}$$

where $x \in \mathbb{R}$ is the state and $u \in \mathbb{R}$ the control input. Assume that the perturbation term $\varphi(t)$ is a bounded and globally Lipschitz continuous function, i.e.

$$|\varphi(t)| \leq \varphi_{max}, \quad |\dot{\varphi}(t)| \leq L. \tag{4.2a}$$

Moreover, the control input for the plant is saturated such that

$$\rho \geq |u|. \tag{4.2b}$$

where $\rho \in \mathbb{R}$ is a given constant.

The objective of control is to drive the state trajectories of x to the origin in finite-time with a control signal that is continuous except at a finite number of switching instants.

A necessary condition of the problem to be solvable is

$$\rho > \varphi_{max}. \tag{4.2c}$$

4.3 Saturated Super Twisting Algorithm

In order to guarantee boundedness and continuity of the control signal, the following dynamic switched control law is proposed:

$$u = \begin{cases} u_c & \text{if } s = 0 \\ \\ u_{STA} & \text{if } s = 1; \end{cases} \tag{4.3a}$$

$$\begin{bmatrix} u_c \\ \dot{z} \end{bmatrix} = \begin{bmatrix} -\rho \text{sign}\,(x) \\ 0 \end{bmatrix}, \quad z(0) = 0 \tag{4.3b}$$

$$\begin{bmatrix} u_{STA} \\ \dot{z} \end{bmatrix} = \begin{bmatrix} -k_1 \lceil x \rfloor^{1/2} + z \\ -k_2 \text{sign}\,(x) \end{bmatrix}, \quad z(t_1) = 0. \tag{4.3c}$$

A dynamic switching law (see Fig. 4.1), defines the value of the binary variable s. The variable is set to $s = 0$ for every initial condition $|x_0| > \delta$. If the state satisfies $|x(t)| \leq \delta$, s is set to $s = 1$ and keeps this value for all future time, even if the state becomes $|x(t)| > \delta$. This condition avoids sliding motions along the switching lines $|x(t)| = \delta$.

We will show that the proposed algorithm can enforce the trajectories to zero in finite-time with only one switch (or any) from RC to STA, fulfilling the saturation in the control input.

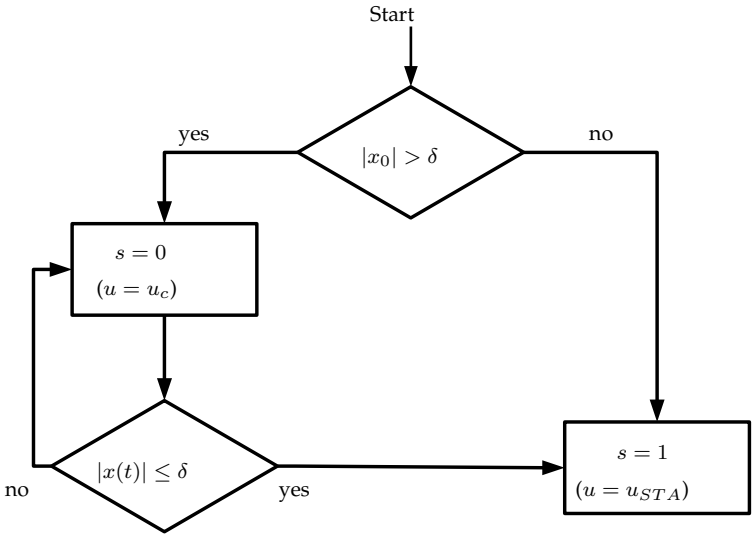

FIGURE 4.1: Principle of the switching law. Only one (or any) transition from RC to STA.

Theorem 3. *Suppose that the perturbation term of system (4.1) satisfies (4.2) with $L > 0$ and $\rho > \varphi_{max} \geq 0$. Then, all the trajectories of system (4.1) in closed-loop with (4.3) will converge to the origin in finite-time if gains satisfy*

$$k_1 > \quad 0, \quad k_2 > \quad 3L + \tfrac{2L^2}{k_1^2}, \tag{4.4}$$

and the switching occurs if $|x(t)| \leq \delta$ is reached where

$$0 \leq \delta \leq \frac{2\rho^2\gamma_2}{(k_1^2 + 4k_2)}, \quad \gamma_2 = \frac{k_1^2 + 8k_2}{2k_1^2 + 8k_2}, \tag{4.5}$$

fulfilling (4.2b) with a continuous control signal and at most only one switch. The maximum perturbation bound is

$$\varphi_{max} < \kappa\rho; \quad \kappa = \frac{2\gamma_2\rho + \sqrt{\delta}k_1 - 2\sqrt{\gamma_3}}{2(\gamma_2 - 1)}, \tag{4.6}$$

where $\gamma_3 = \gamma_2\rho^2 + \delta\left(\left(\frac{k_1^2}{2} + 2k_2\right)(\gamma_2 - 1) + \frac{k_1^2}{4}\right) + \sqrt{\delta}\gamma_2 k_1\rho$. ▲

The proof is given in the *Appendix*.

4.3.1 Principle of operation

Nominal case: STA is a state feedback control law $u = u_{STA}(x, z)$ with integral action that introduces a dynamical extension in the closed-loop system

$$\Sigma_s : \begin{cases} \dot{x} = -k_1\lceil x \rfloor^{1/2} + z \\ \dot{z} = -k_2 \text{sign}\,(x)\,, \end{cases}$$

making dynamics of order two. The saturation of the control signal $|u_{STA}(x, z)| \leq \rho$ can be interpreted as the curves $z = \pm\rho + k_1\lceil x_1 \rfloor^{\frac{1}{2}}$ in the phase plane (x, z) (see black dashed lines in Fig. 4.2).

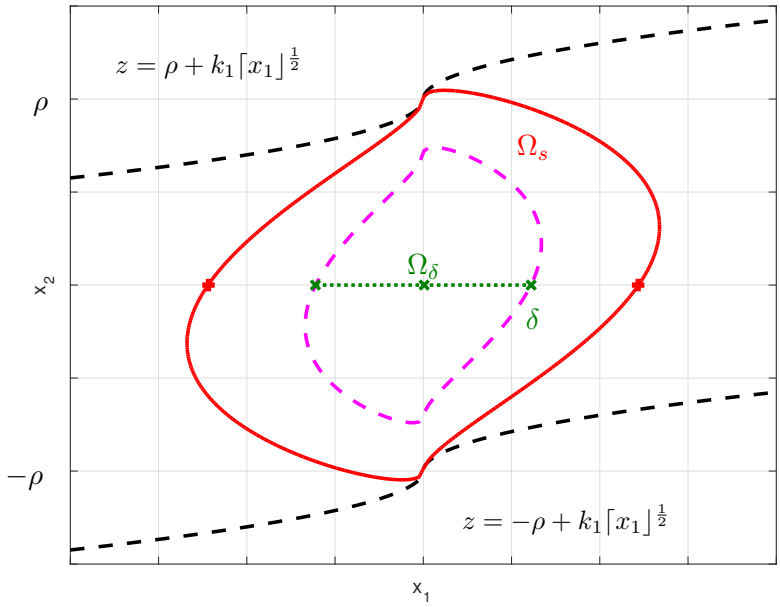

FIGURE 4.2: Nominal case phase plane: saturation planes (dashed), PINS Ω_s with respect to STA (solid), PINS Ω_δ with respect to RC (dotted) which is a subset of Ω_s.

Based on Lyapunov function in Moreno, 2009

$$V_s(x,z) = \xi^T P \xi, \quad P = \begin{bmatrix} p_{11} & -p_{12} \\ -p_{12} & p_{22} \end{bmatrix} > 0, \tag{4.7}$$

with P being a constant, symmetric and positive definite matrix and the vector $\xi^T = [\xi_1 \quad \xi_2] = \left[|x_1|^{1/2}\text{sign}\,(x_1) \quad z\right]$; we find the maximum sublevel set $\Omega_s = \{(x,z) \in \mathbb{R}^2 \mid V_s(x,z) \leq c_s\}$ as a Positively Invariant Set (PINS) such that it is between the saturation curves. Thus, every trajectory of the system starting inside Ω_s fulfills (4.2b) (see Fig. 4.2).

Remark 4. *The structure of Lyapunov function 4.7 used to obtain PINS, is exactly the same as the one used for the stability analysis in Chapters 2 and 3, see Appendix A. Therefore, GSTA can be applied, and the saturation mechanism will be exactly the same.*

△

A second PINS Ω_δ with respect to the closed-loop system

$$\Sigma_c : \begin{cases} \dot{x} = -\rho\text{sign}\,(x) \\ \dot{z} = 0, \end{cases}$$

where $x(0) = x_0, z(0) = 0$, is found as a sublevel set $\Omega_\delta = \{x \in \mathbb{R} \mid V_c(x) \leq c_1\delta\}$, where

$$V_c(x) = c_1|x|, \; c_1 > 0. \tag{4.8}$$

If Ω_δ is a subset of Ω_s, then trajectories driven by RC will converge to Ω_δ in finite-time, and also will reach Ω_s in finite-time. Any starting STA trajectory inside Ω_δ will be also inside Ω_s and then, the STA trajectories will converge to zero fulfilling (4.2b).

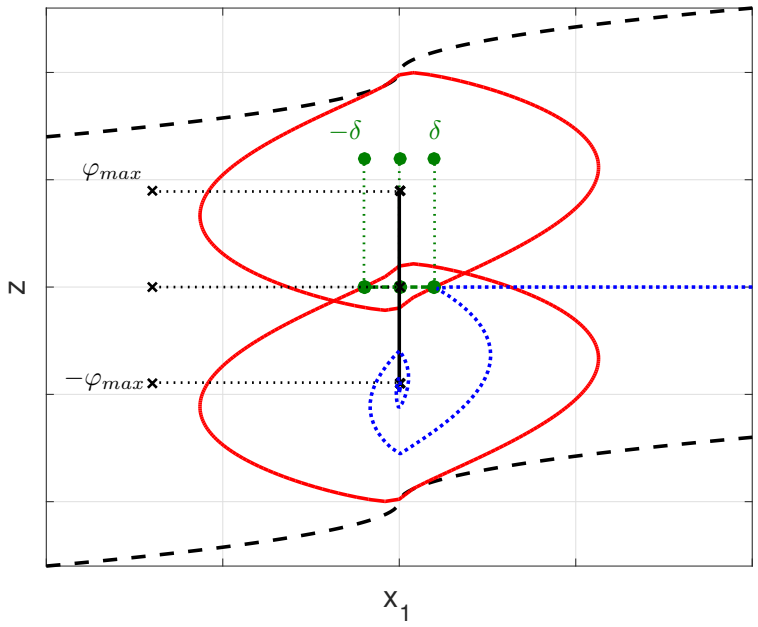

FIGURE 4.3: Phase Plane with perturbation $|\varphi(t)| \leq \varphi_{max}$. Switch of control law in a neighborhood of the origin $|x(t)| \leq \delta$ and a system trajectory (dotted).

Perturbed case: The closed-loop system can be represented by

$$\Sigma_2 : \begin{cases} \dot{x}_1 = -k_1 \lceil x_1 \rfloor^{1/2} + x_2 \\ \dot{x}_2 = -k_2 \text{sign}\,(x_1) + \dot{\varphi}(t) \end{cases} \tag{4.9}$$

where $x_1 = x$, $x_2 = z + \varphi(t)$. The order of the system dynamics is again increased by one.

Lyapunov functions from Moreno and Osorio, 2012, Polyakov and Poznyak, 2009 ensure finite-time convergence of the trajectories to a second order sliding mode $x_1 = x_2 = 0$. Convergence of x_2 to zero in finite-time implies that z converges to $-\varphi(t)$. Then, in the phase plane (x_1, z), the perturbation $\varphi(t)$ acts as displacements of the equilibrium point along the z axis, see Fig. 4.3.

PINS Ω_s should be reduced in its size, adjusting the parameter δ as in (4.5), in order to maintain condition (4.2b). The smaller selected δ, the greater allowed maximum bound φ_{max}.

Note that the maximum allowed value for the bound of the perturbation is less than $\frac{1}{2}\rho$. This is a restrictive drawback of the proposed algorithm as it was expected to have the whole range of control signal to overcome perturbations.

Remark 5. *Note in Fig. 4.3 that the dynamic switching law allows the trajectories of the STA to behave freely inside the PINS Ω_s, even leaving the set $|x(t)| \leq \delta$ without generating high frequency switching along the lines $|x| = \delta$.*

△

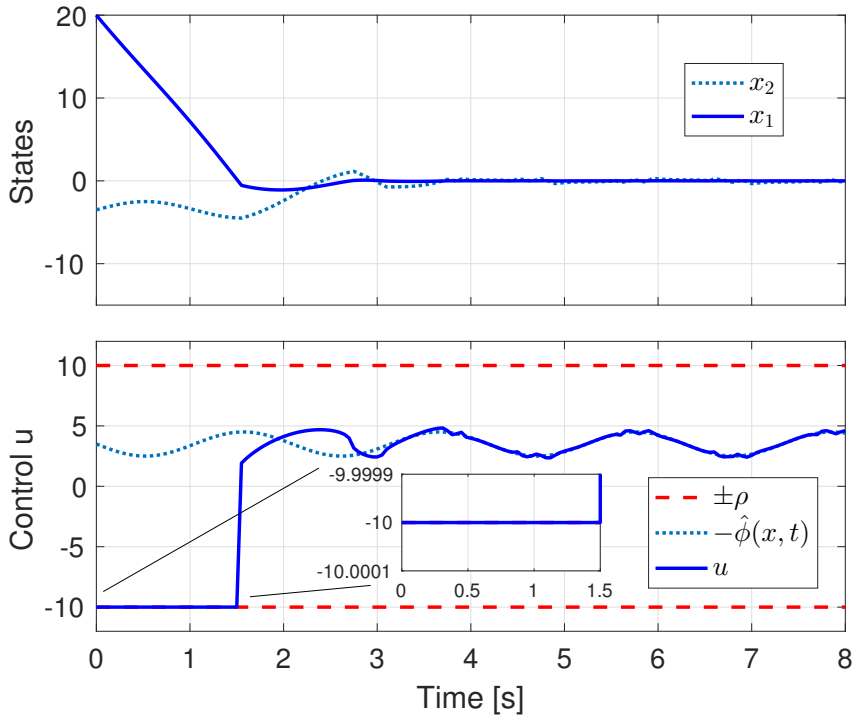

FIGURE 4.4: Finite-time convergence to zero of the states at the maximum rate with saturated control signal $|u| \leq \rho = 10$. Sampling step of $\tau = 0.05s$.

4.3.2 Example 1

Consider system (4.9) with the following perturbation and initial condition:

$$\varphi_{21}(t) = \ sin(3t) - 3.5, \quad x_0 = \ 20.$$

The control input is saturated to $|u| \leq \rho = 10$. The gains were selected as in (4.4) with respect to $\varphi_1(t)$, as $k_1 = 6$ and $k_2 = 10$. Choosing $\delta = 0$, the maximum allowed perturbation in (4.6) is $\varphi_{max} = 4.66$. Note that the perturbation $\varphi_1(t)$ fulfills (4.6).

Fig. 4.5 shows how the system trajectories converge to zero in finite-time. From the initial time $t_0 = 0$ to $t_1 \approx 1.5$ the saturation of the control signal drives the state towards zero with the maximum possible rate. Then, a discontinuity in the control signal produced by the switching law occurs. A Super-Twisting Algorithm reaching phase from second 1.5 to 3.5 takes place. The trajectories converge to zero in finite-time compensating the perturbation.

The original STA Levant, 1993, Theorem 5, p.1257 defined by

$$\begin{aligned} u = & \ u_1 + u_2, \\ \dot{u}_1 = & \begin{cases} -u. & |u| > \rho \\ -\alpha \text{sign}\,(\sigma)\,, & |u| \leq \rho \end{cases} \\ u_2 = & \begin{cases} -\lambda |\sigma_0|^p \text{sign}\,(\sigma) & |\sigma| > \sigma_0 \\ -\lambda |\sigma|^p \text{sign}\,(\sigma) & |\sigma| \leq \sigma_0 \end{cases} \end{aligned}$$

was also simulated with the same gains $\lambda = k_1$, $\alpha = k_2$, and parameters $\rho = 10$, $\sigma_0 = 5$ and $p = \frac{1}{2}$. Results are shown in Fig. 4.5. Note that the saturation level is generated by high frequency switching in the control law producing sliding-modes

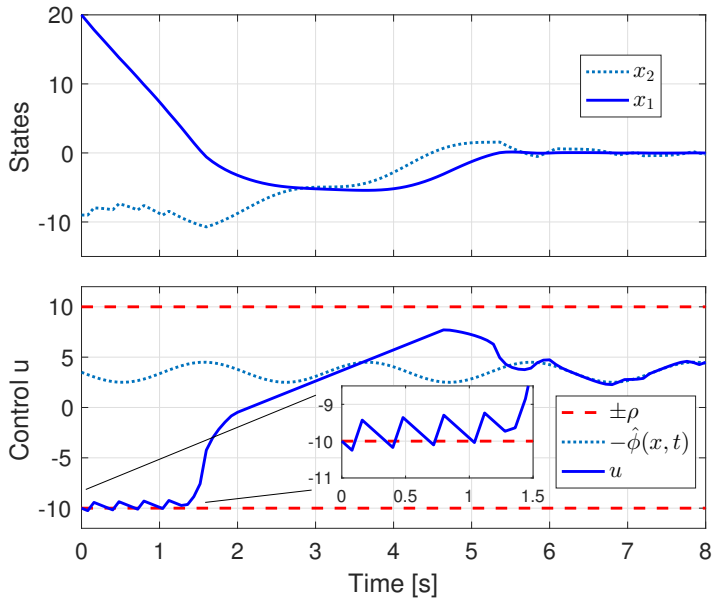

FIGURE 4.5: Levant's original STA. Sampling step of $\tau = 0.05s$.

that can cause undesired stress in the actuator. Note also that the convergence is slightly slower.

4.4 Saturated Super-Twisting with a Perturbation Estimator

In order to overcome restriction (4.6), an estimator of the perturbation based on STA (Davila, Fridman, and Poznyak, 2006) is included into the algorithm stated above. The estimator is defined by

$$\begin{aligned} \dot{\hat{x}}_1 = &\quad \beta_1 \lceil e_1 \rfloor^{1/2} - \hat{x}_2 + u \\ \dot{\hat{x}}_2 = &\quad -\beta_2 \text{sign}\,(e_1)\,, \\ e_1 = &\quad x - \hat{x}_1, \quad e_2 = \hat{x}_2 + \varphi(t), \end{aligned} \tag{4.10}$$

where $\hat{x}_1$ is an estimate of x_1 and $\hat{x}_2$ an estimate of $-\varphi(t)$. In this new scheme, the dynamic switching law is also able to reset the variable to $s = 0$ only if the value of the precalculated STA control signal exceeds $|u_{STA}| > \rho$, see Fig. 4.6. When the control law switches from RC to STA dynamics at time t_i, $i = 0, 1, 2, ...$, $t_0 = 0$, the STA's integrator is reset to the estimation

$$\begin{aligned} z(t_i) = &\quad \hat{x}_{2s}(t_i), \\ \hat{x}_{2s} = &\quad \begin{cases} \rho + k_1 \lceil x \rfloor^{1/2} & \text{if } \hat{x}_2 > \rho + k_1 \lceil x \rfloor^{1/2}, \\ -\rho + k_1 \lceil x \rfloor^{1/2} & \text{if } \hat{x}_2 < -\rho + k_1 \lceil x \rfloor^{1/2}, \\ \hat{x}_2 & \text{otherwise.} \end{cases} \end{aligned} \tag{4.11}$$

With the appropriate selection of $\{k_1, k_2, \beta_1, \beta_2\}$ based on (4.2a), the state x converges to zero in finite-time and z and $\hat{x}_2$ converge to $-\varphi(t)$ in finite-time.

Theorem 4. *Suppose that the perturbation term of system* (4.1) *satisfies* (4.2) *with* $L > 0$ *and* $\rho > \varphi_{max} \geq 0$. *Then, all the trajectories of system* (4.1) *in closed-loop with* (4.3), (4.10)

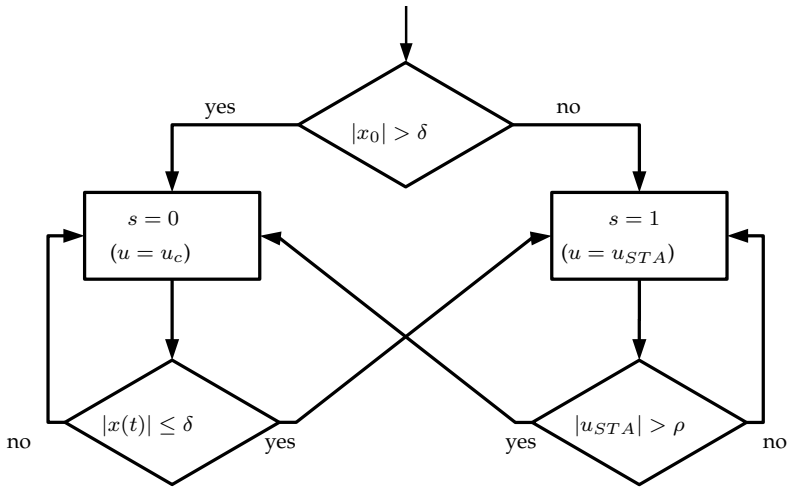

FIGURE 4.6: Principle of the extended switching law.

and (4.11) *will converge to the origin in finite-time if the gains satisfy*

$$k_1 > \quad 0, \quad k_2 > \quad 3L + \tfrac{2L^2}{k_1^2}, \tag{4.12a}$$

$$\beta_1 > \quad 0, \quad \beta_2 > \quad 3L + \tfrac{2L^2}{\beta_1^2}, \tag{4.12b}$$

and the switching from RC to STA occurs if $|x(t)| \leq \delta$ *where*

$$0 \leq \delta \leq \frac{2\rho^2\gamma_2}{(k_1^2 + 4k_2)}, \quad \gamma_2 = \frac{k_1^2 + 8k_2}{2k_1^2 + 8k_2}, \tag{4.13}$$

fulfilling (4.2b) *with a continuous control and a finite number of switches. The maximum allowed perturbation bound is*

$$\varphi_{max} < \rho. \tag{4.14}$$

▲

The proof is given in the *Appendix*.

With the new switching law and estimator, RC and STA dynamics can alternate a finite number of times depending on the instant values of the perturbations. This new scheme is able to compensate perturbations whose maximum bound is $\varphi_{max} < \rho$.

4.4.1 Example 2

Consider system (4.1) with perturbation $\varphi_{22}(t) = \frac{1}{2}sin(\sqrt{5}t) - 8$, and a saturated control input $|u| \leq \rho = 10$. Then, for $\varphi_{max} = 8.5$ and $L = 1.12$ is possible to design $k_1 = \beta_1 = 1$, $k_2 = \beta_2 = 5.9$ and $\delta = 5$. In Fig. 4.7, it can be observed how the state $x_1 = x$ and the virtual state $x_2 = z + \varphi_2$ converge to zero in finite time starting from the initial condition $x_1(0) = 20$. During the first second, the system trajectory is driven to a region around the origin $|x(t)| \leq \delta$ by a saturated control input $u = -10$. Then, the STA is activated at time $t_1 \approx 0.8s$ and a reaching phase (transient process) occurs. The continuous control signal reaches $|u_{STA}| \geq \rho$ in time instant $t \approx 2.8s$, and the saturation ($u = u_c$) is activated and so on. Note that during the change of STA's behavior at times $t_1 \approx 0.8s$, $t_2 \approx 3s$, and $t_3 \approx 4.8s$, the estimator still has wrong estimation values. Nevertheless, the integrator initialization helps

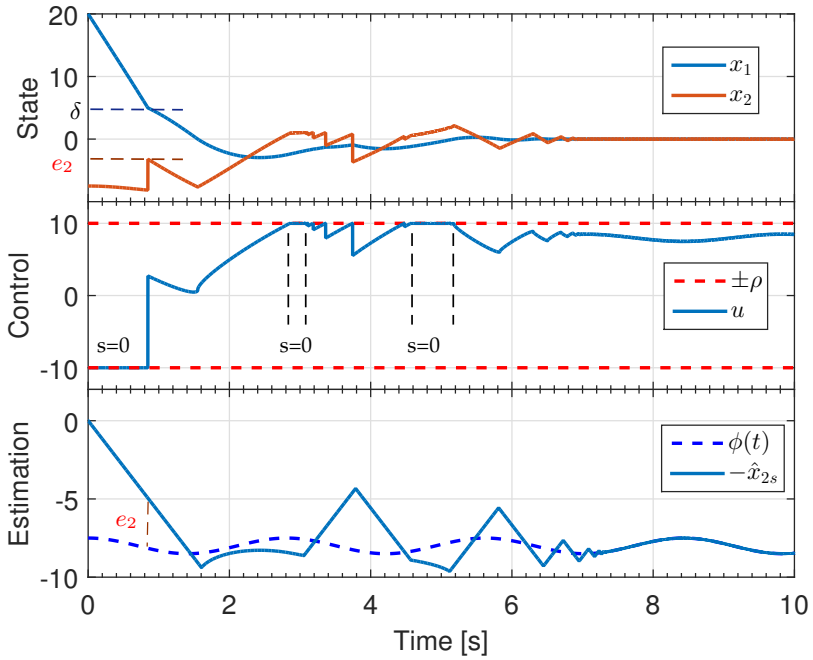

FIGURE 4.7: The selection of gains as in (4.12a) and (4.12b), ensures convergence to zero in finite-time of the state and the estimator. Multiple control switches can occur before the state reaches zero.

the trajectories to converge faster and, at the end of the simulation, this allows to compensate perturbations whose bounds φ_{max} are near to the saturation level ρ.

4.5 Prescribed finite-time convergence gains

An interesting SSTA's behavior occurs when the parameter δ is selected as $\delta = 0$, and the estimation error converges to zero *before* the state reaches $x = 0$. It provides the maximum rate of convergence of the state to zero, and theoretically exactly compensates the perturbation in sliding mode $x = \dot{x} = 0$ with a continuous control signal and with just one switch from RC to STA.

We will show that it is possible to design the gains of the estimator such that the exact value of the perturbation is estimated before the reaching time of the state for every initial condition $x_0 \neq 0$.

Proposition 1. *Suppose that* (4.2a) *and* (4.2b) *are fulfilled. Then, for every initial condition* $x_0 \neq 0$, *the gains of the STA estimator*

$$\beta_1 \geq \max\{2.5\sqrt{\tilde{L}}, 6\sqrt{L}\} \tag{4.15a}$$

$$\beta_2 \geq \max\{1.6\tilde{L} - 2L, 7L\} \tag{4.15b}$$

where

$$\tilde{L} = \frac{\left(\varphi_{max}^2 + \rho\varphi_{max}\right)}{|x_0|}; \tag{4.16}$$

ensure the finite-time convergence of the estimator states to the sliding mode $e_1 = e_2 = 0$ *in a time smaller than*

$$t_1 < T_{cmin} = \frac{|x_0|}{\rho + \varphi_{max}}. \tag{4.17}$$

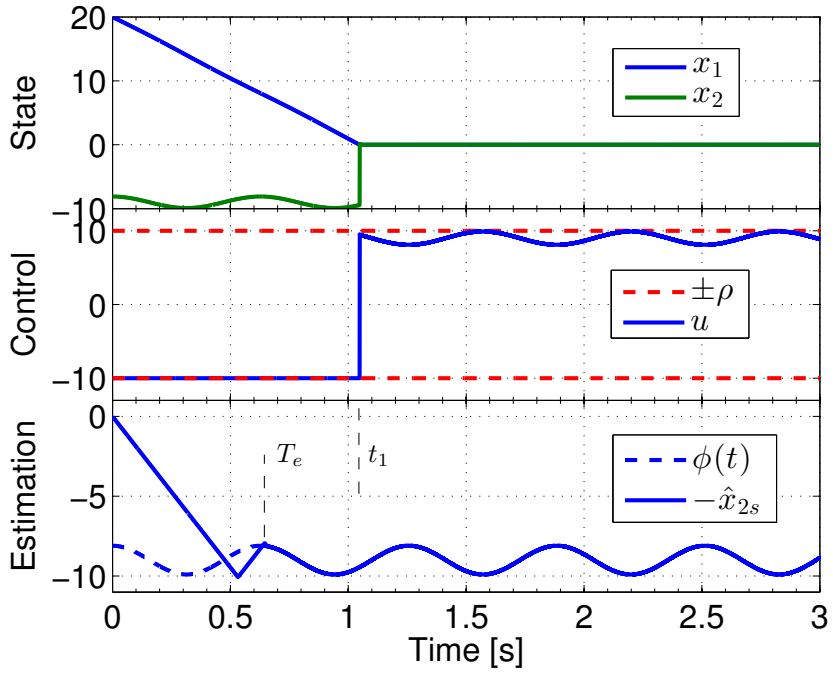

FIGURE 4.8: The selection of the estimator's gains as in (4.15), ensures convergence of the estimator in a finite time T_e smaller than the reaching time of the state t_1.

▲

4.5.1 Example 3

Consider system (4.1) with the perturbation term $\varphi_{23}(t) = 0.9\cos(10t) - 9$, and a saturated control input $|u| \leq \rho = 10$. The controller gains are chosen as $k_1 = 4$, $k_2 = 37.12505$, and $\delta = 0$. Using (4.15) and (4.16), we get $\beta_1 = 19$, and $\beta_2 = 63.5$. The estimation of the state reaching time is $T_{cmin} = \frac{|20|}{10+9.9} = 1.0050s$.

The estimation error in Fig. 4.8 converges to zero before second 1 ($T_e \approx 0.6s$) and then, the state converges to zero. When the state reaches $|x| = \delta = 0$, the STA's integrator is initialized with the exact value of the perturbation $z(t_1) = \hat{x}_{2s}(t_1) = -0.9\cos(10t_1) + 9$. Then, the trajectories are maintained in sliding mode $x = \dot{x} = 0$ for all future time with an *equivalent control* $u = -\hat{\varphi}_{32}(t) = -0.9\cos(10t) + 9$. It is possible to see that two properties are achieved:

- Perturbation is near to the control limit with maximum of $\varphi_{max} = 9.9$.
- The estimation error converges to zero at time $T_e \approx 0.6s$, i.e. faster than the state.

Chapter 5

Experimental Setups

5.1 Velocity Tracking of a Mechanical System

Consider the problem of velocity tracking in mechanical system

$$J_m\ddot{q} + F(q,\dot{q}) = \tau + \omega(t),$$

where $q \in \mathbb{R}$ and $\dot{q} \in \mathscr{Q} \subset \mathbb{R}$ are the state variables and $u \in \mathbb{R}$ the torque control input which is limited to $|\tau| \leq \rho = 0.7Nm$. The terms of the differential equation represent the inertia moment with $J_m = 0.0286K_gm^2$, a bounded function F representing locally Lipschitz unknown dynamics of the system, the saturated torque control input τ, and possibly external Lipschitz disturbances $\omega(t)$.

It is desired to realize exact velocity tracking to a desired trajectory $\dot{q}_d$. By defining the error variable $e_1 = \dot{q} - \dot{q}_d$, the velocity error dynamics are

$$\dot{e}_1 = \bar{\gamma}\left(\tau + \underbrace{\omega(t) - F(q,\dot{q})}_{\varphi(t)}\right) - \ddot{q}_d, \tag{5.1}$$

where $\bar{\gamma} = 1/J_m$, and $\varphi(t) = \omega(t) - F(q,\dot{q})$, a bounded locally Lipschitz perturbation with bounded derivative $|\dot{\varphi}(t)| \leq L$, to be determined experimentally. The perturbation is assumed to be bounded by a constant $|\varphi(t)| \leq \phi_{max} < \rho = 0.7Nm$. Applying the control law $\tau = \frac{\ddot{q}_d}{\bar{\gamma}} + u$, where $u \in \mathbb{R}$ is a new control input, the system becomes

$$\dot{e}_1 = \bar{\gamma}\left(u + \phi(t)\right).$$

Here, we can apply the SSTA as in (4.3). The perturbation estimator is implemented with a slightly difference in the coefficient of control $\bar{\gamma}$

$$\begin{array}{rl} \dot{\hat{x}}_1 = & \beta_1 \lceil e_1 \rfloor^{1/2} - \hat{x}_2 + \bar{\gamma}u \\ \dot{\hat{x}}_2 = & -\beta_2 \text{sign}\left(e_1\right), \quad e_1 = x - \hat{x}_1, \end{array} \tag{5.2}$$

$z(t_i) = \hat{x}_{2s}(t_i)$, and

$$\hat{x}_{2s} = \begin{cases} \rho + \alpha_1 \lceil x \rfloor^{1/2} & \text{if } \frac{\hat{x}_2}{\bar{\gamma}} > \rho + \alpha_1 \lceil x \rfloor^{1/2}, \\ -\rho + \alpha_1 \lceil x \rfloor^{1/2} & \text{if } \frac{\hat{x}_2}{\bar{\gamma}} < -\rho + \alpha_1 \lceil x \rfloor^{1/2}, \\ \frac{\hat{x}_2}{\bar{\gamma}} & \text{otherwise.} \end{cases} \tag{5.3}$$

The SSTA was implemented in the ECP Torsional Model 205. It is an experimental system which consists in three inertial subsystems interconnected through two springs, (see Fig. 5.1). Its design allows the reconfiguration of inertias, springs

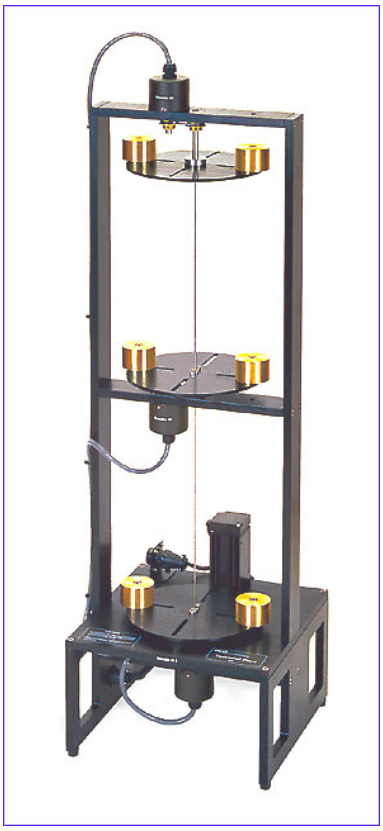

FIGURE 5.1: ECP Model 205: Torsional Plant.

and the interconnection between subsystems. In this experiment only one inertia subsystem will be considered.

Figure 5.2 shows the velocity tracking to a desired polynomial trajectory $\dot{q}_d$ including three steps at second 30, 35, and 45. A STA with a saturation function at its output without any wind-up technique and the SSTA were applied to the plant with the same gains $k_1 = 0.12$, $k_2 = 0.45$ and $\beta = 0$, experimentally adjusted. It is possible to see the overshoots that the integral wind-up produces to the trajectory tracking when STA+sat(u) is used. The SSTA with perturbation estimator is able to reach the desired step levels without overshoots. Control signals of both experiments are depicted in Fig. 5.3. STA+sat(u) integrates the tracking error during all saturation intervals, accumulating an integral control action that produces the overshoots in the state. SSTA jumps from STA to FOSMC behavior when needed and jumps back to STA with the exact amount of integral control action to exactly compensate the dynamics and perturbations of the system avoiding the overshoot. The estimation error and the perturbation estimation is depicted in Fig. 5.4. Video of the experiment can be found at https://goo.gl/O009Qy.

5.2 Controlled Swing-up for a Reaction Wheel Pendulum

5.2.1 Reaction Wheel Pendulum model

A Reaction Wheel Pendulum (RWP) is a weight or bar suspended from a pivot so that it can swing freely with an inertia wheel attached. The disk is actuated by DC-motor and the coupling torque generated by the angular acceleration of the disk can be used to actively control the system. (Fig. 5.5).

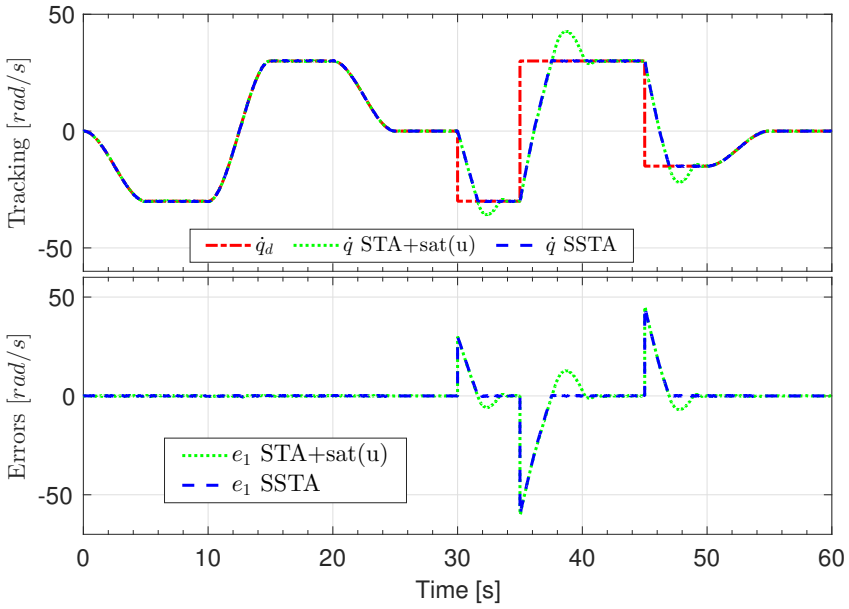

FIGURE 5.2: Desired trajectory $\dot{q}_d$, state $\dot{q}$ when a STA with a saturation block is applied to the plant and $\dot{q}$ when SSTA, for comparison.

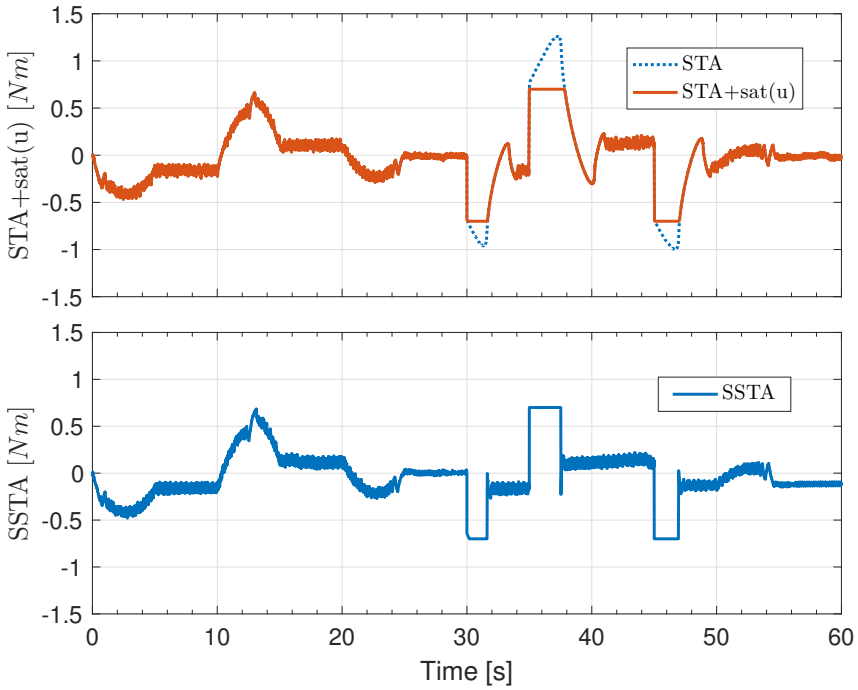

FIGURE 5.3

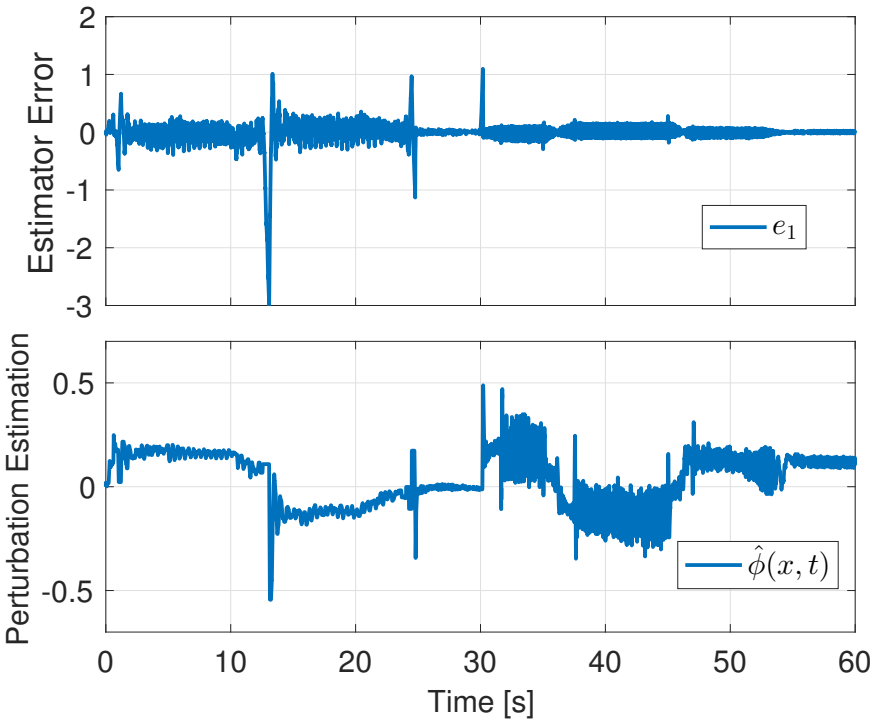

FIGURE 5.4: Estimation error $[rad/s]$ and perturbation estimation $[Nm]$

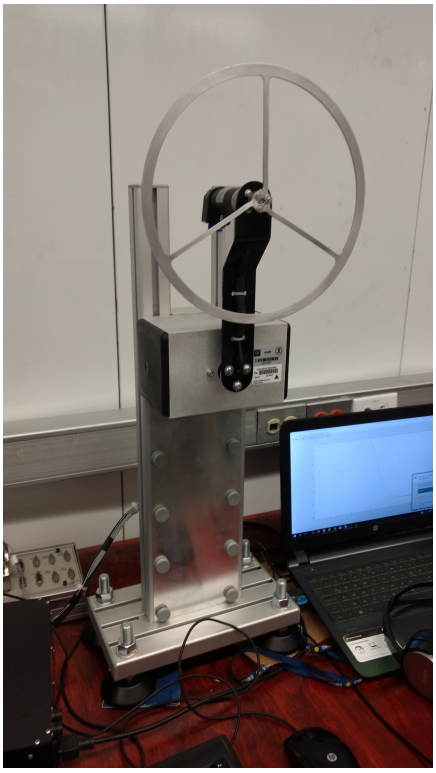

FIGURE 5.5: Reaction Wheel Pendulum in Sliding Mode Control Laboratory.

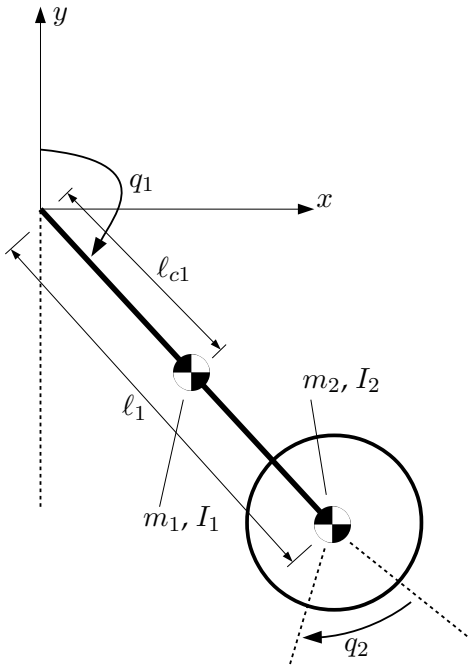

FIGURE 5.6: Frame coordinates and parameters of Reaction Wheel Pendulum.

RWP can be modeled as a two degree of freedom robot

$$\begin{aligned} d_{11}\ddot{q}_1 + d_{12}\ddot{q}_2 + b_1\dot{q}_1 + \eta(q_1) &= 0, \\ d_{21}\ddot{q}_1 + d_{22}\ddot{q}_2 + b_2\dot{q}_2 &= \tau + \varphi(t), \end{aligned} \tag{5.4}$$

where q_1 is the pendulum angle, q_2 is the disk angle, τ is the motor torque input, $\omega(t)$ possible external Lipschitz perturbations and

$$\begin{aligned} d_{11} &= m_1\ell_{c1}^2 + m_2\ell_1^2 + I_1 + I_2 \\ d_{12} &= d_{21} = d_{22} = I_2, \\ \eta(q_1) &= -\bar{m}g\sin(q_1), \\ \bar{m} &= m_1\ell_{c1} + m_2\ell_1 \end{aligned} \tag{5.5}$$

with the parameters shown in Fig. 5.6

5.2.2 Control Design

The objective of control is a tracking trajectory of the pendulum position in order to make a swing-up and stabilize the instable equilibrium point. As the disc angular position is a cyclic variable it will not be taken into account into the model. Then, the reduced model state vector is defined $x^T = [x_1 \quad x_2 \quad x_3] = [q_1 \quad \dot{q}_1 \quad \dot{q}_2]$ and finally, the state space model is given by

$$\begin{aligned} \dot{x}_1 &= x_2, \\ \dot{x}_2 &= -\tfrac{d_{22}}{D}\eta(x_1) - \tfrac{d_{22}b_1}{D}x_2 + \tfrac{d_{12}b_2}{D}x_3 - \tfrac{d_{12}}{D}(\tau + \varphi(t)) \\ \dot{x}_3 &= \tfrac{d_{21}}{D}\eta(x_1) + \tfrac{d_{21}b_1}{D}x_2 - \tfrac{d_{11}b_2}{D}x_3 + \tfrac{d_{11}}{D}(\tau + \varphi(t)) \end{aligned} \tag{5.6}$$

where $D = d_{11}d_{22} - d_{12}d_{21} > 0$.

The tracking errors are defined as $e_1 = x_1 - x_d$, $e_2 = x_2 - \dot{x}_d$ and $e_3 = x_3$, thus the error dynamics are

$$\begin{array}{rl} \dot{e}_1 = & e_2 \\ \dot{e}_2 = & -\frac{d_{22}}{D}\eta(e_1 + x_d) - \frac{d_{22}b_1}{D}(e_2 + \dot{x}_d) + \frac{d_{12}b_2}{D}e_3 - \frac{d_{12}}{D}(\tau + \varphi(t)) - \ddot{x}_d \\ \dot{e}_3 = & \frac{d_{21}}{D}\eta(e_1 + x_d) + \frac{d_{21}b_1}{D}(e_2 + \dot{x}_d) - \frac{d_{11}b_2}{D}e_3 + \frac{d_{11}}{D}(\tau + \varphi(t)) \end{array} \tag{5.7}$$

This can be written as

$$\dot{e} = f(e,t) + g(\tau + \varphi(t)) \tag{5.8}$$

where the error vector is $e^T = [e_1 \;\; e_2 \;\; e_3]$, and

$$\begin{array}{rcl} f(e,t) & = & \begin{bmatrix} x_2 \\ -\frac{d_{22}}{D}\eta(e_1 + x_d) - \frac{d_{22}b_1}{D}(e_2 + \dot{x}_d) + \frac{d_{12}b_2}{D}e_3 - \ddot{x}_d \\ \frac{d_{21}}{D}\eta(e_1 + x_d) + \frac{d_{21}b_1}{D}(e_2 + \dot{x}_d) - \frac{d_{11}b_2}{D}e_3 \end{bmatrix}, \\ g & = & \begin{bmatrix} 0 \\ -\frac{d_{12}}{D} \\ \frac{d_{11}}{D} \end{bmatrix}. \end{array} \tag{5.9}$$

Feedback linearization

In order to take the system into the normal form of Isidori, 1995, a feedback linearization approach was used. It was proved that there exists an output $y = h(e)$, such that it has relative degree equals to the order of the system n. Defining the output as follows

$$y = h(e) = b_1 e_1 + d_{11} e_2 + d_{12} e_3. \tag{5.10}$$

The first derivative of the function output y satisfies the condition

$$\dot{y} = L_f h + L_g h(\tau + \varphi(t)), \tag{5.11}$$

in which $L_f h$ is the Lie derivative of h with respect to f and $L_g h$ the one respect to f and g. The Lie derivative with respect of h to f of the system is

$$\begin{array}{rl} L_f h = & \begin{bmatrix} b_1, & d_{11} & d_{12} \end{bmatrix} \begin{bmatrix} e_2 \\ -\frac{d_{22}}{D}\eta(e_1 + x_d) - \frac{d_{22}b_1}{D}(e_2 + \dot{x}_d) + \frac{d_{12}b_2}{D}e_3 - \ddot{x}_d \\ \frac{d_{21}}{D}\eta(e_1 + x_d) + \frac{d_{21}b_1}{D}(e_2 + \dot{x}_d) - \frac{d_{11}b_2}{D}e_3 \end{bmatrix} \\ = & -\eta(e_1 + x_d) - b_1\dot{x}_d - d_{11}\ddot{x}_d, \end{array} \tag{5.12}$$

and the Lie derivative with respect to f and g is

$$L_g h = \begin{bmatrix} b_1, & d_{11}, & d_{12} \end{bmatrix} \begin{bmatrix} 0 \\ -\frac{d_{12}}{D} \\ \frac{d_{11}}{D} \end{bmatrix} = 0 \tag{5.13}$$

Following the procedure, the higher Lie derivatives were computed as follows

$$\begin{array}{c} \ddot{y} = L_f^2 h + L_g L_f h \tau = L_f^2 h, \;\; L_g L_f h = 0, \\ y^{(3)} = L_f^3 h + L_g L_f^2 h \tau = L_f^3 h, \;\; L_g L_f^2 h \neq 0, \end{array} \tag{5.14}$$

where

$$\begin{aligned} L_f^2 h = & -\dot{\eta}(e_1 + x_d)e_2 - b_1\ddot{x}_d - d_{11}x_d^{(3)}, \\ L_f^3 h = & -\ddot{\eta}(e_1 + x_d)e_2^2 + \dot{\eta}(e_1 + x_d)\left[\frac{d_{21}}{D}\eta(e_1 + x_d) + \frac{d_{21}b_1}{D}(e_2 + \dot{x}_d) - \frac{d_{11}b_2}{D}e_3\right] \\ & -b_1 x_d^{(3)} - d_{11}x_d^{(4)} \\ L_g L_f^2 h = & \frac{d_{12}}{D}\dot{\eta}(e_1 + x_d). \end{aligned} \tag{5.15}$$

It is possible to see that the relative degree of the system is $n = 3$, with respect to the output mentioned in equation (5.10).

Defining new state variables as

$$\begin{aligned} z_1 = & \quad h(e) = b_1 e_1 + d_{11}e_2 + d_{12}e_3, \\ z_2 = & \quad L_f h(e) = -\eta(e_1 + x_d) - b_1\dot{x}_d - d_{11}\ddot{x}_d \\ z_3 = & \quad L_f^2 h(e) = -\dot{\eta}(e_1 + x_d)e_2 - b_1\ddot{x}_d - d_{11}x_d^{(3)} \end{aligned} \tag{5.16}$$

This is a local diffeomorphism. The system now is presented in term of the new state variable as follows

$$\dot{z_1} = z_2, \tag{5.17}$$
$$\dot{z_2} = z_3, \tag{5.18}$$
$$\dot{z_3} = L_f^3 h + L_g L_f^2 h(\tau + \varphi(t)). \tag{5.19}$$

Defining the transformation for the feedback linearization

$$\begin{aligned} \tau = & \frac{1}{L_g L_f^2 h}\left(u - L_f^3 h\right) \\ = & \frac{D}{d_{12}\dot{\eta}(e_1 + x_d)}\left\{u + \ddot{\eta}(e_1 + x_d)e_2^2 + b_1 x_d^{(3)} + d_{11}x_d^{(4)} + \right. \\ & \left. \dot{\eta}(e_1 + x_d)\left[-\frac{d_{22}}{D}\eta(e_1 + x_d) - \frac{d_{22}b_1}{D}(e_2 + \dot{x}_d) + \frac{d_{12}b_2}{D}e_3\right]\right\} \end{aligned} \tag{5.20}$$

Now the system can be presented as a chain of integrators of the following form

$$\dot{z_1} = z_2 \tag{5.21}$$
$$\dot{z_2} = z_3 \tag{5.22}$$
$$\dot{z_3} = u + L_g L_f^2 h\varphi(t). \tag{5.23}$$

Sliding Mode Design

We apply the classical SMC design for a relative degree one sliding variable. Reduced order system is taken as

$$\dot{z_1} = z_2 \tag{5.24}$$
$$\dot{z_2} = z_3 = u_v \tag{5.25}$$

and the variable z_3 is taken as virtual control u_v. A linear controller

$$u_v = -c_1 z_1 - c_2 z_2, \tag{5.26}$$

can be designed such that the the origin of the reduced order closed-loop system

$$\dot{z_1} = z_2 \tag{5.27}$$
$$\dot{z_2} = -c_1 z_1 - c_2 z_2 \tag{5.28}$$

is an asymptotically stable equilibrium point. Gains c_1 and c_2 can be designed with pole placement or LQR methods, nevertheless, they will be adjusted experimentally in the lab. The sliding variable has the form

$$\sigma = z_3 + c_1 z_1 + c_2 z_2. \tag{5.29}$$

Sliding variable dynamics are

$$\dot{\sigma} = u + \varphi(t) + c_1 z_2 + c_2 z_3 \tag{5.30}$$

and the nominal equivalent control can be applied as

$$u = -c_1 z_2 - c_2 z_3 + \nu \tag{5.31}$$

such that the closed-loop becomes

$$\dot{\sigma} = \nu + \varphi(t). \tag{5.32}$$

Nevertheless, note that the control law (5.20) strongly depends on the known parameters of the system. If parametric uncertainty is taken into account the applied control law has the form

$$\tau = \frac{1}{\tilde{L}_g \tilde{L}_f^2 h} \left(u - \tilde{L}_f^3 h \right) \tag{5.33}$$

The closed-loop system with parametric uncertainty in the control law is

$$\dot{z_1} = z_2 \tag{5.34}$$
$$\dot{z_2} = z_3 \tag{5.35}$$
$$\dot{z_3} = \underbrace{\frac{L_g L_f^2 h}{\tilde{L}_g \tilde{L}_f^2 h}}_{\gamma(e)} u + \underbrace{\frac{L_f^3 h - \tilde{L}_f^3 h}{\tilde{L}_g \tilde{L}_f^2 h} + \frac{L_g L_f^2 h}{\tilde{L}_g \tilde{L}_f^2 h} \varphi(t)}_{\bar{\varphi}(e,t)}. \tag{5.36}$$

Here the coefficient of control $\tilde{L}_g \tilde{L}_f^2 h$ and $\tilde{L}_f^3 h$ cannot be completely compensated and the uncertainties become state dependent.

Sliding variable dynamics can be represented as

$$\dot{\sigma} = \gamma(e) u + \bar{\varphi}(e,t) + c_1 z_2 + c_2 z_3 \tag{5.37}$$

and if the nominal equivalent control (5.31) is applied, the closed-loop is

$$\dot{\sigma} = \gamma(e)\nu + \underbrace{c_1(1-\gamma(e))z_2 + c_2(1-\gamma(e))z_3 + \bar{\varphi}(e,t)}_{\tilde{\varphi}(\sigma,t)} \tag{5.38}$$

Note that the sliding variable $\sigma = \sigma(z)$ is dependent of state z and the state $z = z(e)$ is dependent of e. Then, the sliding variable dynamics can be represented by functions dependent on σ, i.e. $\tilde{\gamma}(\sigma) = \gamma(e)$ and $\tilde{\varphi}(\sigma,t) = c_1(1-\gamma(e))z_2 + c_2(1-\gamma(e))z_3 + \bar{\varphi}(e,t)$.

$$\dot{\sigma} = \tilde{\gamma}(\sigma)\nu + \tilde{\varphi}(\sigma,t) \tag{5.39}$$

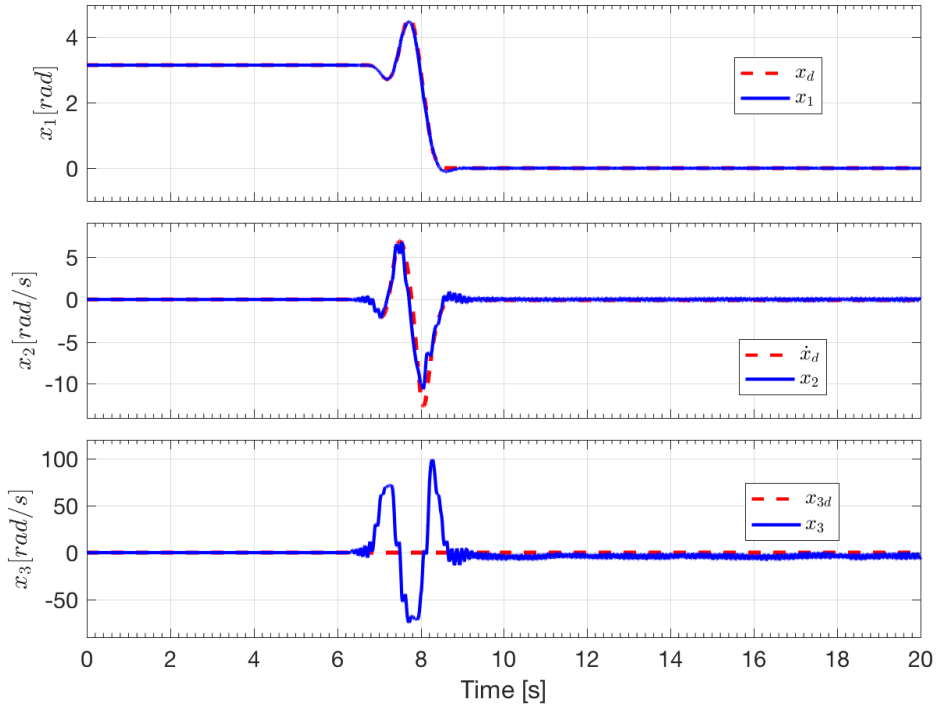

FIGURE 5.7: Trajectory tracking of pendulum position and velocity and stabilization of the wheel velocity.

Here the sliding variable matches the problem presented in Chapter 2 and 3.

5.2.3 Experimental Results

Reaction Wheel pendulum of the Sliding Mode Control laboratory was built in the Institute of Automation and Control, Graz University of Technology, Graz, Austria. Its actuator consists of a 12[v] DC Motor and quadrature encoders to read the pendulum angular position and disk angular position (see Fig. 5.5).

Fig. 5.7 shows the system trajectories of pendulum position, velocity and wheel velocity, following a predefined desired trajectory $x_d(t)$, $\dot{x}_d$ and x_{3d}. The trajectory was previously designed by the method presented in Graichen, 2006. Once the system has reached the instable equilibrium point Fig. 5.8 shows the precision in steady state.

Fig. 5.9 and 5.10 show the tracking errors of pendulum position and velocity and the regulation error of wheel velocity. Even when there is a maximum error of 0.18 [rad] in error tracking of the pendulum position, the control strategy was able to swing-up the pendulum to the instable equilibrium point and stabilize it.

Fig. 5.11 shows the evolution of sliding variable and Fig. 5.12 control signal produced by the SSTA. The gains for the GSTA were selected as $k_1 = 2$, $k_2 = 3.5$ and $\beta = 12$ and for the sliding surface $c_1 = 30$ and $c_2 = 15$. Note that the magnitude of control signal and SSTA gains are remarkable big. This is due to the parameter values of the ratio $\frac{1}{\tilde{L}_g \tilde{L}_f^2 h}$ in the control law (5.33).

The control input signal applied to the system is depicted in Fig. 5.13. It was saturated at 10[v] in order to protect the actuator.

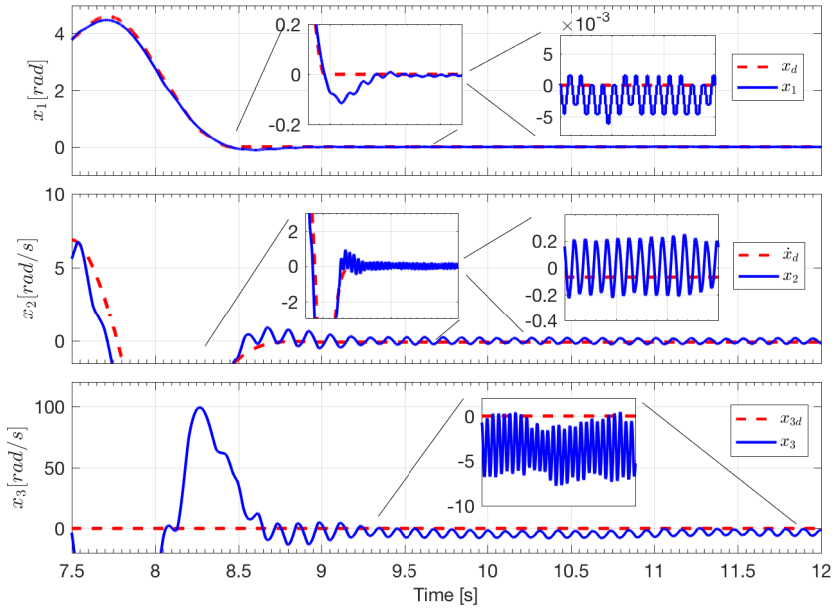

FIGURE 5.8: States and trajectories. Zoom.

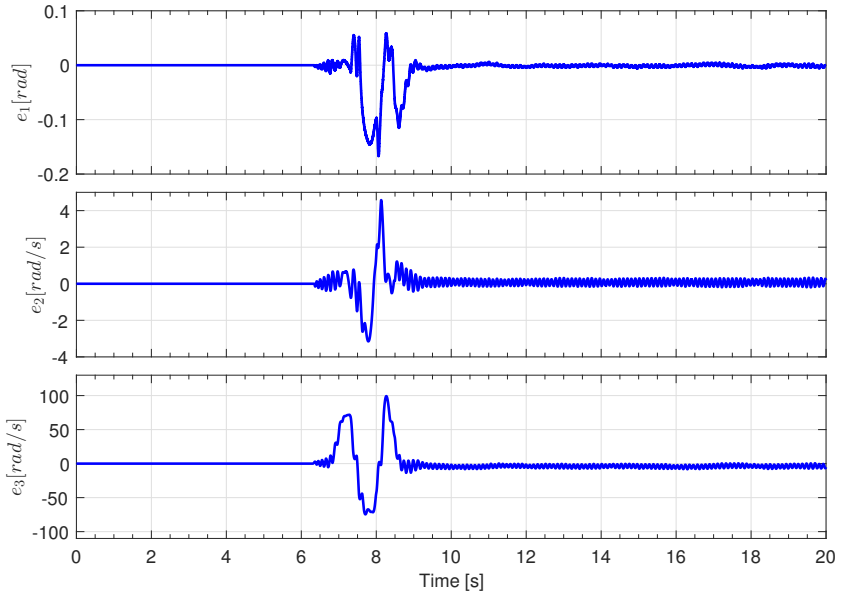

FIGURE 5.9: Tracking errors of pendulum position and velocity. Regulation error of wheel velocity.

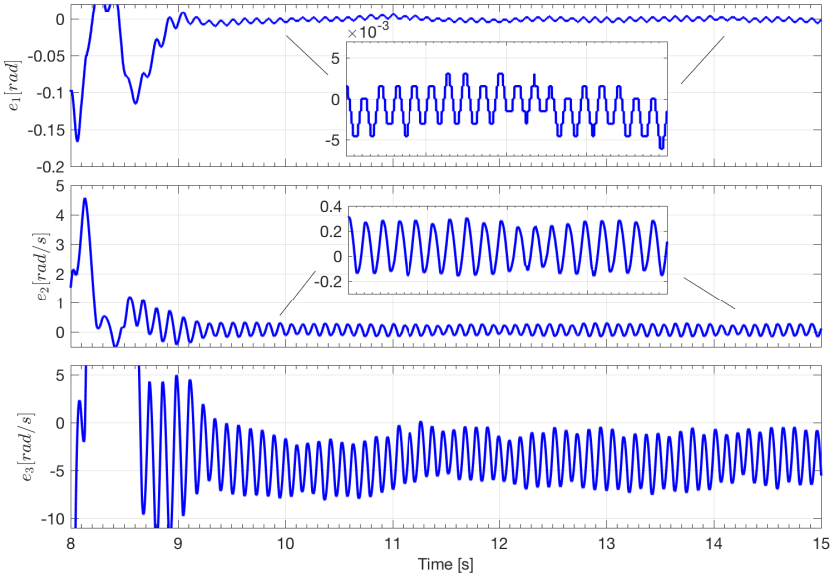

FIGURE 5.10: Error dynamics. Zoom.

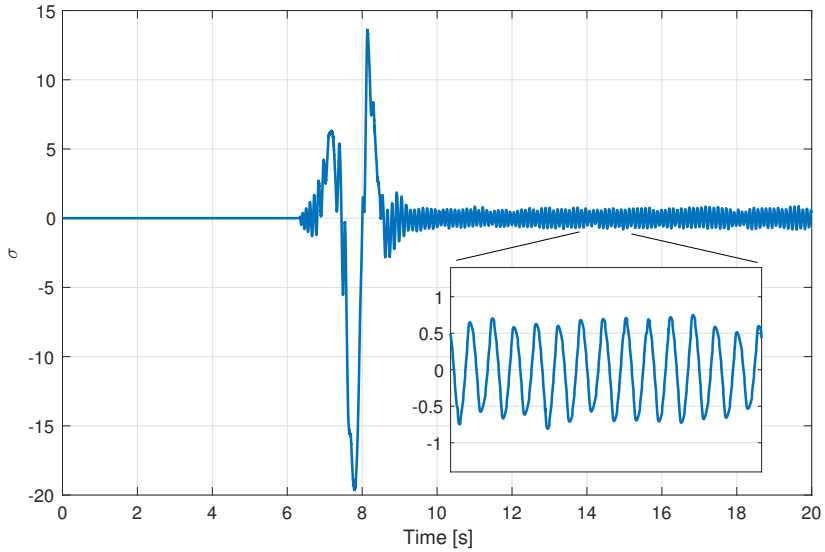

FIGURE 5.11: Evolution of sliding variable.

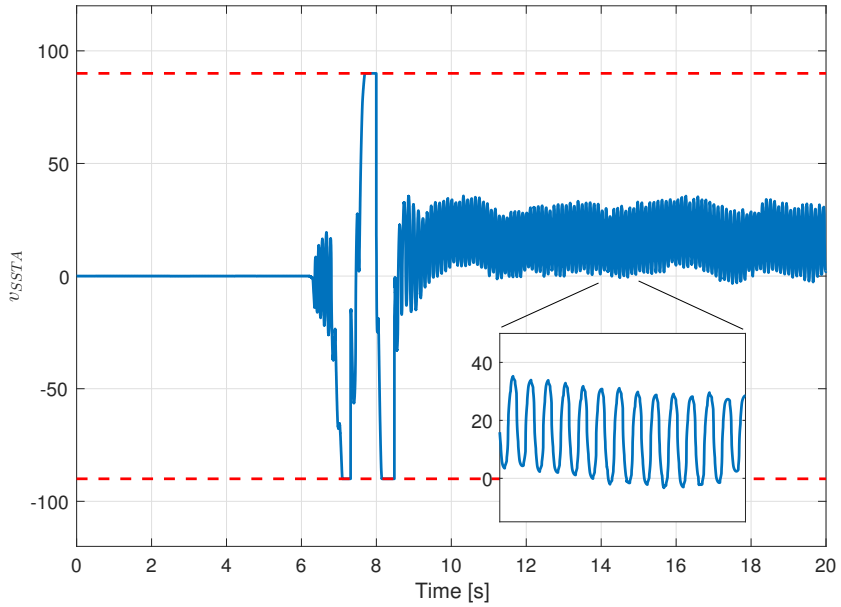

FIGURE 5.12: Saturated SSTA control signal at 90

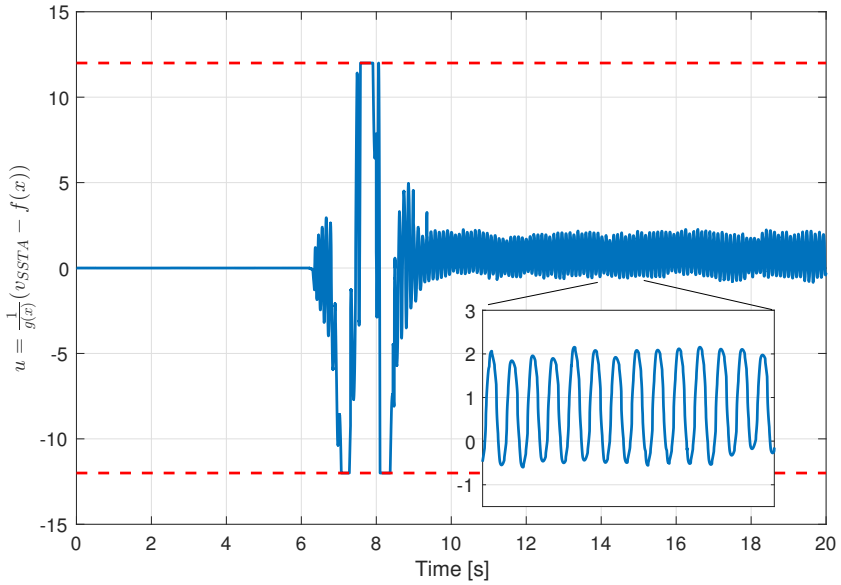

FIGURE 5.13: Control signal of feedback linearization and SSTA.

5.3 Model Predictive Output Integral Sliding Mode Control

A combination of model predictive control with output integral sliding mode techniques is proposed. The output integral sliding mode controller protects the nominal control provided by the predictive controller against matched perturbations. The entire concept exploits output information only. The control strategy is tested in the laboratory on a mass positioning system.

Consider a linear time invariant system

$$\dot{x}(t) = Ax(t) + Bu(t) + B\varphi(t) \tag{5.40a}$$
$$y(t) = Cx(t) \tag{5.40b}$$

with state vector $x \in \mathbb{R}^n$, initial state $x(0) = x(t=0)$, inputs $u \in \mathbb{R}^m$, matched perturbations $\varphi \in \mathbb{R}^m$ and system matrices $A \in \mathbb{R}^{n\times n}$, $B \in \mathbb{R}^{n\times m}$ and $C \in \mathbb{R}^{p\times n}$. System (5.40) is subject to constraints

$$u_{min} \leq u(t) \leq u_{max} \tag{5.41a}$$
$$\dot{u}_{min} \leq \dot{u}(t) \leq \dot{u}_{max} \tag{5.41b}$$
$$x_{min} \leq x(t) \leq x_{max} \tag{5.41c}$$
$$y_{min} \leq y(t) \leq y_{max}\ . \tag{5.41d}$$

The main goal is to design an output tracking controller for system (5.40) that does not need full state measurements and fulfills all constraints (5.41) for all $t \geq 0$. Therefore, the following assumptions are stated:

Assumption 1. *Input and output matrices have full rank, i.e.* $\mathrm{rank}(B) = m$ *and* $\mathrm{rank}(C) = p$.

Assumption 2. *The pair* (A, B) *is controllable,* (A, C) *is observable.*

Assumption 3. *The initial state is unknown but bounded* $||x(0)|| \leq \mu$.

Assumption 4. *The matched perturbation is unknown but bounded* $||\varphi(t)|| \leq \varphi_{max}$, *and also its time derivative* $||\dot{\varphi}(t)|| \leq d_{max}$ *for all* $t \geq 0$.

Assumption 5. *The dimensions of inputs, outputs and states fulfill* $m < p < n$.

Assumption 6. $\mathrm{rank}\,(CB) = m$.

5.3.1 Overall Structure

Figure 5.14 shows the overall structure of the proposed control loop, where the control signal u consists of two parts

$$u = u_0 + u_1\ , \tag{5.42}$$

which are both bounded to fulfill (5.41a). A nominal control u_0 results from a MPC that is designed to control the nominal system, i.e. the system without disturbances. An OISM controller acts as a protector of the nominal behavior against matched perturbations and contributes with u_1 to the control signal. For the estimation of the systems states, an OISM observer is used. It takes advantage of the nominal control and the measured outputs y and provides the estimates $\hat{x}$ to the MPC and the OISM controller, see Fig. 5.14.

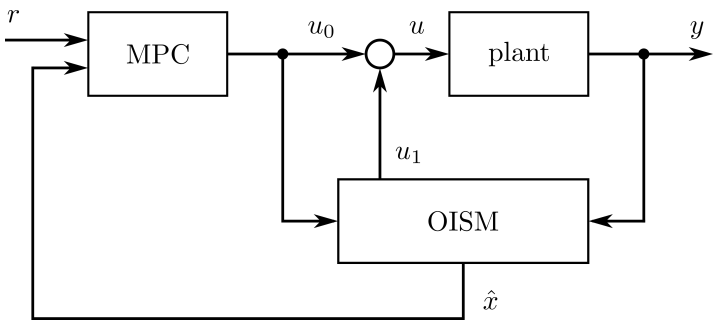

FIGURE 5.14: Overall structure of the control loop to track desired references r for the outputs y under the presence of disturbances φ. The OISM block consists of an OISM observer and an OISM controller

For the realization of this control loop, a small sampling time $T_{S,Plant}$ is used for the OISM observer and controller to get quasi-continuous characteristics. In contrast, a much bigger sampling time $T_{S,MPC}$ is used to do the optimization in the MPC.

5.3.2 Model Predictive Controller

In the chosen classical version of the MPC, the discretized version of model (5.40) is used:

$$x_{k+1} = A_d\, x_k + B_d\, u_k \tag{5.43a}$$
$$y_k = C_d\, x_k \tag{5.43b}$$

The change of the control signals between two subsequent time instants Δu_k are considered as optimization variables. Thus, u_k is replaced by $u_k = u_{k-1} + \Delta u_k$. As a consequence, a prediction based on model (5.43) is given by

$$\overline{y}_{k+1} = F_d x_k + G_d u_{k-1} + H_d \overline{\Delta u}_k \tag{5.44}$$

using the control horizon N_C and the prediction horizon N_P, see e.g. Maciejowski, 2002. Vectors $\overline{y}_{k+1} \in \mathbb{R}^{pN_P}$ and $\overline{\Delta u}_k \in \mathbb{R}^{mN_C}$ consists of the values of the predicted outputs and the changes of the control signal over the corresponding horizons, respectively. Matrices $F_d \in \mathbb{R}^{pN_P \times n}$, $G_d \in \mathbb{R}^{pN_P \times m}$ and $H_d \in \mathbb{R}^{pN_P \times mN_C}$ are built up using the system matrices in (5.43). In cost function

$$J(\overline{\Delta u}_k) = \left(\overline{y}_{k+1} - \overline{r}_{k+1}\right)^T Q \left(\overline{y}_{k+1} - \overline{r}_{k+1}\right) + \overline{\Delta u}_k^T R\, \overline{\Delta u}_k \tag{5.45}$$

the difference between the predicted outputs (5.44) and the reference trajectories over the prediction horizon $\overline{r}_{k+1} \in \mathbb{R}^{pN_P}$ is weighted by Matrix $Q \in \mathbb{R}^{pN_P \times pN_P}$. The change of the control signals contribute to J with a weight $R \in \mathbb{R}^{mN_C \times mN_C}$. Inserting (5.44) in (5.45) yields

$$J(\overline{\Delta u}_k) = \overline{\Delta u}_k^T \left(H_d^T Q H_d + R\right) \overline{\Delta u}_k + 2\overline{\Delta u}_k^T H_d^T Q \overline{e}_k \tag{5.46}$$

using vector $\overline{e}_k = F_d x_k + G_d u_{k-1} - \overline{r}_{k+1}$. Additionally, all constraints (5.41) are written in terms of $\overline{\Delta u}_k$, i.e.

$$W \overline{\Delta u}_k \leq \bar{w} \tag{5.47}$$

with a constant matrix $W \in \mathbb{R}^{2(2mN_C + nN_P + pN_p) \times mN_C}$,

and a vector $\bar{w} \in \mathbb{R}^{2(2mN_C+nN_P+pN_p)}$ that depends on u_{k-1} and the actual value of x_k. Note that due to (5.42), the admissible control for the MPC is limited depending on the maximal value of u_1. The resulting optimization problem is to minimize (5.46) subject to (5.47) which is a quadratic program Maciejowski, 2002.

Of course, there exist a lot of extensions of this formulation. However, the goal in this work is to keep the MPC as simple as possible and use an OISM controller to get rid of the matched perturbations. This additional controller as well as the MPC need the states of the system that are estimated in the next Section.

5.3.3 Output Integral Sliding Mode Observer

The main idea behind the OISM observer is to reconstruct the observability matrix $\mathscr{O} \in \mathbb{R}^{pl \times n}$ so that

$$\mathscr{O} = \begin{bmatrix} C \\ CA \\ \vdots \\ CA^{l-1} \end{bmatrix} \tag{5.48}$$

has full rank, i.e. $\operatorname{rank}(\mathscr{O}) = n$, where l represents the observability index Fridman, Poznyak, and Bejarano, 2014. Then, $\mathscr{O}$ is used to determine the states based on the measured outputs and auxiliary variables as described below.

The estimation is carried out step-by-step in a hierarchical structure. The basis for that is a classical Luenberger observer of the form

$$\dot{\tilde{x}} = A\tilde{x} + Bu + L\left(y - C\tilde{x}\right)$$

with matrix gain $L \in \mathbb{R}^{n \times p}$. To get exponentially stable dynamics for the error $e = x - \tilde{x}$, matrix $(A - LC)$ has to be Hurwitz, i.e. all real parts of the eigenvalues have to be negative. As a result an upper bound for e can be stated as

$$||e|| \leq \gamma e^{-\eta t}\left(\mu + ||\tilde{x}(0)||\right) ,$$

Constants γ and η are both positive.

The step-by-step procedure starts to reconstruct CAx using a first auxiliary system, then to determine CA^2x by means of a second auxiliary system and so on as far as CA^{l-1}, see Fridman, Poznyak, and Bejarano, 2014. For the k-th step, the auxiliary system has the following form

$$\dot{x}_a^{(k)} = A^k\tilde{x} + A^{k-1}Bu + \tilde{L}\left(C\tilde{L}\right)^{-1} v^{(k)} , \tag{5.49}$$

where $\tilde{L}$ is designed such that $C\tilde{L}$ is invertible. Output injection $v^{(k)}$ is given by

$$v^{(k)} = \alpha_k(t)\frac{s^{(k)}}{||s^{(k)}||} \tag{5.50}$$

with

$$\alpha_k(t) > ||CA^k||\,||x - \tilde{x}|| , \tag{5.51}$$

e.g.

$$\alpha_k(t) = ||CA^k||\gamma e^{-\eta t}\left(\mu + ||\tilde{x}(0)||\right) + \lambda \tag{5.52}$$

and $\lambda > 0$. In (5.50), a sliding variable

$$s^{(k)} = \begin{cases} y - Cx_a^{(1)} & \text{for} \quad k = 1 \\ v_{eq}^{(k-1)} + CA^{k-1}\tilde{x} - Cx_a^{(k)} & \\ & \text{for} \quad k = 2, \ldots, (l-1) \end{cases} \tag{5.53}$$

is used. Its construction uses the outputs for $k = 1$. For $k = 2, \ldots, (l-1)$, the equivalent control belonging to the previous step is taken into account, see Bejarano, Fridman, and Poznyak, 2007; Fridman, Poznyak, and Bejarano, 2014. By the choice of the initial values

$$s^{(k)}(0) = \begin{cases} y(0) - Cx_a^{(1)}(0) & \text{for} \quad k = 1 \\ v_{eq}^{(k-1)}(0) + CA^{k-1}\tilde{x}(0) - Cx_a^{(k)}(0) & \\ & \text{for} \quad k = 2, \ldots, (l-1) \end{cases} \tag{5.54}$$

one gets

$$s^{(k)}(0) = 0, \quad \dot{s}^{(k)}(0) = 0 \quad \Rightarrow \quad s^{(k)} = 0 \quad \forall t \geq 0.$$

and as a consequence

$$CA^k x = CA^k \tilde{x} + v_{eq}^{(k)} \quad \text{for} \quad k = 2, \ldots, (l-1)\,. \tag{5.55}$$

This means that sliding mode is enforced at the very beginning (integral sliding mode) and $CA^k x$ is reconstructed for all $t \geq 0$. A combination of relations (5.53) and (5.55) yields

$$\begin{aligned} Cx &= C\tilde{x} + Cx_a^{(1)} - C\tilde{x} && \text{(5.56a)} \\ CAx &= CA\tilde{x} + v_{eq}^{(1)} && \text{(5.56b)} \\ &\vdots \qquad\qquad \vdots & \\ CA^{l-1}x &= CA^k\tilde{x} + v_{eq}^{(l-1)}\,. && \text{(5.56c)} \end{aligned}$$

Using (5.48), equations (5.56) can be written as

$$\mathscr{O}x = \mathscr{O}\tilde{x} + v_{eq} \tag{5.57}$$

with

$$v_{eq} = \begin{bmatrix} Cx_a^{(1)} - C\tilde{x} \\ v_{eq}^{(1)} \\ \vdots \\ v_{eq}^{(l-1)} \end{bmatrix}\,. \tag{5.58}$$

The hierarchical OISM observer takes advantage of (5.57) to estimate the states of the system but needs filtering to get v_{eq}, e.g. with filter constant τ and differential equation

$$\tau \dot{x}_f^{(k)} + x_f^{(k)} = v_{eq}^{(k)}\,.$$

Finally, the OISM observer take the form

$$\dot{\hat{x}} = \tilde{x} + \mathscr{O}^{+} v_f\,,$$

with the estimated states $\hat{x}$ and the left inverse of the observability matrix

$$\mathscr{O}^{+} = (\mathscr{O}^{T}\mathscr{O})^{-1}\mathscr{O}^{T} .$$

Additionally $v_{eq}^{(k)}$ has to be replaced by $v_{f}^{(k)}$ in relations (5.53), (5.54) and (5.58).

5.3.4 Continuous Output Integral Sliding Mode Controller

In this section an OISM controller is designed. It relies on the OISM observer stated above that provides estimates $\hat{x}$. For this combination, the sliding variable

$$s = G\left(y - y(0) - \int_0^t \left[CA\hat{x}(\tau) + CBu_0(\tau)\right]d\tau\right)$$

was proposed in Bejarano, Fridman, and Poznyak, 2007. Here, $G \in \mathbb{R}^{m\times p}$ must be chosen such that $\det(GCB) \neq 0$ holds. In this paper, the nominal control u_0 stem from the MPC described in Section 5.3.2.

Here the Saturated Super-Twisting is used to determine control signal u_1 that contributes to the input variable u of the plant, see Fig. 5.14. It yields

$$u_1 = (GCB)^{-1}u_{SSTA} \tag{5.59}$$

The closed-loop system with $s_1 = s$, $s_2 = z + GCB\varphi + GCA(x - \hat{x})$, becomes

$$\begin{aligned} \dot{s}_1 = &\quad -\alpha_1 \lceil s \rfloor^{\frac{1}{2}} + s_2 \\ \dot{s}_2 = &\quad -\alpha_2 |s|^0 \text{sign}\,(s) + GCB\dot{\varphi} + GCA^2((x - \hat{x}) + \varphi) \end{aligned} \tag{5.60}$$

where the bound of the derivative of the perturbation is estimated by

$$L > ||GCB||d_{max} + ||GCA^2||(||x - \hat{x}|| + \varphi_{max}).$$

then, the SSTA α_1 and α_2 can be calculated as in the previous Chapters.

In sliding mode the equivalent control is given by the amount of integral control

$$z = u_{1,eq} = -(GCB)^{-1}GCA(x - \hat{x}) - \varphi$$

and it depends on the matched perturbation φ and as a consequence, system (5.40) takes the form

$$\dot{x}(t) = \tilde{A}x(t) + B(GCB)^{-1}GCA\hat{x} + Bu_0(t) \tag{5.61a}$$

$$y(t) = Cx(t) \tag{5.61b}$$

with $\tilde{A} = A - B(GCB)^{-1}GCA$. As shown in Bejarano, Fridman, and Poznyak, 2007, system (5.61) is not observable for $p \leq m$. Therefore, assumption 5 was made in the actual problem statement.

In literature, there exist work focusing on how to design matrix G. In Castaños and Fridman, 2006 a constant input matrix B is used and it is shown that there exist optimal choices for this matrix, e.g. $G = B^{+}$, that enables one to completely eliminate the matched perturbations and do not amplify the unmatched ones. It was extended in Rubagotti et al., 2011, where a state dependent B was used. Inspired by that, also the pseudo-inverse

$$G = (CB)^{+} \tag{5.62}$$

can be used for the OISM controller, leading to a simplification of control law (5.59).

In a next step, the hierarchical OISM observer shown in Section 5.3.3 is modified to be able to operate together with the OISM controller and the plant in closed loop, i.e. on model (5.61). This yields a modified Luenberger observer

$$\dot{\hat{x}} = \tilde{A}\tilde{x} + Bu_0 + B(CB)^{+}CA\hat{x} + L\left(y - C\tilde{x}\right)$$

with L such that $\hat{A} = (\tilde{A} - LC)$ is Hurwitz and changed dynamics for the auxiliary states

$$\dot{x}_a^{(k)} = \tilde{A}^k\tilde{x} + \tilde{A}^{k-1}B\left[u_0 + (CB)^{+}CA\hat{x}\right] + \tilde{L}\left(C\tilde{L}\right)^{-1}v^{(k)},$$

cf. differential equations (5.49). Additionally, matrix A is changed to $\tilde{A}$ in (5.51)-(5.54) and filtering is applied once more to realize v_{eq}. This combination of OISM observer and controller ensures that sliding mode is enforced from the very beginning although only output information is used.

5.3.5 Laboratory Experiment

The proposed combination of MPC and OISM control is tested in the laboratory on a mass spring system with motor Figure (5.15).

FIGURE 5.15: Laboratory experiment: Spring-mass system.

Figure 5.16 shows the functional principle of the system. If a voltage is applied

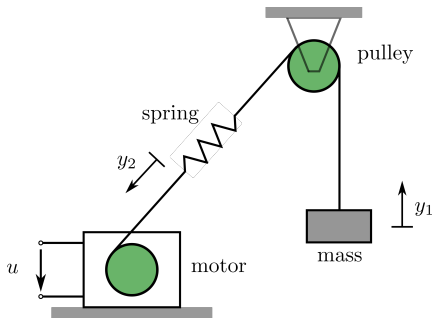

FIGURE 5.16: Functional principle of the laboratory experiment

at input u, a motor winds up a cord that is fixed at the left hand side of a spring

(spring constant c). The right hand side of the spring is led through a deflection pulley (viscous friction coefficient d) to mass m, see Fig. 5.16.

Due to the motor electronics, position y_2 at the left hand side of the spring is related to the integral of u via gain V_c. Consequently, the laboratory system can be modeled (with respect to a equilibrium point) as a linear time-invariant system

$$\dot{x}(t) = \begin{bmatrix} 0 & 1 & 0 \\ -\frac{c}{m} & -\frac{k_P}{m} & \frac{c}{m} \\ 0 & 0 & 0 \end{bmatrix} x(t) + \begin{bmatrix} 0 \\ 0 \\ V_c \end{bmatrix} u(t) \tag{5.63}$$

where the state vector combines position y_2 with position y_1 and velocity $\dot{y}_1$ of the mass such that

$$x = \begin{bmatrix} y_1 & \dot{y}_1 & y_2 \end{bmatrix}^T .$$

Only the two positions can be measured by means of encoders at the motor and pulley, i.e.

$$y(t) = \begin{bmatrix} 1 & 0 & 0 \\ 0 & 0 & 1 \end{bmatrix} x(t)$$

Mass $m = 0.18\,kg$ was measured using a scale, the remaining parameters in (5.63) were identified using frequency domain identification based on FFT resulting in $V_c = 0.0859\,mV^{-1}s^{-1}$, $c = 3.8398\,Nm^{-1}$ and $k_P = 0.0415\,kgs^{-1}$.

The mass positioning system is connected via an interface card to a computer. Matlab/Simulink[1] together with real-time control Software QUARC[2] is used to realize the proposed structure with sampling times $T_{S,MPC} = 100\,ms$ and $T_{S,Plant} = 1\,ms$ for the OSIM block in Fig. 5.14.

In the following subsections, two experiments are carried out to show the performance of the stated control strategy. The matched perturbations are applied as an additional part to the control signal u with $|\varphi(t)| < 2\,V$. The following constraints are used in the examples:

$$\begin{aligned} -5\,V \leq \quad & u(t) \quad \leq 5\,V \\ -0.4\,m \leq \quad & x_1(t) \quad \leq 0.5\,m \\ -1\,ms^{-1} \leq \quad & x_2(t) \quad \leq 1\,ms^{-1} \\ -0.5\,m \leq \quad & x_3(t) \quad \leq 0.4\,m \end{aligned}$$

The parameters of the MPC are chosen as $N_P = 15$, $N_C = 5$, $Q_i = \text{diag}\left(\begin{bmatrix} 100 & 1 \end{bmatrix}\right)$ and $R_i = 0.01$. Matrices Q_i and R_i represent the weightings at each time instant of the prediction resp. control horizon, so they are used to build up Q and R for (5.46). OISM observer and controller are tuned with α according to (5.52), $\lambda = \varphi_{max} + 0.1$, $\beta = 2\,V$ and G consistent with (5.62).

5.3.6 Results

Three different settings are tested in the laboratory and presented in this section for comparison. For all three cases, the same smooth reference trajectories (green curves in Figures 5.17, 5.22 and 5.25) are used and same disturbance (green sinusoidal in Figures. 5.24 and 5.27) for cases (II) and (III) is used.

[1] http://www.mathworks.com
[2] http://www.quanser.com

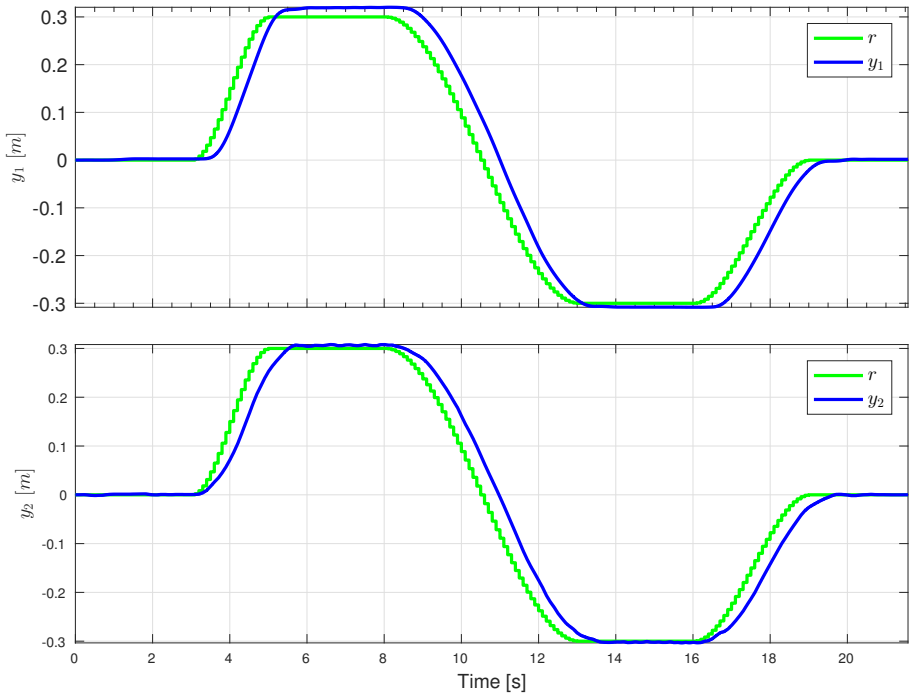

FIGURE 5.17: ① System outputs and the reference trajectories.

In setting ① the proposed MPC nominal controller without OISM controller (i.e. the SSTA is turned off) is applied to the system without external matched perturbations. MPC is allowed to utilize $3\,V$ as maximal value for u_0. Figs. 5.17 and 5.18 and 5.19 show the closed-loop nominal trajectories of the output and states, and nominal control signal. System trajectories ① in graphic 5.17 and 5.18 are considered as nominal closed-loop system behavior.

In setting ②, MPC nominal controller without the OISM controller, (i.e. the SSTA is still turned off) and the external matched perturbation $\varphi(t)$ are applied to the plant. Fig. 5.17 and 5.18 show that the trajectory tracking is strongly affected by the matched perturbation $\varphi(t)$. The effect of the perturbation can be limited by the MPC control signal alone but not eliminated.

Setting ③ uses $3\,V$ for the MPC and $2\,V$ for the SSTA. The application of an OISM controller allows the theoretically exact compensation of the matched Lipschitz perturbation when the design conditions are met. The resulting trajectory tracking can be seen in Figures 5.25 and 5.26, controllers signals in 5.19, and the OISM sliding surface and the SSTA control signal is depicted in Figure 5.28.

During the entire experiments, the OISM observer operates in sliding mode as shown in Figures 5.21 and 5.30. Two sliding variables are used in the observer for the mass positioning system because $l = 1$. In Figures 5.20 and 5.29, the performance of the Luenberger observer and OISM observer are compared. In contrast to the Luenberger observer, the OISM observer completely rejects the acting perturbations. In the last experiment the disturbance does not affect both observers, because the OISM controller completely eliminates the matched disturbance, see Figure 5.29. As illustrated in Figures 5.25 to 5.29 the combination of OISM observer and controller performs very well at the real world system.

The OISM controller is not used solely to track the reference trajectory. This is because this methodology does not provide any possibility to guarantee that the

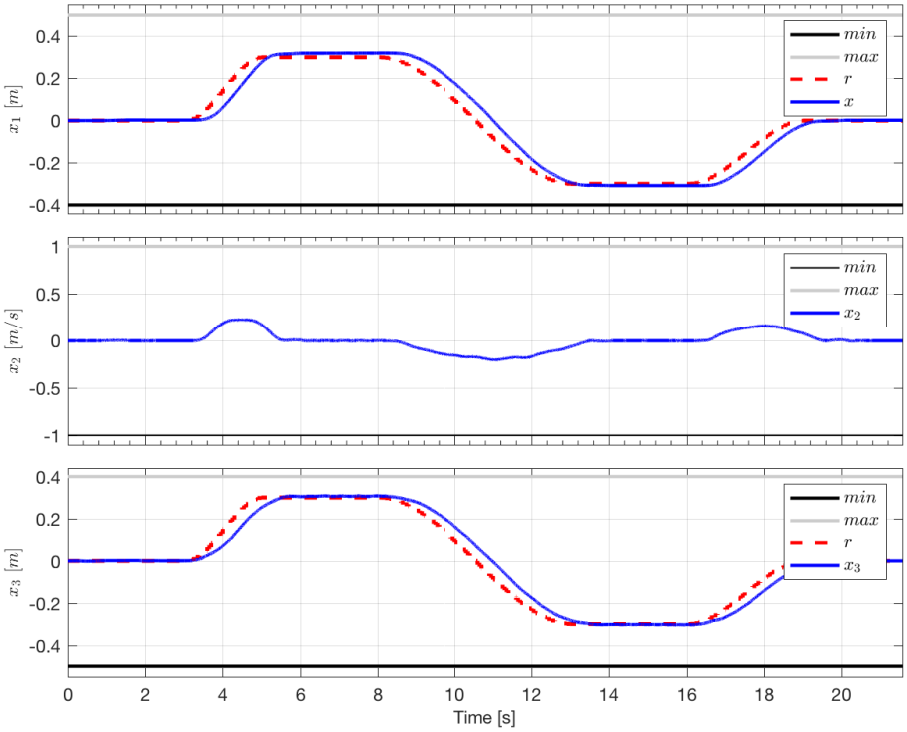

FIGURE 5.18: ① System states and the reference trajectories.

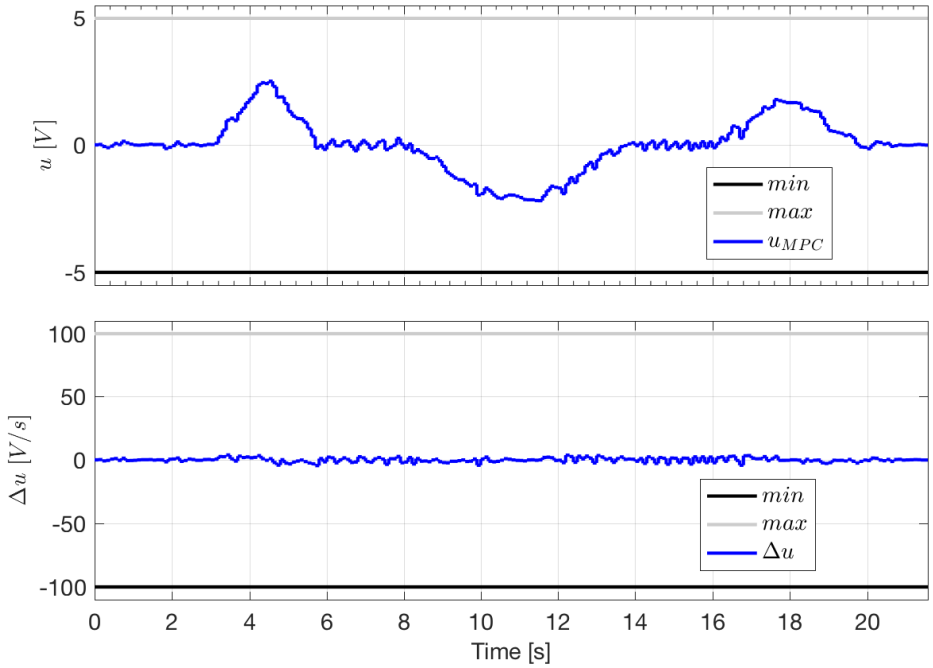

FIGURE 5.19: ① Control signal of the MPC nominal controller without perturbation.

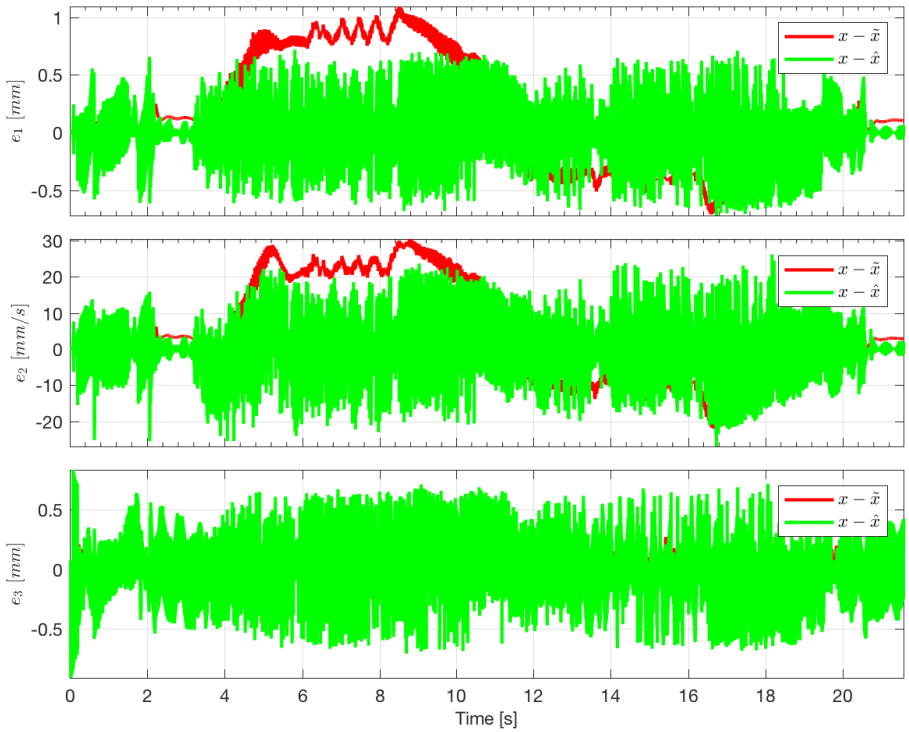

FIGURE 5.20: ① Observation errors of the Luengerber observer and the OISM observer.

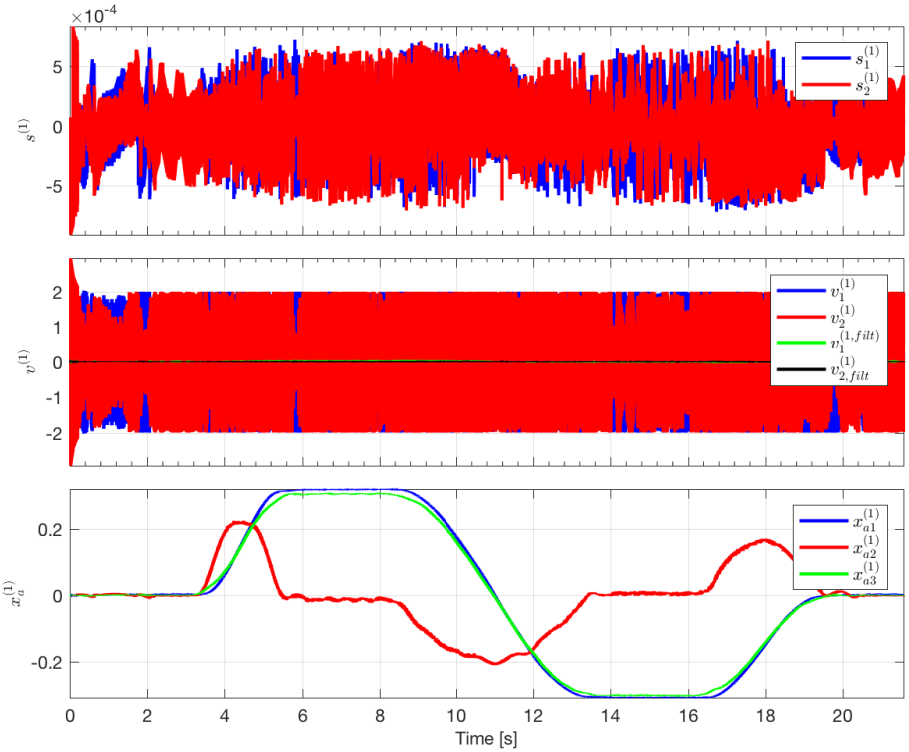

FIGURE 5.21: ① Sliding variables $s^{(k)}$ of the OISM observer ($k \in 1, 2$, error injection input $v^{(k)}$, and the states of the auxiliary subsystems $a^{(k)}$.

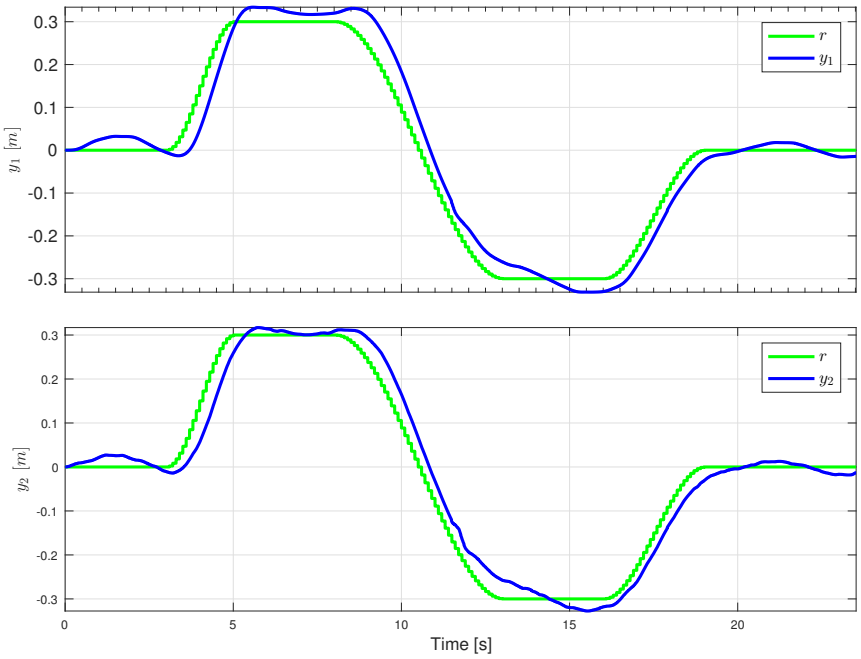

FIGURE 5.22: Ⅱ System outputs and the reference trajectories.

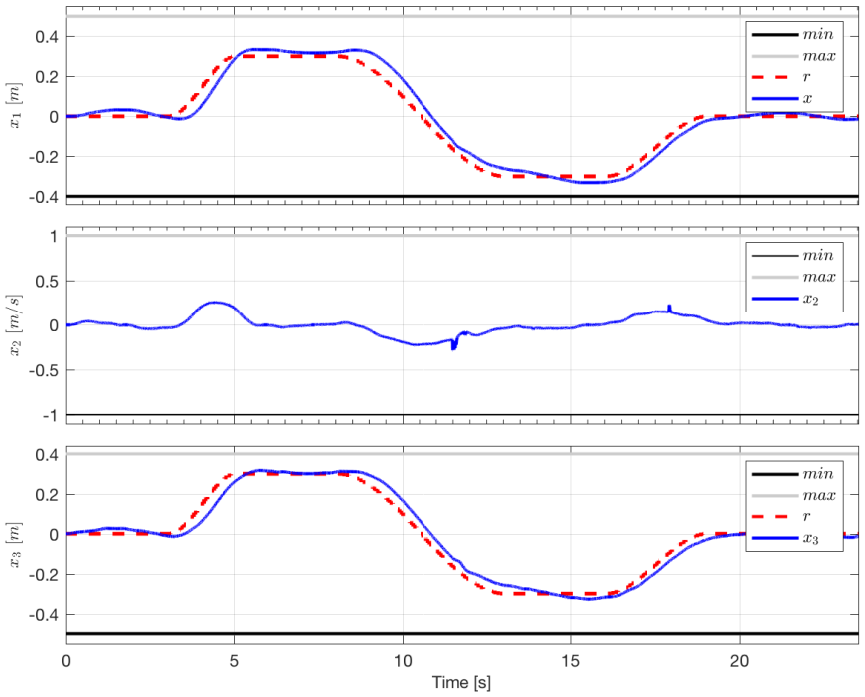

FIGURE 5.23: Ⅱ System states and the reference trajectories.

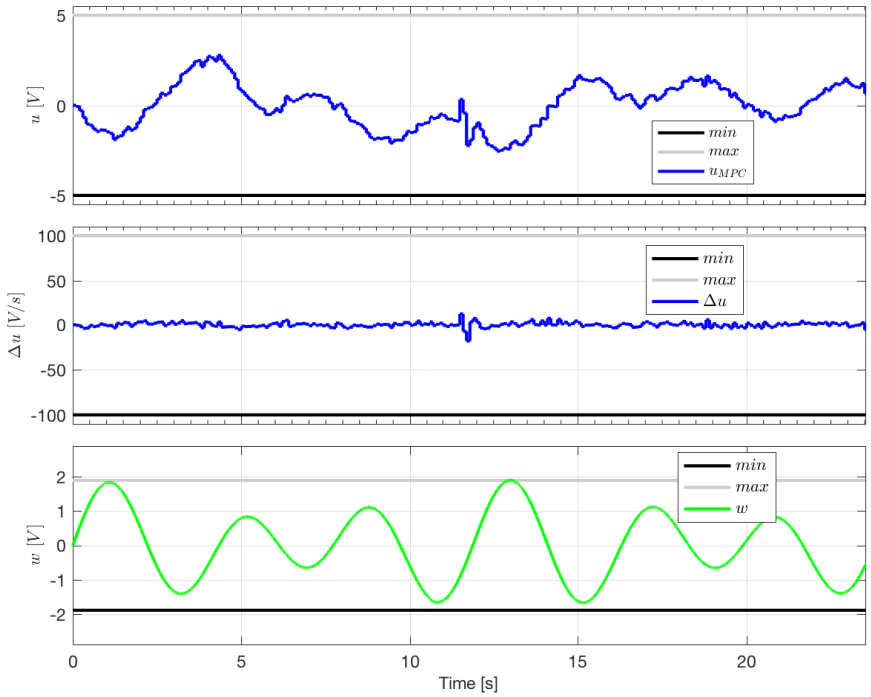

FIGURE 5.24: ⓘⓘ Control signal of the MPC nominal controller and perturbation.

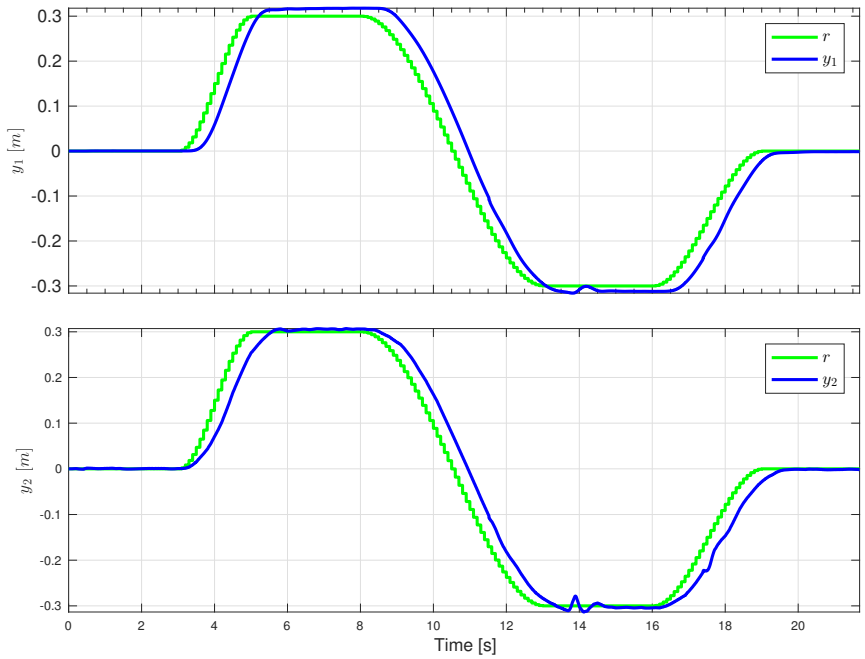

FIGURE 5.25: ⓘⓘⓘ System outputs and the reference trajectories.

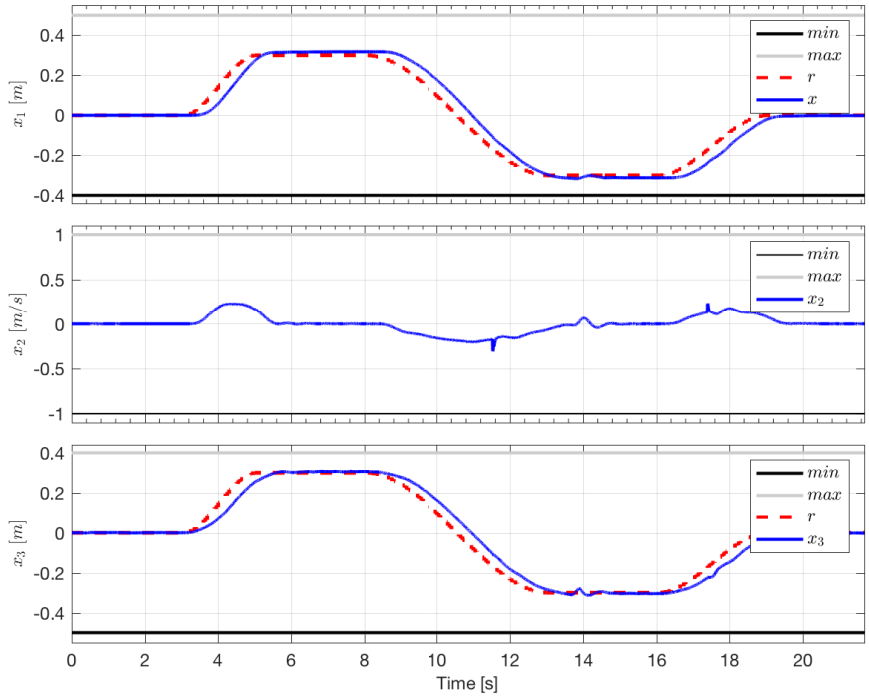

FIGURE 5.26: (III) System states and the reference trajectories.

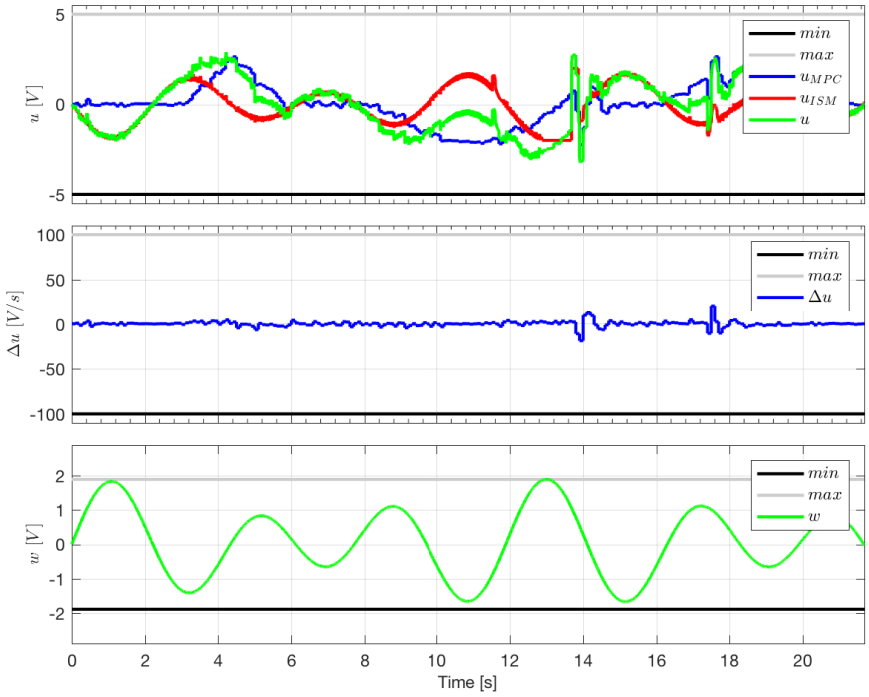

FIGURE 5.27: (III) Control signal of the MPC nominal controller, OISM controller and perturbation.

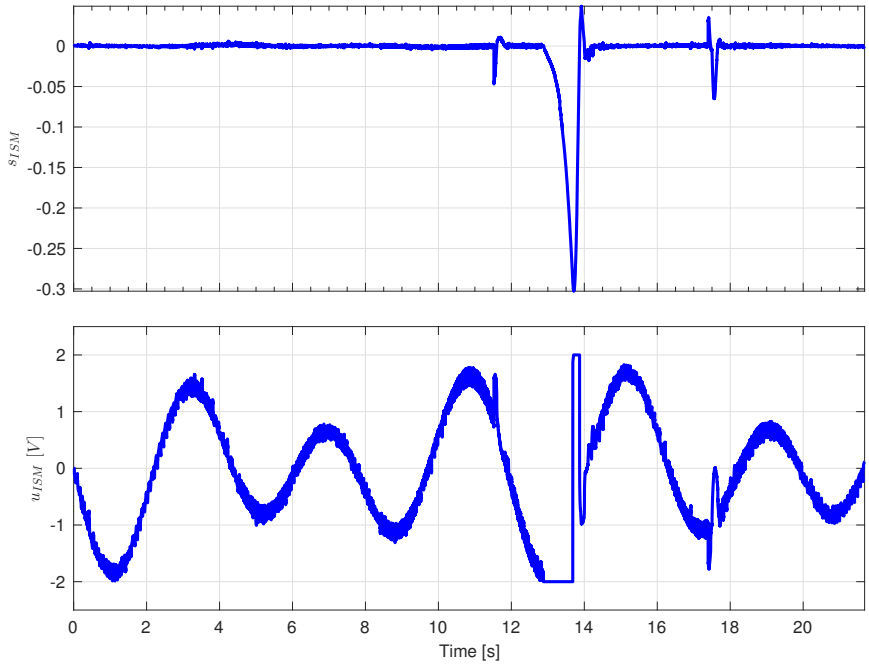

FIGURE 5.28: ⓘⓘⓘ Sliding variable and control signal of OISM.

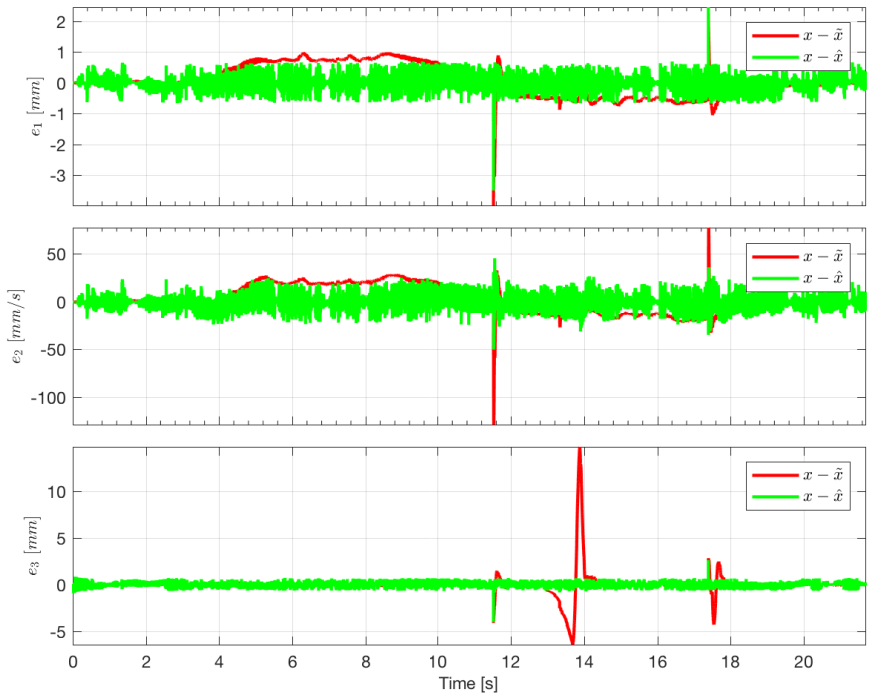

FIGURE 5.29: ⓘⓘⓘ Observation errors of the Luengerber observer and the OISM observer.

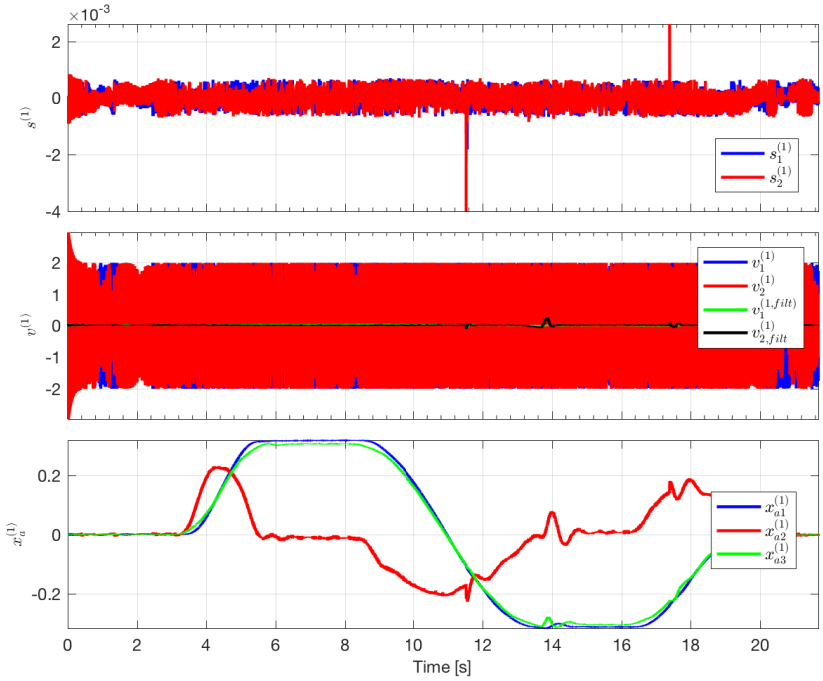

FIGURE 5.30: ⓘⓘⓘ Sliding variables $s^{(k)}$ of the OISM observer ($k \in 1, 2$, error injection input $v^{(k)}$, and the states of the auxiliary subsystems $a^{(k)}$.

state constraints (5.41) are fulfilled during output tracking.

Chapter 6

Conclusions

Control systems in presence of heavy uncertainties and perturbations is one of the main subjects in modern control systems theory. When realistic scenarios are considered, implementation of control feedback laws make evident problems related with parametric uncertainty, non-modeled dynamics, or saturation in the control input due to the limitation in the actuators, among others.

In this work, two of this main problems of implementations are addressed: when parametric uncertainty in mathematical models and in the applied control law is considered perturbation of the system become dependent on the state and time and the coefficient of control also becomes uncertain; when saturation in the control input is considered, it can generate undesired overshoots in presence of integral control laws that can affect the performance or even the stability of the closed-loop.

In Chapters 2 and 3, the problem of state dependent perturbations and uncertain coefficient of control is analyzed. It is shown that during the STA design for systems with the state dependent perturbation or/and uncertain control coefficient the problem of an algebraic loop in the gain design appears. All known methodologies for gain design are unable to solve the problem of the algebraic loop, and moreover, It is shown that the classic STA is unable to maintain the stability properties in presence of state dependent perturbations.

GSTA was proposed in order to overcome the problem of the algebraic loop in the gain design and to ensure the stability properties of the origin in the closed-loop system.

Based on strict non-smooth Lyapunov function Moreno, 2011 the sufficient conditions for global finite-time stability are found. Moreover, it turns out that in case when perturbations and control coefficient are time-dependent the analysis performed in this chapter provides much less restrictive conditions for global finite-time convergence than those reported in literature.

In Chapter 4 two different versions of SSTA are presented. Both versions use a dynamic switching law based on Positively Invariant Sets obtained from level curves of the Lyapunov function in Moreno and Osorio, 2008.

Relay Controller ensures the system trajectories to reach a Positively Invariant Set in finite-time where the STA's continuous control signal is able to drive system trajectory to zero in finite-time fulfilling the saturation condition.

In order to increment the maximum bound of the perturbation supported by the SSTA, the second version also includes a perturbation estimator allowing to set the STA's integrator to theoretically exact value of perturbation.

In Chapter 5, three different experiments in mechanical systems are performed in order to show the SSTA's benefits presented in this work when it is used as a tool in the control design.

The first experiment is the velocity trajectory tracking of a simple rotational system. It shows the advantage in performance of the SSTA with estimator, allowing to

completely avoid the overshoots in the transient process, i.e. it completely removes the wind-up effect.

The second one, a classical Feedback Linearization control is applied to a Reaction Wheel Pendulum. It is known that this control technique is strongly affected by parametric uncertainty. In this case, classical sliding variable design can be applied and, Generalized SSTA can ensure the system trajectories convergence to the sliding surface un spite of state dependent perturbations, uncertain control coefficient and with a saturated control signal.

The third one, a combination of MPC with a OISM observer and controller is proposed to join the advantages of both methods. Namely the ability of the MPC to consider constraints explicitly and the abilities of the OISM techniques to get a theoretically exact estimation of the states and to completely suppress matched perturbation for all times using output information only.

In this work it is shown, theoretically and experimentally, that GSTA is able to compensate a wider class of perturbations and uncertainties than in other previous works. As GSTA is one of the most important CHOSM algorithms, all the properties and advantages presented here, represent new directions in further research in CHOSM theory.

Even when SMC has been hardly criticized by its implementation issues, our experimental results allows us to understand and to show the benefits of the SCM implementation in the real world. The present work shows the advantages and great benefits of SMC on implementation issues.

Appendix A

Appendix A

A.1 State Dependent Perturbations and Uncertain Coefficient of Control

Proof of the General Case Theorem.

A.1.1 Separation of Perturbations

Consider the first order system

$$\dot{x} = \gamma(x,t)u + \varphi(x,t). \tag{A.1}$$

The terms $\varphi(x,t)$ and $\gamma(x,t)$ are uncertain functions dependent on the state and time. The control coefficient function is assumed to be bounded by positive constants

$$0 < k_m \leq \gamma(x,t) \leq k_M. \tag{A.2}$$

Terms of perturbation are

$$\varphi(x,t) = \varphi_1(x,t) + \varphi_2(x,t)$$

such that the first term is vanishing at the origin bounded by

$$|\varphi_1(x,t)| \leq \alpha|\phi_1(x)| \tag{A.3}$$

and the second term has its total derivative such that

$$\frac{d}{dt}\left(\frac{\varphi_2(x,t)}{\gamma(x,t)}\right) = \underbrace{\frac{1}{\gamma}\frac{\partial\varphi_2}{\partial t} - \frac{\varphi_2}{\gamma^2}\frac{\partial\gamma}{\partial t}}_{\delta_1(x_1,t)} + \underbrace{\left(\frac{1}{\gamma}\frac{\partial\varphi_2}{\partial x_1} - \frac{\varphi_2}{\gamma^2}\frac{\partial\gamma}{\partial x_1}\right)}_{\delta_2(x_1,t)}\dot{x}_1 \tag{A.4}$$

$$= \delta_1(x_1,t) + \delta_2(x_1,t)\dot{x}_1 \tag{A.5}$$

Moreover, the partial derivatives of the perturbation are bounded by positive constants

$$|\delta_1(x_1,t)| \leq \quad \bar{\delta}_1, \quad |\delta_2(x_1,t)| \leq \quad \bar{\delta}_2. \tag{A.6}$$

A.1.2 Closed-Loop

System (A.1) closed-loop with the Generalized STA can be written as

$$\dot{x} \quad = -k_1\gamma(x,t)\phi_1(x) + \varphi_1(x,t) + \gamma(x,t)\left[z + \tfrac{\varphi_2(x,t)}{\gamma(x,t)}\right],$$

and expressing the system with the change of variables $x_1 = x$ and $x_2 = z + \frac{\varphi_2(x_1,t)}{\gamma(x_1,t)}$, with $\bar{x} = [x_1 \quad x_2]^T$,

$$\dot{x}_1 = \gamma(x_1,t)\left[-k_1\phi_1(x_1) + \frac{\varphi_1(x,t)}{\gamma(x_1,t)} + x_2\right], \tag{A.7a}$$

$$\dot{x}_2 = -k_2\phi_2(x_1) + \frac{d}{dt}\left(\frac{\varphi_2(x_1,t)}{\gamma(x_1,t)}\right) \tag{A.7b}$$

The first equation can be rewritten as

$$\dot{x}_1 = \gamma(x_1,t)\left(-\tilde{k}_1\phi_1(x_1) + x_2\right)$$

where

$$\tilde{k}_1 = k_1 - \frac{\varphi_1(x,t)}{\gamma(x_1,t)\phi_1(x_1)}, \tag{A.8}$$

and note that from (A.2) and (2.9),

$$\left|\frac{\varphi_1(x,t)}{\gamma(x_1,t)\phi_1(x_1)}\right| \leq \frac{\alpha}{\gamma(x_1,t)}\frac{|\phi_1(x_1)|}{\phi_1(x_1)} \leq \frac{\alpha}{k_m}.$$

From (3.5), we rewrite the second equation as

$$\begin{aligned}
\dot{x}_2 &= -k_2\phi_2(x_1) + \delta_1(x_1,t) + \delta_2(x_1,t)\dot{x}_1 \\
&= -k_2\phi_2(x_1) + \delta_1(x_1,t) + \delta_2(x_1,t)\gamma(x_1,t)\left(-\tilde{k}_1\phi_1(x_1) + x_2\right) \\
&= -k_2\phi_2(x_1) + \delta_1(x_1,t) - \delta_2(x_1,t)\gamma(x_1,t)\tilde{k}_1\phi_1(x_1) + \delta_2(x_1,t)\gamma(x_1,t)x_2.
\end{aligned}$$

Due to the fact that $\phi_2(x_1) = \phi_1(x_1)\phi_1'(x_1)$,

$$\begin{aligned}
\dot{x}_2 &= \phi_1'(x_1)\left[-k_2\phi_1(x_1) + \frac{\delta_1(x_1,t)}{\phi_1'(x_1)} - \frac{\delta_2(x_1,t)\tilde{k}_1\gamma(x_1,t)}{\phi_1'(x_1)}\phi_1 + \frac{\delta_2(x_1,t)\gamma(x_1,t)}{\phi_1'(x_1)}x_2\right] \\
&= \gamma(x_1,t)\phi_1'(x_1)\left[-\left(\frac{k_2}{\gamma(x_1,t)} + \frac{\delta_2(x_1,t)}{\phi_1'(x_1)}\tilde{k}_1\right)\phi_1(x_1) + \frac{\delta_1(x_1,t)}{\gamma(x_1,t)\phi_1'(x_1)} + \frac{\delta_2(x_1,t)}{\phi_1'(x_1)}x_2\right].
\end{aligned}$$

A.1.3 Representation of Lyapunov candidate derivative in quadratic form

Now consider the candidate Lyapunov function

$$V = \xi^T P\xi, \quad P = \begin{bmatrix} p_1 & -1 \\ -1 & p_2 \end{bmatrix}, \quad \xi^T = [\phi_1(x_1) \;\; x_2] \tag{A.9}$$

Whose derivative along the trajectories of the system

$$\begin{aligned}
\dot{V} &= 2\phi_1'(x_1)\left[p_1\phi_1(x_1)-x_2\right]\gamma(x_1,t)\left[-\tilde{k}_1\phi_1(x_1)+x_2\right]+\\
&+ 2\left[p_2x_2-\phi_1(x_1)\right]\gamma(x_1,t)\phi_1'(x_1)\left[-\left(\frac{k_2}{\gamma(x_1,t)}+\frac{\delta_2(x_1,t)}{\phi_1'(x_1)}\tilde{k}_1\right)\phi_1(x_1)+\right.\\
&+ \left.\frac{\delta_1(x_1,t)}{\gamma(x_1,t)\phi_1'(x_1)}+\frac{\delta_2(x_1,t)}{\phi_1'(x_1)}x_2\right]\\
&= 2\gamma(x_1,t)\phi_1'(x_1)\left\{\left[p_1\phi_1(x_1)-x_2\right]\left[-\tilde{k}_1\phi_1(x_1)+x_2\right]+\right.\\
&+ \left[p_2x_2-\phi_1(x_1)\right]\left[-\left(\frac{k_2}{\gamma(x_1,t)}+\frac{\delta_2(x_1,t)}{\phi_1'(x_1)}\tilde{k}_1\right)\phi_1(x_1)+\right.\\
&+ \left.\left.\frac{\delta_1(x_1,t)}{\gamma(x_1,t)\phi_1'(x_1)}+\frac{\delta_2(x_1,t)}{\phi_1'(x_1)}x_2\right]\right\}.
\end{aligned}$$

After several algebraic manipulations, it is possible to group the terms

$$\begin{aligned}
\dot{V} &= 2\gamma(x_1,t)\phi_1'(x_1)\left\{-\left[\tilde{k}_1\left(p_1-\frac{\delta_2(x_1,t)}{\phi_1'(x_1)}\right)-\frac{k_2}{\gamma(x_1,t)}\right]\phi_1^2(x_1)+\right.\\
&+\left[\tilde{k}_1\left(1-\frac{\delta_2(x_1,t)}{\phi_1'(x_1)}\right)+p_1-p_2\frac{k_2}{\gamma(x_1,t)}-\frac{\delta_2(x_1,t)}{\phi_1'(x_1)}\right]\phi_1(x_1)x_2\\
&-\left.\left[1-\frac{p_2\delta_2(x_1,t)}{\phi_1'(x_1)}\right]x_2^2+\frac{p_2\delta_1(x_1,t)}{\gamma(x_1,t)\phi_1'(x_1)}x_2-\frac{\delta_1(x_1,t)}{\gamma(x_1,t)\phi_1'(x_1)}\phi_1(x_1)\right\}
\end{aligned}$$

The last two terms can be rewritten as

$$\frac{p_2\delta_1(x_1,t)}{\gamma(x_1,t)\phi_1'(x_1)}x_2-\frac{\delta_1(x_1,t)}{\gamma(x_1,t)\phi_1'(x_1)}\phi_1(x_1)=\frac{p_2\delta_1(x_1,t)}{\gamma(x_1,t)\phi_2(x_1)}\phi_1(x_1)x_2-\frac{\delta_1(x_1,t)}{\gamma(x_1,t)\phi_2(x_1)}\phi_1^2(x_1).$$

then, substituting,

$$\begin{aligned}
\dot{V} &= 2\gamma(x_1,t)\phi_1'(x_1)\left\{-\left[\tilde{k}_1\underbrace{\left(p_1-\frac{\delta_2(x_1,t)}{\phi_1'(x_1)}\right)}_{\tilde{p}_1}-\underbrace{\frac{1}{\gamma(x_1,t)}\left(k_2-\frac{\delta_1(x_1,t)}{\phi_2(x_1)}\right)}_{\tilde{k}_2}\right]\phi_1^2(x_1)+\right.\\
&+\left[\tilde{k}_1\underbrace{\left(1-\frac{p_2\delta_2(x_1,t)}{\phi_1'(x_1)}\right)}_{\tilde{h}}+\underbrace{p_1-\frac{\delta_2(x_1,t)}{\phi_1'(x_1)}}_{\tilde{p}_1}-\underbrace{\frac{p_2}{\gamma(x_1,t)}\left(k_2-\frac{\delta_1(x_1,t)}{\phi_2(x_1)}\right)}_{p_2\tilde{k}_2}\right]\phi_1(x_1)x_2\\
&-\left.\left[\underbrace{1-\frac{p_2\delta_2(x_1,t)}{\phi_1'(x_1)}}_{\tilde{h}}\right]x_2^2\right\}.
\end{aligned}$$

From functions on GSTA controller $\phi_1'(x) = \left(\frac{1}{2|x_1|^{\frac{1}{2}}} + \beta\right)$, and $\phi_2(x) = \frac{1}{2}\lceil x \rfloor^0 + \frac{3}{2}\beta\lceil x \rfloor^{\frac{1}{2}} + \beta^2 x$ we have

$$\left|\frac{1}{\phi_1'(x)}\right| \leq \frac{1}{\beta}; \quad \left|\frac{1}{\phi_2(x)}\right| = \left|\frac{\text{sign}\,(x)}{\frac{1}{2} + \frac{3}{2}\beta|x|^{\frac{1}{2}} + \beta^2|x|}\right| \leq 2.$$

Several terms can be grouped as *perturbed* bounded terms,

$$\begin{array}{rclcrcl}
\tilde{p}_1 & = & \left(p_1 - \frac{\delta_2(x_1,t)}{\phi_1'(x_1)}\right) & \Rightarrow & \tilde{p}_1 \in \left[\underline{p}_1, \bar{p}_1\right] & = & \left[p_1 - \frac{\bar{\delta}_2}{\beta}, p_1 + \frac{\bar{\delta}_2}{\beta}\right], \\
\tilde{k}_2 & = & \frac{1}{\gamma(x_1,t)}\left(k_2 - \frac{\delta_1(x_1,t)}{\phi_2(x_1)}\right) & \Rightarrow & \tilde{k}_2 \in \left[\underline{k}_2, \bar{k}_2\right] & = & \left[\frac{1}{k_M}\left(k_2 - 2\bar{\delta}_1\right), \frac{1}{k_m}\left(k_2 + 2\bar{\delta}_1\right)\right], \\
\tilde{k}_1 & = & k_1 - \frac{\varphi_1(x,t)}{\gamma(x_1,t)\phi_1(x_1)} & \Rightarrow & \tilde{k}_1 \in \left[\underline{k}_1, \bar{k}_1\right] & = & \left[k_1 - \frac{\alpha}{k_m}, k_1 + \frac{\alpha}{k_m}\right], \\
\tilde{h} & = & 1 - \frac{p_2\delta_2(x_1,t)}{\phi_1'(x_1)} & \Rightarrow & \tilde{h} \in \left[\underline{h}, \bar{h}\right] & = & \left[1 - \frac{p_2\bar{\delta}_2}{\beta}, 1 + \frac{p_2\bar{\delta}_2}{\beta}\right].
\end{array} \tag{A.10}$$

and rewritten in a matrix form,

$$\begin{array}{rcl}
\dot{V} & = & 2\gamma(x_1,t)\phi_1'(x_1)\left\{-\underbrace{\left[\tilde{k}_1\tilde{p}_1 - \tilde{k}_2\right]}_{q_1(t)}\phi_1^2(x_1)\right. \\
& - & \left.\underbrace{\left[p_2\tilde{k}_2 - (\tilde{k_1}\tilde{h} + \tilde{p}_1)\right]}_{q_3(t)}\phi_1(x_1)x_2 - \underbrace{\tilde{h}}_{q_2(t)}x_2^2\right\} \\
& = & -2\gamma(x_1,t)\phi_1'(x_1)\xi^T Q(t)\xi
\end{array} \tag{A.11}$$

where

$$Q(t) = \begin{bmatrix} q_1(t) & q_3(t) \\ q_3(t) & q_2(t) \end{bmatrix} = \begin{bmatrix} \tilde{k}_1\tilde{p}_1 - \tilde{k}_2 & \frac{1}{2}\left(p_2\tilde{k}_2 - (\tilde{k_1}\tilde{h} + \tilde{p}_1)\right) \\ \frac{1}{2}\left(p_2\tilde{k}_2 - (\tilde{k_1}\tilde{h} + \tilde{p}_1)\right) & \tilde{h} \end{bmatrix}. \tag{A.12}$$

If matrix $Q(t)$ is positive definite then the time derivative $\dot{V}$ is negative definite.

A.1.4 Positiveness of matrix $Q(t)$

The determinant of matrix $Q(t)$ can be expressed as

$$\det Q(t) = a_{\tilde{p}_1}\tilde{p}_1^2 + b_{\tilde{p}_1}\tilde{p}_1 + c_{\tilde{p}_1}, \tag{A.13}$$

where

$$\begin{array}{rcl}
a_{\tilde{p}_1} & = & -\frac{1}{4}, \\
b_{\tilde{p}_1} & = & \frac{1}{2}\left(\tilde{h}\tilde{k}_1 + \tilde{k}_2 p_2\right), \\
c_{\tilde{p}_1} & = & -\frac{1}{4}\left(\tilde{h}\tilde{k}_1 - \tilde{k}_2 p_2\right)^2 - \tilde{h}\tilde{k}_2.
\end{array}$$

Note that the coefficient $a_{\tilde{p}_1}$ is negative, then, in order to get the positiveness of $\det Q(t)$, the discriminant of the second degree equation $\det Q(t) = 0$ must be positive, and the constant value p_1 should be selected within the interval defined by the

two real roots of $\det Q(t) = 0$.

$$\Delta_{\tilde{p}_1}(x_1,t) = b_{p_1}^2 - 4a_{p_1}c_{p_1} = \tilde{h}\tilde{k}_2\left(\tilde{k}_1 p_2 - 1\right) > 0, \tag{A.14}$$

For the $\tilde{h} > 0$ factor

$$1 > \frac{\delta_2(x,t)p_2}{\phi_1'(x_1)} \tag{A.15}$$

$$\frac{1}{p_2} > \frac{\bar{\delta}_2}{\beta}. \tag{A.16}$$

For $\tilde{k}_2 > 0$ factor

$$k_2 > 2\bar{\delta}_1.$$

For $\tilde{k}_1 p_2 - 1 > 0$ factor, we get $p_2 > \frac{1}{\tilde{k}_1}$, and taking into account (A.10)

$$p_2 > \frac{1}{k_1 - \frac{\alpha}{k_m}}$$

$$p_2 > \frac{k_m}{k_1 k_m - \alpha}$$

Then, a possible selection of p_2 is

$$p_2 = \frac{k_m + \epsilon}{k_1 k_m - \alpha}, \quad \text{for } \epsilon > 0. \tag{A.17}$$

Finally, from (A.16) and (A.17) we get $\frac{k_1 k_m - \alpha}{k_m + \epsilon} > \frac{\bar{\delta}_2}{\beta}$, and consequently

$$k_1 > \frac{\bar{\delta}_2}{\beta}\frac{(k_m + \epsilon)}{k_m} + \frac{\alpha}{k_m}. \tag{A.18}$$

The two real roots of the quadratic equation $\det Q(t) = 0$ are

$$p_1^+ = \tilde{h}\tilde{k}_1 + \tilde{k}_2 p_2 + \frac{\delta_2(x,t)}{\phi_1'(x_1)} + 2\sqrt{\Delta_{\tilde{p}_1}(x_1,t)}. \tag{A.19a}$$

$$p_1^- = \underbrace{\tilde{h}\tilde{k}_1 + \tilde{k}_2 p_2 + \frac{\delta_2(x,t)}{\phi_1'(x_1)}}_{p_{1c}} - 2\sqrt{\Delta_{\tilde{p}_1}(x_1,t)}. \tag{A.19b}$$

The two real roots define the endpoints of an interval wich is a set of all possible values for p_1 such that $Q(t) > 0$. However, the endpoints are dependent on perturbed bounded terms ($\tilde{h}$, $\tilde{k}_1$, $\tilde{k}_2$ and $\delta_2(x,t)/\phi_1'(x_1)$) which make each endpoint to move from a minumum value (p_{1min}^+, p_{1min}^-) to a maximum value (p_{1Max}^+, p_{1Max}^-). A valid selection of a constant p_1 must belong to an intersection set between the minor endpoint at its maximum value (p_{1Max}^-) and the maximum end point at its minumum value (p_{1min}^+) as shown in Figure A.1.

$$p_1 \in \left(p_{1Max}^-, p_{1min}^+\right). \tag{A.20}$$

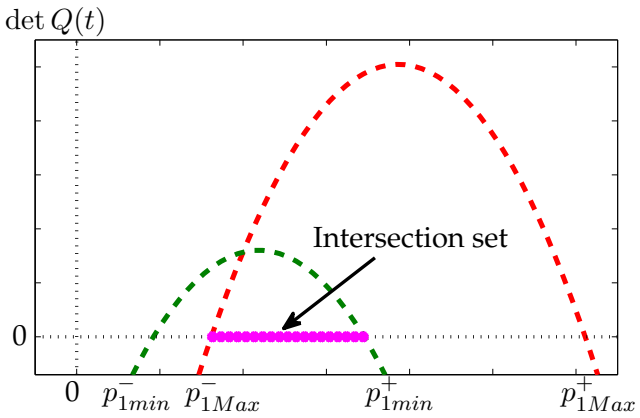

FIGURE A.1: Intersection set: Possible values for selecting p_1.

Some possible bounds for the terms in (A.19) are $0 < \underline{p}_{1c} \leq p_{1c} \leq \bar{p}_{1c}$, and $0 < \underline{\Delta}_{\tilde{p}_1}(x_1,t) \leq \Delta_{\tilde{p}_1}(x_1,t) \leq \bar{\Delta}_{\tilde{p}_1}(x_1,t)$, where

$$\begin{aligned}
\bar{p}_{1c} &= \bar{h}\bar{k}_1 + \bar{k}_2 p_2 - \frac{\bar{\delta}_2}{\beta}, \\
\underline{p}_{1c} &= \underline{h}\underline{k}_1 + \underline{k}_2 p_2 + \frac{\bar{\delta}_2}{\beta}, \\
\bar{\Delta}_{\tilde{p}_1}(x_1,t) &= \bar{h}\bar{k}_2\left(\bar{k}_1 p_2 - 1\right), \\
\underline{\Delta}_{\tilde{p}_1}(x_1,t) &= \underline{h}\underline{k}_2\left(\underline{k}_1 p_2 - 1\right).
\end{aligned}$$

and note that possible upper and lower bounds for p^-_{1Max}, p^+_{1min} are

$$p^-_{1Max} \geq \bar{h}\bar{k}_1 + \bar{k}_2 p_2 - \frac{\bar{\delta}_2}{\beta} - 2\sqrt{\underline{h}\underline{k}_2\left(\underline{k}_1 p_2 - 1\right)} \tag{A.21}$$

$$p^+_{1min} \leq \underline{h}\underline{k}_1 + \underline{k}_2 p_2 + \frac{\bar{\delta}_2}{\beta} + 2\sqrt{\underline{h}\underline{k}_2\left(\underline{k}_1 p_2 - 1\right)}. \tag{A.22}$$

Then p_1 should be selected within

$$p_1 \in \left(\bar{h}\bar{k}_1 + \bar{k}_2 p_2 - \frac{\bar{\delta}_2}{\beta} - 2\sqrt{\underline{h}\underline{k}_2\left(\underline{k}_1 p_2 - 1\right)}, \underline{h}\underline{k}_1 + \underline{k}_2 p_2 + \frac{\bar{\delta}_2}{\beta} + 2\sqrt{\underline{h}\underline{k}_2\left(\underline{k}_1 p_2 - 1\right)}\right). \tag{A.23}$$

A.1.5 Intersection set

In order to guarantee a non-empty intersection set the next condition must hold

$$p^+_{1min} > p^-_{1Max}. \tag{A.24}$$

Then, (A.24) can be rewritten as

$$\underline{p}_{1c} + 2\sqrt{\underline{\Delta}_{\tilde{p}_1}(x_1,t)} > \bar{p}_{1c} - 2\sqrt{\underline{\Delta}_{\tilde{p}_1}(x_1,t)}.$$

After several algebraic manipulations, the last inequality can be expressed as

$$a_{k_2} K_2^2 + b_{k_2} K_2 + c_{k_2} > 0, \tag{A.25}$$

where

$$\begin{aligned} a_{k_2} &= -\tfrac{(1+\epsilon)(k_M-k_m)}{\underline{k}_1 k_m}, \\ b_{k_2} &= 4\sqrt{\underline{h}\epsilon}, \\ c_{k_2} &= -\tfrac{2(1+\epsilon)}{\underline{k}_1 k_m}\left(\tfrac{\bar{\delta}_2\alpha}{\beta}+2\bar{\delta}_1\right)-2\left(\tfrac{\bar{\delta}_2\epsilon}{\beta}+\tfrac{\alpha}{k_m}\right), \end{aligned}$$

and with a change of variable $K_2^2 = \underline{k}_2$.

Solutions of the last inequality belong to the interior of the interval defined by

$$\begin{aligned} K_2 &= \frac{-b_{k_2}}{2a_{k_2}} \pm \frac{2\sqrt{\Delta_{k_2}}}{2a_{k_2}} \\ &= \frac{2\sqrt{\underline{h}\epsilon}\underline{k}_1 k_m}{(1+\epsilon)(k_M-k_m)} \pm \frac{\underline{k}_1 k_m}{2(1+\epsilon)(k_M-k_m)}\sqrt{\Delta_{k_2}} \end{aligned}$$

where

$$\Delta_{k_2} = b_{k_2}^2 - 4a_{k_2}c_{k_2} = 16\underline{h}\epsilon - 8\left(\frac{(1+\epsilon)(k_M-k_m)}{\underline{k}_1 k_m}\right)\left(\frac{(1+\epsilon)}{\underline{k}_1 k_m}\left[\frac{\bar{\delta}_2\alpha}{\beta}+2\bar{\delta}_1\right]+\frac{\bar{\delta}_2\epsilon}{\beta}+\frac{\alpha}{k_m}\right).$$

Finally, gain k_2 can be selected within the interval

$$k_2 \in \left(k_M\left(2\sqrt{\underline{h}\epsilon}\bar{c}-\frac{\bar{c}}{2}\sqrt{\Delta_{k_2}}\right)^2+2\bar{\delta}_1, k_M\left(2\sqrt{\underline{h}\epsilon}\bar{c}+\frac{\bar{c}}{2}\sqrt{\Delta_{k_2}}\right)^2+2\bar{\delta}_1\right), \tag{A.26}$$

$$\underline{h} = 1-\frac{\bar{\delta}_2}{\beta}\frac{k_m+\epsilon}{(k_1 k_m-\alpha)}, \quad \bar{c} = \frac{\underline{k}_1 k_m}{(1+\epsilon)(k_M-k_m)}, \quad \underline{k}_1 = k_1-\frac{\alpha}{km}.$$

A.1.6 Guarantee the existence of the interval for gain k_2

In order to have an interval between two real roots, the discriminant Δ_{k_2} must be greater or equals to zero $\Delta_{k_2} \geq 0$. It is possible to express the last inequality as

$$a_{k_1}\underline{k}_1^2 + b_{k_1}\underline{k}_1 + c_{k_1} > 0 \tag{A.27}$$

where

$$\begin{aligned} a_{k_1} &= 16\epsilon, \\ b_{k_1} &= -\tfrac{8(1+\epsilon)}{k_m}\left(\tfrac{\alpha}{k_m}(k_M-k_m)+\tfrac{\bar{\delta}_2\epsilon}{\beta}(k_M+k_m)\right), \\ c_{k_1} &= -\tfrac{8(1+\epsilon)^2}{k_m^2}(k_M-k_m)\left(\tfrac{\bar{\delta}_2\alpha}{\beta}+2\bar{\delta}_1\right). \end{aligned}$$

It is worth it to note that, the coefficient a_{k_1} is positive and the discriminant $\Delta_{k_1} = b_{k_1}^2 - 4a_{k_1}c_{k_1}$ of (A.27) is always positive

$$\Delta_{k_1} = \frac{64(1+\epsilon)^2}{k_m^2}\left[\underbrace{\left(\frac{\alpha}{k_m}(k_M-k_m)+\frac{\bar{\delta}_2\epsilon}{\beta}(k_M+k_m)\right)^2+8\epsilon(kM-km)\left(\frac{\bar{\delta}_2\alpha}{\beta}+2\bar{\delta}_1\right)}_{\Lambda_{k_1}}\right] > 0.$$

Then, there is always possible to find a gain k_1 to ensure the existence of a valid selection interval for the gain k_2. Selecting the k_2 gain, is possible to ensure that the interior set of parables p_1 is not empty, and therefore, to ensure the positiveness of

$\det Q(t)$. Gain k_1 can be selected as

$$k_1 > \frac{-b_{k_2}}{2a_{k_2}} + \frac{\sqrt{b_{k_2}^2 - 4a_{k_2}c_{k_2}}}{2a_{k_2}} + \frac{\alpha}{k_m}, \tag{A.28}$$

$$> \frac{(1+\epsilon)}{4\epsilon k_m}\left(\frac{\alpha}{k_m}(k_M - k_m) + \frac{\bar{\delta}_2\epsilon}{\beta}(k_M + k_m)\right) + \frac{(1+\epsilon)}{4\epsilon k_m}\sqrt{\Lambda_{k_1}} + \frac{\alpha}{k_m}. \tag{A.29}$$

We have shown that if (A.29) and (A.26) are satisfied, $\det Q(t) > 0$. However the condition (A.29) does not imply (A.18) for every case. Condition (A.18) and (A.29) when $\delta_1(x_1, t) = 0$, $\alpha = 0$ are

$$k_1 > \frac{\bar{\delta}_2}{\beta}\left(1 + \frac{\epsilon}{k_m}\right), \quad k_1 > \frac{(1+\epsilon)}{2k_m}\frac{\bar{\delta}_2}{\beta}(k_M + k_m) \tag{A.30}$$

by modifying the factor $(k_M + k_m)$ to $(k_M + k_m + 2)$ we achieve

$$\frac{\bar{\delta}_2}{\beta}\left(1 + \frac{\epsilon}{k_m}\right) \leq \frac{(1+\epsilon)}{2}\frac{\bar{\delta}_2}{\beta}\left(\frac{k_M}{k_m} + 1 + \frac{2}{k_m}\right) \tag{A.31}$$

$$\frac{\bar{\delta}_2}{\beta} + \frac{\bar{\delta}_2}{\beta}\frac{\epsilon}{k_m} \leq \frac{\bar{\delta}_2}{2\beta}\left(\frac{k_M}{k_m} + 1\right) + \frac{\bar{\delta}_2}{\beta}\frac{\epsilon}{k_m} + \frac{\bar{\delta}_2}{\beta k_m} + \frac{\epsilon\bar{\delta}_2}{2\beta}\left(\frac{k_M}{k_m} + 1\right). \tag{A.32}$$

then (A.29) always imply (A.18).

Finally, condition (A.29) ensures that the term $\tilde{h} = q_2(t) > 0$. It can be seen that if $\det Q(t) = q_1(t)q_2(t) - q_3^2(t) > 0$ and $q_2(t) > 0$, $q_1(t)$ is also positive definite. Therefore, matrix $Q(t)$ is positive definite.

A.1.7 Finite-time convergence and Convergence Time

Based on Moreno, 2009, recall the standard inequality for quadratic forms

$$\lambda_{min}\{P\}||\xi||_2^2 \leq \xi^T P\xi \leq \lambda_{max}\{P\}||\xi||_2^2,$$

and

$$||\xi||_2^2 = \xi_1^2 + \xi_2^2 = \phi_1^2(x_1) + x_2^2 = |x_1| + 2\beta|x_1|^{\frac{3}{2}} + \beta^2 x_1^2 + x_2^2 \tag{A.33}$$

is the Euclidean norm of ξ, and note that the inequality

$$|x_1|^{\frac{1}{2}} \leq ||\xi||_2 \leq \frac{V^{\frac{1}{2}}(x_1, x_2)}{\lambda_{min}^{\frac{1}{2}}\{P\}}$$

is satisfied. Since $Q(t)$ is definite positive and all its elements are bounded, then $Q(t) - \varepsilon\mathbb{I} > 0$, for $\varepsilon > 0$ and $\mathbb{I}$ the identity matrix, we can rewrite

$$\begin{aligned}
\dot{V} &\leq -2\gamma(x_1, t)\phi_1'(x_1)\xi^T Q(t)\xi \leq -2k_m\phi_1'(x_1)\xi^T\varepsilon\mathbb{I}\xi \\
&\leq -2k_m\varepsilon\phi_1'(x_1)||\xi||_2^2 \leq -\frac{k_m\varepsilon}{|x_1|^{\frac{1}{2}}}||\xi||_2^2 - 2k_m\varepsilon\beta||\xi||_2^2 \\
&\leq -\frac{k_m\varepsilon\lambda_{min}^{\frac{1}{2}}\{P\}}{\lambda_{max}\{P\}}V^{\frac{1}{2}}(x_1, x_2) - \beta\frac{2k_m\varepsilon}{\lambda_{max}\{P\}}V(x_1, x_2) \\
&\leq -\mu_1 V^{\frac{1}{2}}(x_1, x_2) - \mu_2 V(x_1, x_2),
\end{aligned}$$

where

$$\mu_1 = \frac{k_m \varepsilon \lambda_{min}^{\frac{1}{2}}\{P\}}{\lambda_{max}\{P\}}, \quad \mu_2 = \beta \frac{2k_m \varepsilon}{\lambda_{max}\{P\}}.$$

that shows that the system trajectories converge in finite time.

Since the solution of the differential equation

$$\dot{v} = -\mu_1 v^{\frac{1}{2}} - \mu_2 v, \quad v(0) = v_0 \geq 0$$

is given by

$$v(t) = \exp\left(-\mu_2 t\right)\left[v_0^{\frac{1}{2}} + \frac{\mu_1}{\mu_2}\left(1 - \exp\left(\frac{\mu_2}{2}t\right)\right)\right]^2,$$

if $\mu_1 \geq 0$ and $\mu_2 > 0$. If follows from (A.34) and the comparison principle that $V(t) \leq v(t)$, when $V(x_1(0), x_2(0)) \leq v_0$. Therefore, $x_1(t)$ and $x_2(t)$ converge to zero in finite-time and reaches that value at most after a time given by

$$T = \frac{2}{\mu_2} \ln\left(\frac{\mu_2}{\mu_1} V^{\frac{1}{2}}(x_1(0), x_2(0)) + 1\right) \tag{A.34}$$

A.1.8 Proof of Theorem 2

When there is no uncertain control coefficient, the bounds of the function $\gamma(x_1, t)$ are, with loss of generality

$$k_M = k_m = 1$$

and quadratic term in inequality (A.25) become zero. Then, the condition for gain k_2 is

$$k_2 > \frac{1}{16\underline{h}\epsilon} c_{k_2}^2 + 2\bar{\delta}_1 \tag{A.35a}$$

$$> \frac{1}{4\underline{h}\epsilon}\left(\frac{(1+\epsilon)}{(k_1 - \alpha)}\left(\frac{\bar{\delta}_2 \alpha}{\beta} + 2\bar{\delta}_1\right) + \frac{\bar{\delta}_2 \epsilon}{\beta} + \alpha\right)^2 + 2\bar{\delta}_1 \tag{A.35b}$$

Condition from quadratic inequality (A.27) reduces to

$$k_1 > \frac{2(1+\epsilon)\bar{\delta}_2}{\beta} + \alpha, \tag{A.36}$$

the same as in (A.18).

Proof of the Corollary 1

When there is no state dependent perturbations, the function $\delta_2(x,t) = 0$, then the conditions are simply reduced as

$$k_2 \in \left[k_M\left(2\sqrt{\epsilon}\bar{c} - \frac{\bar{c}}{2}\sqrt{\Delta_{k_2}}\right)^2 + 2\bar{\delta}_1, k_M\left(2\sqrt{\epsilon}\bar{c} + \frac{\bar{c}}{2}\sqrt{\Delta_{k_2}}\right)^2 + 2\bar{\delta}_1\right], \tag{A.37}$$

$$\Delta_{k_2} = 16\epsilon - 8\left(\frac{(1+\epsilon)(k_M - k_m)}{\underline{k}_1 k_m}\right)\left(\frac{(1+\epsilon)}{\underline{k}_1 k_m} 2\bar{\delta}_1 + \frac{\alpha}{k_m}\right).$$

$$\underline{h} = 1 - \frac{\bar{\delta}_2}{\beta}\frac{k_m + \epsilon}{(k_1 k_m - \alpha)}, \quad \bar{c} = \frac{\underline{k}_1 k_m}{(1+\epsilon)(k_M - k_m)}, \quad \underline{k}_1 = k_1 - \frac{\alpha}{km}.$$

Gain k_1 can be selected as

$$k_1 > \frac{(1+\epsilon)}{4\epsilon k_m}\left(\frac{\alpha}{k_m}(k_M-k_m)\right)+\frac{(1+\epsilon)}{4\epsilon k_m}\sqrt{\Lambda_{k_1}}+\frac{\alpha}{k_m}. \tag{A.38}$$

$$\Lambda_{k_1}=\left(\frac{\alpha}{k_m}(k_M-k_m)\right)^2+16\epsilon(k_M-k_m)\bar{\delta}_1.$$

A.2 Saturated Super-Twisting Algorithm: Stability Analysis

A.2.1 Saturated STA without perturbation estimator.

When control law (4.3) is in the state $s=0$ (RC behavior), system (4.1) in closed-loop is

$$\Sigma_1:\begin{cases}\dot{x}_1=-\rho\text{sign}\,(x_1)+\phi(t)\\ \dot{z}=0,\end{cases}$$

with $x_1=x$, $z(0)=0$. Note that the integrator dynamics is kept equal to zero and the order of Σ_1 can be considered as one. On the other hand, when the condition $s=1$ holds (STA behavior), system (4.1) in closed-loop is

$$\Sigma_2:\begin{cases}\dot{x}_1=-\alpha_1\lceil x_1\rfloor^{1/2}+x_2\\ \dot{x}_2=-\alpha_2\text{sign}\,(x_1)+\dot{\phi}(t)\end{cases}$$

with $x_1=x$, $x_2=z+\phi(t)$, and $\bar{x}=[x_1 \quad x_2]^T$. The order of the dynamics is two.

Nominal Case

Consider function

$$V_c(x_1)=c_1|x_1|,\ c_1>0, \tag{A.39}$$

as a Lyapunov candidate for the system Σ_1 without perturbations, i.e. function $\phi(t)=0$. Since the time derivative along the trajectories of the system is

$$\dot{V}_c(x_1)=-c_1\rho<0,$$

then,(A.39) is a strict Lyapunov function for the nominal system Σ_1.

Now consider the function $V_s(\xi)$ in Moreno and Osorio, 2012, with respect to the vector $\xi^T=[\xi_1 \quad \xi_2]=\left[|x_1|^{1/2}\text{sign}\,(x_1) \quad x_2\right]$, as a Lyapunov candidate for the system Σ_2 without perturbations ($\phi(t)=0$) Moreno and Osorio, 2012

$$V_s(\bar{x})=\xi^TP\xi,\quad P=\begin{bmatrix}p_{11} & -p_{12}\\ -p_{12} & p_{22}\end{bmatrix}>0, \tag{A.40}$$

with P being a constant, symmetric and positive definite matrix, as a strict Lyapunov function candidate. Since the derivative of the vector ξ is given by

$$\dot{\xi}=\frac{1}{|x_1|^{1/2}}A\xi,\quad A=\begin{bmatrix}-\frac{1}{2}\alpha_1 & \frac{1}{2}\\ -\alpha_2 & 0\end{bmatrix};$$

the derivative along the trajectories of the unperturbed system Σ_2 is

$$\dot{V}_s(\bar{x})=-\frac{1}{|x_1|^{1/2}}\xi^TQ\xi\le 0,$$

where P and Q are related by the Algebraic Lyapunov Equation (ALE) $A^TP+PA=-Q$. Since A is Hurwitz iff $\alpha_1>0$, $\alpha_2>0$, for every $Q=Q^T>0$ there exists a solution $P=P^T>0$ for the ALE; Therefore, V_s is a strict Lyapunov function for the nominal system Σ_2. Moreover, a trajectory starting at any initial condition $\bar{x}_0$ at time $t=0$ reaches the origin in a time smaller than $T_s(\bar{x}_0)$,

$$T_s(\bar{x}_0)=\frac{2}{\gamma_1}V^{1/2}(\bar{x}_0),\quad \gamma_1=\frac{\lambda_{min}^{1/2}\{P\}\lambda_{min}^{1/2}\{Q\}}{\lambda_{max}^{1/2}\{P\}} \tag{A.41}$$

where γ_1 is a constant depending on the gains α_1, α_2, and Q as shown in Moreno and Osorio, 2012. $\lambda_{min}\{\cdot\}$ and $\lambda_{max}\{\cdot\}$ represent the minimum and maximum eigenvalues of the argument.

Positive Invariant Sets

To prove the stability of the combination of systems Σ_1 and Σ_2, it will be shown that the trajectories of system (4.1) reach a positively invariant set (PINS) Ω_δ with respect to Σ_1 in finite time. If Ω_δ is a subset of a second PINS Ω_s with respect to Σ_2, then, the set Ω_s is also reached in finite-time. In this second set $|u_{STA}|\leq\rho$ has to be satisfied for every $\xi\in\Omega_s$. Then, as $\dot{V}_s\leq 0$ holds for every ξ in Ω_s, the trajectories will converge to the origin in finite time fulfilling (4.2b).

STA is a state feedback control law $u=u_{STA}(x,z)$ with integral action that introduces a dynamical extension in the closed-loop system. The saturation of the control signal $|u_{STA}(x,z)|=\rho$ can be interpreted as the curves $z=\pm\rho+\alpha_1\lceil x_1\rfloor^{\frac{1}{2}}$ in the phase plane (x,z) (see Fig. A.2). We define the set $\Omega_\rho=\{(x,z)\in\mathbb{R}^2\mid |z-\alpha_1\lceil x_1\rfloor^{\frac{1}{2}}|\leq\rho\}$ where the control signal does not exceed the saturation level, see the region between the two black-dashed lines in Fig. A.2. Evaluating Lyapunov function $V_s(x,z)$ in the curve $z=\rho+\alpha_1\xi_1$ (the second curve $z=-\rho+\alpha_1\xi_1$ omitted for symmetry) we get

$$\begin{aligned}V_s(x,\rho+\alpha_1\xi_1)=\ & (p_{22}\alpha_1^2-2p_{12}\alpha_1+p_{11})|x|+\\ & +(2\alpha_1p_{22}\rho-2p_{12}\rho)\lceil x\rfloor^{\frac{1}{2}}+p_{22}\rho^2.\end{aligned}$$

The minimum value of this function is obtained and used as the constant for the Lyapunov level curve,

$$V_s(x,z)=c_s, \tag{A.42}$$

where

$$c_s=\rho^2\gamma_2,\quad \gamma_2=\frac{(p_{11}p_{22}-p_{12}^2)}{p_{22}\alpha_1^2-2p_{12}\alpha_1+p_{11}} \tag{A.43}$$

is a constant depending on the elements of the matrix P of (A.40) and α_1. The maximum sublevel set of $V_s(x,z)$ contained in Ω_ρ is $\Omega_s=\{(x,z)\in\Omega_\rho\mid V_s\leq c_s\}$, where the derivative $\dot{V}_s$ is negative for every (x,z). (see Fig. A.2).

On the other hand, as V_c is a Lyapunov function for Σ_1, the set $\Omega_\delta=\{(x,z)\in\mathbb{R}^2\mid V_c\leq c_1\delta, z=0\}$ is a PINS with respect to Σ_1, see Fig. A.2. Moreover, the one-dimensional set Ω_δ will be a subset of the two-dimensional set Ω_s if δ is smaller than the endpoints of the interval defined by

$$V_s(x,0)=p_{11}|x|\leq c_s\quad\Rightarrow\quad |x|\leq\frac{c_s}{p_{11}}.$$

Then, if the parameter δ is selected within

$$0 \leq \delta \leq \frac{c_s}{p_{11}}, \tag{A.44}$$

Ω_δ is a subset of Ω_s.

Let's define $\Lambda = \{x \in \mathbb{R} \mid c_1\delta \leq V_c \leq c_1|x_0|\}$ for some initial condition $x_0 = x(0)$. In this set, Lyapunov function (A.39) satisfies

$$\dot{V}_c = -c_1\rho, \quad \forall x_1 \in \Lambda \tag{A.45}$$

Since $\dot{V}_c$ is negative in Λ, every trajectory starting in Λ must move in a direction of decreasing V_c. In fact, the trajectories behaves as if the origin was finite-time stable. The function V_c will continue decreasing until the trajectory enters Ω_δ in finite-time and stays therein for all future time.

Note that if $c_1 = 1/\rho$, equation (A.45) becomes $\dot{V}_c = -1$, and for $t_0 = 0$,

$$V_c(x) = V_c(x_0) - t = \frac{|x_0|}{\rho} - t.$$

This shows that V_c reduces to δ/ρ in time

$$T_c(x_0, \rho, \delta) = \frac{|x_0| - \delta}{\rho}. \tag{A.46}$$

Once the trajectories have entered the set Ω_δ, the finite-time convergence of trajectories to the origin is ensured by the dynamics of system Σ_2 in set Ω_s, and the total convergence time can be estimated as

$$T_T = T_c(x_0, \rho, \delta) + T_s(\bar{x}_\delta).$$

where $\bar{x}_\delta = [\delta, \ 0]^T$, $T_s(\bar{x}_\delta) = (p_{11}|\delta|)^{1/2}$ according to (A.41)■

A.2.2 Perturbed Case

We will show that the functions (A.39) and (A.40) are also Lyapunov functions for the perturbed systems $\Sigma_{1,2}$, if the gains are properly selected.

Relay Controller

Consider function (A.39) as Lyapunov function candidate for the perturbed system Σ_1 with perturbation $\phi = \phi(t)$. The time derivative along the trajectories of the system is

$$\begin{aligned} \dot{V}_c(x) &= c_1 sign(x)\left(-\rho sign(x) + \phi(t)\right) \\ &= -c_1\rho + c_1 sign(x)\phi(t) \\ &\leq -c_1(\rho - \phi_{max}). \end{aligned}$$

Assuming that the perturbation bound is less than the saturation level, i.e. $\rho = \phi_{max} + \epsilon_\rho$ such that $\rho > \phi_{max}$ is fulfilled, i.e. $\epsilon_\rho > 0$, yields

$$\dot{V}_c(x) \leq -c_1\epsilon_\rho < 0.1 \tag{A.47}$$

Then, (A.39) is also a Lyapunov function for the perturbed closed-loop system Σ_1.

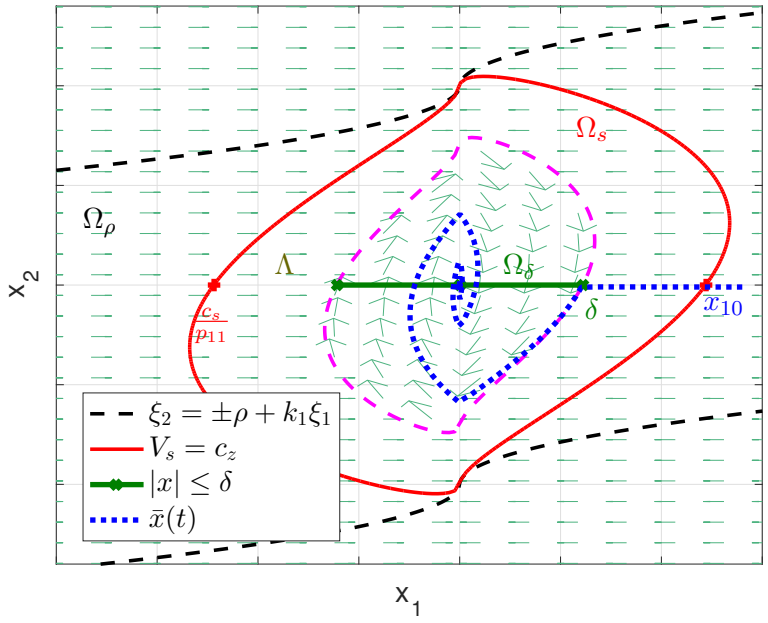

FIGURE A.2: Phase Plane: Subset Ω_ρ where $|u| \leq \rho$ holds (black-dashed). PINS Ω_s with respect to Σ_2 (red). PINS Ω_δ with respect to Σ_1 (green). Set Λ (brown). A trajectory of the system beginning in x_0, switches to the STA behavior when it comes inside Ω_δ (blue).

Super-Twisting Algorithm

Consider the Lyapunov function of the form (A.40), where

$$P = \begin{bmatrix} p_{11} & -p_{12} \\ -p_{12} & p_{22} \end{bmatrix} = \frac{1}{2}\begin{bmatrix} 4\alpha_2 + \alpha_1^2 & -\alpha_1 \\ -\alpha_1 & 2 \end{bmatrix} > 0. \tag{A.48}$$

as candidate for the perturbed system Σ_2 Moreno and Osorio, 2008. Recalling Moreno and Osorio, 2008, Theorem 3: Suppose that the perturbation term of the system Σ_2 is globally bounded by (4.2a) for some positive constant $L \geq 0$. Then the origin $x = 0$ is an equilibrium point that is globally finite-time stable if the gains satisfy (4.4). Moreover, all trajectories converge to the origin in a time upper-bounded by

$$\tilde{T}_s(\bar{x}_0) = \frac{2}{\tilde{\gamma}_1} V_s^{1/2}(\bar{x}_0), \quad \tilde{\gamma}_1 = \frac{\lambda_{min}^{1/2}\{P\}\lambda_{min}^{1/2}\{\tilde{Q}\}}{\lambda_{max}^{1/2}\{P\}}.$$

with

$$\tilde{Q} = \frac{\alpha_1}{2}\begin{bmatrix} 2\alpha_2 + \alpha_1^2 - 2L & -\left(\alpha_1 + \frac{2L}{\alpha_1}\right) \\ -\left(\alpha_1 + \frac{2L}{\alpha_1}\right) & 1 \end{bmatrix}.$$

The time derivative along the trajectories of the system is

$$\dot{V}_s(\bar{x}) = -\frac{1}{|x_1|^{1/2}}\xi^T Q \xi + \dot{\phi}(t) q_2^T \xi,$$

where $q_2^T = [-\alpha_1 \quad 2]$. Using the bounds on the perturbation it can be shown that

$$\dot{V}_s(\bar{x}) \leq -\frac{1}{|x_1|^{1/2}}\xi^T \tilde{Q}\xi.$$

$\dot{V}$ is negative definite if $\tilde{Q} > 0$. It is easy to see that this is the case if the gains are as in (4.4).

Positive Invariant Sets

In the perturbed system case, it is not possible to evaluate the Lyapunov function $V_s(x_1, x_2)$, since $x_2 = z + \phi(t)$, and the perturbation is unknown. Then, it is necessary to find any possible PINS in the $(x_1, z) \in \mathbb{R}^2$ space to ensure that the trajectories of the system does not exceed the bound of the control signal. Convergence of x_2 to zero in finite-time implies that z converges to $-\phi(t)$. Then, in the phase plane (x_1, z), the perturbation $\phi(t)$ acts as displacements of the equilibrium point along the z axis, see Fig. 4.3. A sublevel set whose boundary intersects the curve $z = \rho + \alpha_1\xi_1$ in one point is defined by

$$V_s(\xi_1, z - \phi_{max}) \leq c_\rho, \quad c_\rho = (\phi_{max} - \rho)^2\gamma_2. \tag{A.49}$$

A sublevel set whose boundary intersects the axis $z = 0$ in two points when $\delta > 0$ (and at the origin when $\delta = 0$) is defined by

$$V_s(\xi_1, -\phi_{max}) \leq c_\delta,$$

$$c_\delta = \delta p_{11} + \phi_{max}^2 p_{22} + 2\phi_{max}\sqrt{\delta}p_{12}. \tag{A.50}$$

Both conditions are obtained by setting $c_\rho = c_\delta$, and solving for ϕ_{max}, we get the maximum allowed bound for the perturbation

$$\phi_{max} \leq \frac{\gamma_2\rho + \sqrt{\delta}p_{12} - \sqrt{\gamma_3}}{\gamma_2 - p_{22}}, \tag{A.51}$$

where $\gamma_3 = (p_{12}^2 + \gamma_2 p_{11} - p_{11}p_{22})\delta + 2\gamma_2 p_{12}\rho\sqrt{\delta} + \gamma_2 p_{22}\rho^2$. Finally, from (A.43), (A.44), and (A.48) we get (4.5) and (4.6).

A.2.3 Saturated STA with perturbation estimator.

The error dynamics of estimator (4.10) are

$$\begin{aligned} \dot{e}_1 &= -\beta_1 \lceil e_1 \rfloor^{1/2} + e_2 \\ \dot{e}_2 &= -\beta_2 \text{sign}\,(e_1) + \dot{\phi} \end{aligned} \tag{A.52}$$

where $e_2 = \hat{x}_2 + \phi(t)$ and $\bar{e} = [e_1 \quad e_2]^T$. Note that the structure of the error dynamics are the same as in Σ_2, therefore the design of the gains β_1 and β_2 to assure the convergence of the errors to zero in finite-time is analogue, and can be defined as in (4.12b).

SSTA behaviors

Proposition 2. *When the parameter is selected as $\delta = 0$ and the estimation error converges to zero before the state reaches $x_1 = 0$, a nominal-like behavior will occur (see Fig. A.3).*

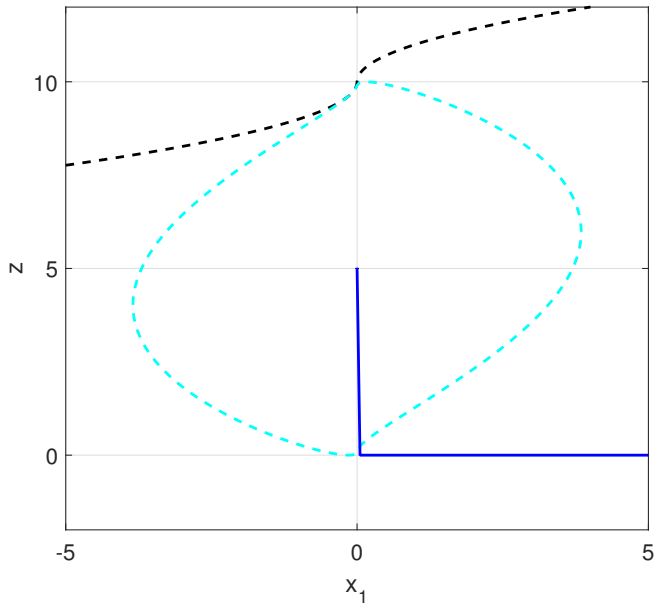

FIGURE A.3: Proposition 2: Nominal-like behavior; $\delta = 0$ and $e_2 = 0$

During the interval $x(t) \in [x_0, 0)$, the RC will enforce the trajectories to reach zero, then, the STA controller will keep the trajectories in $x_1 = x_2 = 0$, with the equivalent control $u = -\hat{\phi}(t)$.

Proof. The time derivative of the Lyapunov function V_c along the solutions of system (A.47) ensures the convergence of the state to zero in finite-time when Ω_δ contains only the origin $x_1 = 0$. When the estimator is in sliding mode, $e_1 = e_2 = 0$, it implies that $\hat{x}_2 = -\hat{\phi}(t)$, then, after initialize $z(t_i) = \hat{x}_2(t_i)$, the system is

$$\begin{aligned} \dot{x}_1(t_i) = &\quad u(t_i) + \phi(t_i) \\ = &\quad -\alpha_1 \lceil x_1(t_i) \rfloor^{1/2} + z(t_i) + \phi(t_i) \\ = &\quad -\alpha_1 \lceil 0 \rfloor^{1/2} - \hat{\phi}(t_i) + \phi(t_i) = 0 \end{aligned} \quad . \tag{A.53}$$

Then the trajectories will stay in sliding mode $x_1 = x_2 = 0$ for all future time.■

Proposition 3. *When the condition (4.6) is not fulfilled, the trajectories of the system may exhibit a switched periodic motions, see Fig. A.4. Nevertheless, as e_2 tends to zero (i.e. $\hat{x}_2(t) \to -\phi(t)$) in finite-time, the amplitude of the periodic motions will decrease to zero also in finite-time. After a finite number of oscillations there will be a last STA reaching phase converging to zero in finite-time without returning to the RC behavior.*

Proof. For every ϵ_ϕ such that $|\rho - \phi_{max}| \leq \epsilon_\phi$, there exist sufficiently small initial conditions $x(t_i) = [0 \;\; e_2]^T$ such that

$$V_s(0, e_2) \leq \gamma_2 (\rho - \phi_{max})^2, \tag{A.54}$$

holds. PINS will not exceed the saturation lines and the trajectories will converge to zero in finite-time fulfilling (4.2b), i.e., using the fact that the estimation error will be $e_2 = 0$ after a finite-time, it is clear that $V(0, 0) = 0 < \gamma_2 \epsilon_\phi^2$.

△

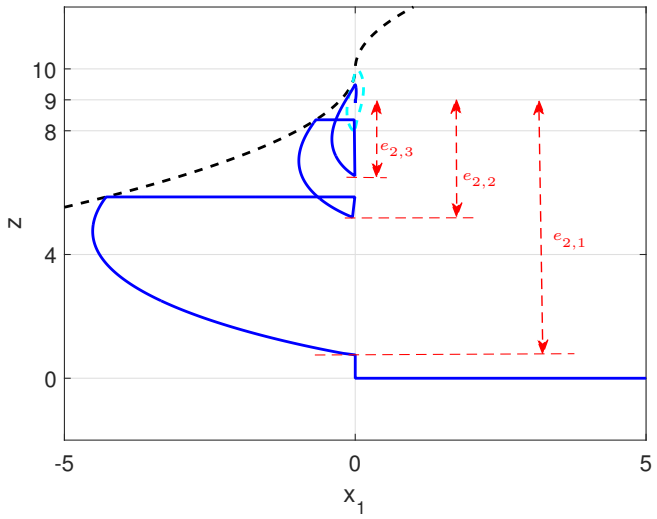

FIGURE A.4: Proposition 3: $\delta = 0$ and $e_2 \neq 0$. Different error estimations $e_2(t_i) = e_{2,i}$, $i = 1, 2, 3$.

A.3 Estimator preescribed convergence time gains

The estimation of the minimum reaching time T_{cmin} of the RC is made considering the case when the perturbation helps the system trajectories to converge. Then, Lyapunov function derivative (A.47) has the form

$$\dot{V}_c \leq -c_1 \left(\rho + \phi_{max}\right).$$

If we select $c_1 = 1/(\rho + \phi_{max})$, the Lyapunov function derivative becomes $\dot{V}_c = -1$, and for $t_0 = 0$,

$$V_c(x) = V_c(x_0) - t = \frac{|x_0|}{\rho + \phi_{max}} - t.$$

This shows that V_c reduces to zero in time (4.17).

Consider the Lyapunov function in Polyakov and Poznyak, 2009

$$V_e = \begin{cases} \dfrac{k^2}{4}\left(\dfrac{e_2\lceil e_1 \rfloor^0}{\gamma} + k_0 e^{m(\bar{e})}\sqrt{s(\bar{e})}\right)^2 & e_1 e_2 \neq 0 \\ \dfrac{2\bar{k}e_2^2}{\alpha_1^2} & e_1 = 0 \\ \dfrac{|e_1|}{2} & e_2 = 0 \end{cases} \tag{A.55}$$

where k, $\bar{k}$ and k_0 are design parameters depending on L and the gains β_1 and β_2. $s(\bar{e})$ and $m(\bar{e})$ are non-linear functions of the state, and $g = 8\gamma/\alpha_1^2$ with $\gamma(\bar{e}) := \alpha_2 - L\text{sign}\left(e_1 e_2\right)$.

Note that with the knowledge of the initial condition x_0 it is possible to set $\hat{x}_1(0) = x_0$, and therefore $e_1(0) = x_0 - \hat{x}_1(0) = 0$ to use the second case of (A.55).

We choose a parametrization of the estimator gains

$$\beta_1 = 2\sqrt{(9L + \epsilon)}, \tag{A.56a}$$

$$\beta_2 = 7L + \epsilon, \tag{A.56b}$$

with $\epsilon > 0$, such that the conditions of Polyakov and Poznyak, 2009, Theorem 1, Lemma 5 hold, i.e.

$$\beta_2 = 7L + \epsilon > 5L$$

and

$$\begin{array}{rcccl} 32L & < & \beta_1^2 & < & 8(\alpha_2 - L) \\ 32L & < & (2\sqrt{9L+\epsilon})^2 & < & 8((7L+\epsilon) - L) \\ 32L & < & 36L + 4\epsilon & < & 48L + 8\epsilon. \end{array}$$

The parameter g may take two possible values $g^- = 8(\beta_2 - L)/\beta_1^2, g^+ = 8(\beta_2 + L)/\beta_1^2$ depending on the values of $\gamma \in \{\beta_2 + L, \beta_2 - L\}$. The term g also can vary depending on the selection of the parameter ϵ. Therefore the limits of g^- and g^+ when $\epsilon \to 0$ and $\epsilon \to \infty$ are taken:

$$\begin{array}{ll} \lim\limits_{\epsilon \to 0} g^- = 4/3, & \lim\limits_{\epsilon \to \infty} g^- = 2, \\ \lim\limits_{\epsilon \to 0} g^+ = 16/9, & \lim\limits_{\epsilon \to \infty} g^+ = 2. \end{array} \tag{A.57}$$

The whole range of variation of g depending on γ and ϵ is $g \in [g_m,\ g_M] = [4/3,\ 2]$.

The parameter $\bar{k}$ should belong to a intersection set of the intervals $I(g_m) \cap I(g_M) \neq 0$, where the interval $I(g)$,

$$I(g) = \left(\frac{2}{g} + \frac{e^{(1/\sqrt{g-1})(-(\pi/2) - arctan(1/\sqrt{g-1}))}}{\sqrt{g}}, \frac{e^{(1/\sqrt{g-1})((\pi/2) - arctan(1/\sqrt{g-1}))}}{\sqrt{g}} \right). \tag{A.58}$$

Evaluating the numeric endpoints of g, $I(g^-) = [1.5093,\ \ 2.1448]$ and $I(g^+) = [1.0670,\ \ 1.5509]$, $\bar{k}$ can be selected as $\bar{k} = 1.5301$.

Using Polyakov and Poznyak, 2009, Theorem 1, we ensure that the time derivative of (A.55) along the trajectories of the system satisfies

$$\dot{V}_e \leq -k\sqrt{V}_e \leq -k_{min}\sqrt{V}_e \tag{A.59}$$

and if the bound for $|e_2(0)| = |\phi(0)| = \phi_{max}$, the reaching time estimate can be referred to as

$$T_e \leq \frac{2}{k_{min}} \sqrt{V_e(0, \phi_{max})}, \tag{A.60}$$

$$\begin{array}{rl} k_{min} := & \frac{\alpha_1}{\sqrt{8}} \min\limits_{\substack{g \in \{g^-, g^+\} \\ \epsilon \in \{0, \infty\}}} f(g, \epsilon), \\ f(g, \epsilon) = & \left| g\bar{k} - \sqrt{g} e^{\left(\frac{arctan\left(\frac{-1}{\sqrt{g-1}}\right) + \left(\frac{\pi(\alpha_1^2 g - 8\alpha_2)}{16L}\right)}{\sqrt{g-1}} \right)} \right|. \end{array} \tag{A.61}$$

Evaluating f with the two limits g_m and g_M, $f(g, \epsilon) \in [f_m,\ f_M] = [2.0277,\ 11.8608]$, and then, $k_{min} = \frac{\alpha_1}{\sqrt{8}} f_m$.

From (A.55), and (A.60), and setting the reaching time of the estimator T_e less than the minimum reaching time of the state T_{cmin}, we have

$$T_e \leq \frac{8\bar{k}\phi_{max}}{\beta_1^2 f_m} \leq T_{cmin}. \tag{A.62}$$

Substituting (4.17) and solving for β_1,

$$\beta_1 \geq \sqrt{\frac{8\bar{k}}{f_m}\frac{\left(\phi_{max}^2 + \rho\phi_{max}\right)}{|x_0|}}, \tag{A.63}$$

and finally we get (4.15a).

From parametrization (A.56a), we solve for ϵ,

$$\epsilon = \frac{1}{4}\beta_1^2 - 9L. \tag{A.64}$$

Substituting (A.64) in parametrization (A.56b), we get

$$\beta_2 = \frac{1}{4}\beta_1^2 - 2L,$$

using the equality case of (A.63),

$$\beta_2 \geq \frac{2\bar{k}}{f_m}\frac{\left(\phi_{max}^2 + \rho\phi_{max}\right)}{|x_0|} - 2L \tag{A.65}$$

and finally we get (4.15b).

Note that the value of the gains β_1 and β_2 tends to zero and to $-2L$, respectively, as x_0 tends to infinity because in this expressions the restriction $\epsilon > 0$ disappeared. Therefore, the conditions (4.15) are expressed as the maximum of two values: when $\epsilon > 0$, and $\epsilon = 0$, respectively.

Bibliography

Bejarano, F.J., L. Fridman, and A. Poznyak (2007). "Output Integral Sliding Mode Control Based on Algebraic Hierarchical Observer". In: *International Journal of Control* 80.3, pp. 443–453.

Bernuau, E. et al. (2013). "Verification of ISS, IISS and IOSS properties applying weighted homogeneity". In: *Systems and Control Letters* 62.12, pp. 1159 –1167. ISSN: 0167-6911. DOI: http://dx.doi.org/10.1016/j.sysconle.2013.09.004. URL: http://www.sciencedirect.com/science/article/pii/S0167691113001916.

Boiko, I. and L. Fridman (2005). "Analysis of chattering in continuous sliding-mode controllers". In: *IEEE Transactions on Automatic Control* 50.9, pp. 1442–1446. ISSN: 0018-9286. DOI: "10.1109/TAC.2005.854655".

Castaños, F. and L. Fridman (2006). "Analysis and Design of Integral Sliding Manifolds for Systems With Unmatched Perturbations". In: *IEEE Transactions on Automatic Control* 51.5, pp. 853–858.

Castillo, I. et al. (2016a). "Saturated Super-Twisting Algorithm based on Perturbation Estimator". In: *2016 IEEE 55th Conference on Decision and Control (CDC)*, pp. 7325–7328. DOI: 10.1109/CDC.2016.7799400.

Castillo, I. et al. (2016b). "Saturated Super-Twisting Algorithm: Lyapunov based approach". In: *2016 14th International Workshop on Variable Structure Systems (VSS)*, pp. 269–273. DOI: 10.1109/VSS.2016.7506928.

Davila, J., L. Fridman, and A. Poznyak (2006). "Observation and identification of mechanical systems via second order sliding modes". In: *International Journal of Control* 79.10, pp. 1251–1262. DOI: 10.1080/00207170600801635. eprint: http://dx.doi.org/10.1080/00207170600801635. URL: http://dx.doi.org/10.1080/00207170600801635.

Fridman, L., A. Poznyak, and F. J. Bejarano (2014). *Robust Output LQ Optimal Control via Integral Sliding Modes*. Birkhäuser.

Gonzalez, T., Moreno J. A., and L. Fridman (2012). "Variable Gain Super-Twisting Sliding Mode Control". In: *IEEE Transactions on Automatic Control* 57.8, pp. 2100–2105. ISSN: 0018-9286. DOI: 10.1109/TAC.2011.2179878.

Graichen, K. (2006). "Feedforward Control Design for Finite-Time Transition Problems of Nonlinear Systems with Input and Output Constraints". PhD Thesis. Stuttgart University.

Guzmán, E. and J. A. Moreno (2015). "Super-twisting observer for second-order systems with time-varying coefficient". In: *IET Control Theory Applications* 9.4, pp. 553–562. ISSN: 1751-8644. DOI: 10.1049/iet-cta.2014.0348.

Hippe, P. (2006). *Windup in control: its effects and their prevention*. Springer Science & Business Media.

Isidori, Al (1995). "Nonlinear control systems () Springer". In: *London, UK*.

Levant, A. (1993). "Sliding order and sliding accuracy in sliding mode control". In: *International Journal of Control* 58.6, pp. 1247–1263. DOI: 10.1080/00207179308923053. eprint: http://dx.doi.org/10.1080/00207179308923053. URL: http://dx.doi.org/10.1080/00207179308923053.

Levant, A. (1998). "Robust exact differentiation via sliding mode technique". In: *Automatica* 34.3, pp. 379 –384. ISSN: 0005-1098. DOI: http://dx.doi.org/10.1016/S0005-1098(97)00209-4. URL: http://www.sciencedirect.com/science/article/pii/S0005109897002094.

— (2010). "Chattering Analysis". In: *IEEE Trans. Autom. Control* 55, pp. 1380 –1389.

Maciejowski, J.M. (2002). *Predictive Control with Constraints*. Pearson Education Limited.

Moreno, J. (2011). "Lyapunov Approach for Analysis and Design of Second Order Sliding Mode Algorithms. State of the Art". In: *Sliding Modes after the first Decade of the 21st Century*. Ed. by L. Fridman, J. A. Moreno, and R. Iriarte. Vol. 412. Lecture Notes in Control and Information Sciences. Springer-Verlag Berlin Heidelberg, pp. 113–149. ISBN: 978-3-642-22164-4. DOI: 10.1007/978-3-642-22164-4.

Moreno, J. A. (2009). "A linear framework for the robust stability analysis of a Generalized Super-Twisting Algorithm". In: *Electrical Engineering, Computing Science and Automatic Control,CCE,2009 6th International Conference on*, pp. 1–6. DOI: 10.1109/ICEEE.2009.5393477.

Moreno, J. A. and M. Osorio (2008). "A Lyapunov approach to second-order sliding mode controllers and observers". In: *Decision and Control, 2008. CDC 2008. 47th IEEE Conference on. Cancun, México*, pp. 2856–2861. DOI: 10.1109/CDC.2008.4739356.

— (2012). "Strict Lyapunov functions for the super-twisting algorithm". In: *Automatic Control, IEEE Transactions on* 57.4, pp. 1035–1040.

Orlov, Yury, Yannick Aoustin, and Christine Chevallereau (2011). "Finite Time Stabilization of a Perturbed Double Integrator-Part I: Continuous Sliding Mode-Based Output Feedback Synthesis". In: *IEEE Transactions on Automatic Control* 56.3, pp. 614–618. ISSN: 0018-9286. DOI: 10.1109/TAC.2010.2090708.

Pérez-Ventura, U. and L. Fridman (2016). "Chattering measurement in SMC and HOSMC". In: *Variable Structure Systems (VSS), 2016 14th International Workshop on*. IEEE, pp. 108–113.

Picó, J. et al. (2013). "Stability preserving maps for finite-time convergence: Super-twisting sliding-mode algorithm". In: *Automatica* 49.2, pp. 534 –539. ISSN: 0005-1098. DOI: http://dx.doi.org/10.1016/j.automatica.2012.11.022. URL: http://www.sciencedirect.com/science/article/pii/S0005109812005584.

Polyakov, A. and A. Poznyak (2009). "Reaching Time Estimation for "Super-Twisting" Second Order Sliding Mode Controller via Lyapunov Function Designing". In: *IEEE Transactions on Automatic Control* 54.8, pp. 1951–1955. ISSN: 0018-9286. DOI: 10.1109/TAC.2009.2023781.

Rubagotti, M. et al. (2011). "Integral Sliding Mode Control for Nonlinear Systems With Matched and Unmatched Perturbations". In: *IEEE Transactions on Automatic Control* 56.11, pp. 2699–2704.

Shtessel, Y., M. Taleb, and F. Plestan (2012). "A novel adaptive-gain supertwisting sliding mode controller: Methodology and application". In: *Automatica* 48.5, pp. 759 –769. ISSN: 0005-1098. DOI: http://dx.doi.org/10.1016/j.automatica.2012.02.024. URL: http://www.sciencedirect.com/science/article/pii/S0005109812000751.

Utkin, V. (2016). "Discussion Aspects of High-Order Sliding Mode Control". In: *IEEE Transactions on Automatic Control* 61.3, pp. 829–833. ISSN: 0018-9286. DOI: 10.1109/TAC.2015.2450571.

Utkin, V. I. (1992). *Sliding Modes in Control and Optimization*. Springer-Verlag Berlin Heidelberg.

— (2013). "On Convergence Time and Disturbance Rejection of Super-Twisting Control". In: *IEEE Transactions on Automatic Control* 58.8, pp. 2013–2017. ISSN: 0018-9286. DOI: 10.1109/TAC.2013.2251812.

Utkin, V. I. and A. S. Poznyak (2013). "Adaptive sliding mode control with application to super-twist algorithm: Equivalent control method". In: *Automatica* 49.1, pp. 39 –47. ISSN: 0005-1098. DOI: http://dx.doi.org/10.1016/j.automatica.2012.09.008. URL: http://www.sciencedirect.com/science/article/pii/S0005109812004694.